

AUTOMATED SEPARATION OF KRYPTON

from Small Atmospheric Air
Samples for Measurement
with Atom Trap Trace Analysis

A Dissertation submitted in
Candidacy for the Degree
of Doctor of Philosophy to
the Faculty of Mathematics,
Informatics and Natural
Sciences, Department of
Physics, at Universität
Hamburg

BY SIMON HEBEL
HAMBURG 2018

This thesis was written and research conducted at
University of Hamburg
Carl Friedrich von Weizsäcker-Centre for Science and Peace Research
Beim Schlump 83
D-20144 Hamburg
Germany

Gutachter der Dissertation:	Prof. Dr. Gerald Kirchner Dr. Roland Purtschert
Zusammensetzung der Prüfungskommission:	Prof. Dr. Gerald Kirchner Dr. Roland Purtschert Prof. Dr. Daniela Pfannkuche Prof. Dr. Volkmar Vill Prof. Dr. Götz Neuneck
Vorsitzende der Prüfungskommission:	Prof. Dr. Daniela Pfannkuche
Datum der Disputation:	19. Juli 2018
Vorsitzender Fach-Promotionsausschuss Physik:	Prof. Dr. Wolfgang Hansen
Leiter des Fachbereichs Physik:	Prof. Dr. Michael Potthoff
Dekan der Fakultät MIN:	Prof. Dr. Heinrich Graener

Abstract

The isotope krypton-85 has applications in the environmental sciences and nuclear verification. In particular, it can serve as an indicator and tracer of nuclear reprocessing activities such as the production of plutonium from irradiated targets and fuel rods, an activity that is subject to regulations by the Nuclear Non-Proliferation Treaty. To employ Kr-85 for the verification of the aforementioned treaty, a sampling and measurement system is required that can determine the Kr-85 concentration of small air samples which are easy to acquire and transport.

To overcome the inherent limitations of radiometric Kr-85 measurements, which require large sample volumes and long measurement times due to low abundance and long half-life, a new measurement method called atom trap trace analysis has been established in which krypton isotopes can be selectively cooled and trapped using magneto-optical traps. These systems can determine the Kr-85 concentration in krypton volumes as low as 1 μL within a few hours, enabling the processing of large numbers of samples. One such system is currently under development at the Centre for Science and Peace Research at the University of Hamburg.

Currently, an air separation system able to extract krypton from a 1 L air sample with sufficient yield and purity for measurement is not available. The aim of this thesis is to develop and build such a system which can operate in a fully automated manner.

This is achieved by examining and adapting existing air separation methods, which commonly operate on larger air samples. The resulting system, named “Krypton-Abtrennungs-Anlage” (KAA, *german: krypton separation line*), is based on gas chromatography using a temperature controlled, activated charcoal column and a helium carrier to split the air into a fraction containing argon, nitrogen and oxygen, and a fraction containing methane and krypton. The latter is purified using a getter device to rid the sample of methane, but also any remaining nitrogen. Script controlled automation and logging of the procedure necessitates only minimal operator intervention, requiring about 2 hours per sample including regeneration, 15–30 minutes of which require the operator’s attention.

The performance of the separation line is characterised using radiometric measurements on large air samples and test samples enriched in Kr, showing a yield of around 38 %. This yield includes the sample transfer from separation to measurement, that is from Hamburg, Germany to Bern, Switzerland, and is sufficient for supplying the atom trap trace analysis with krypton samples using a sample size of 2 L of air.

Zusammenfassung

Das Isotop Krypton-85 findet Verwendung in den Umweltwissenschaften und in der nuklearen Verifikation. Insbesondere stellt es einen Indikator für nukleare Aufbereitungsaktivitäten wie die Produktion von Plutonium dar, welche als proliferationsrelevante Aktivität durch den Nichtverbreitungsvertrag reguliert ist. Um Kr-85 für die Verifikation dieses Vertrages nutzen zu können, wird ein System benötigt, das kleine, leicht zu transportierende Luftproben sammeln, aufbereiten und ihren Kr-85-Gehalt bestimmen kann.

Radiometrische Messungen von Kr-85 benötigen große Luftproben im Kubikmeterbereich und lange Messzeiten von mehreren Tagen. Diese Einschränkungen können durch die Verwendung eines neuartigen Messverfahrens mittels magneto-optischer Atomfallen (atom trap trace analysis) umgangen werden, das einzelne Kryptonisotope selektiv kühlen und einfangen kann. Auf diese Weise kann die Kr-85-Konzentration kleiner Kryptonproben von 1 μL innerhalb weniger Stunden bestimmt werden, was die Sammlung und Verarbeitung einer größeren Zahl von Proben ermöglicht. Ein solches System wird derzeit am Zentrum für Naturwissenschaft und Friedensforschung der Universität Hamburg entwickelt.

Zur Zeit ist kein Abtrennungssystem verfügbar, das eine hochreine Kryptonfraktion aus einer 1 L großen Luftprobe mit hoher Ausbeute extrahieren kann. Das Ziel dieser Dissertation ist die Entwicklung eines solchen Systems, welches automatisiert betrieben werden kann.

Dies wird durch die Anpassung gängiger Luftseparationsmethoden an kleine Proben erreicht. Das so entwickelte System, die „Kryptonabtrennungsanlage“ (KAA), basiert auf einer Gaschromatographie mit Aktivkohlesäule und präziser Temperaturregelung und Helium als Trägergas, um die Luftprobe in eine Argon-Stickstoff-Sauerstoff-Fraktion und eine Krypton-Methan-Fraktion aufzuteilen. Letztere wird mittels eines Getters von Methan und Restgasen gereinigt. Durch die skriptgesteuerte Automatisierung und Auswertung dauert dieser Prozess etwa 2 Stunden einschließlich Regenerationszeit, von denen nur 15–30 Minuten manuell betreut werden müssen.

Die Kryptonabtrennungsanlage wurde getestet und charakterisiert mittels radiometrischer Messung von großen Luftproben und angereicherten, kleinen Luftproben, wobei eine durchschnittliche Ausbeute von 38 % nachgewiesen wurde. Diese Ausbeute schließt alle Transferprozesse und den Transport von Hamburg nach Bern mit ein und ist ausreichend, um Kryptonproben für die Vermessung abzutrennen, wenn die Größe der Luftprobe 2 L beträgt.

Contents

1. Introduction	9
1.1. History of krypton-85 measurement	9
1.2. Production of krypton-85	10
1.3. Potential for krypton-85 in treaty verification	11
1.3.1. The Non-Proliferation Treaty	12
1.3.2. Other treaties	13
2. Theory of gas separation	14
2.1. Adsorption	14
2.1.1. Adsorption isotherms	14
2.1.1.1. Langmuir isotherm	14
2.1.1.2. BET isotherm	15
2.1.2. Adsorption forces	17
2.2. Chromatography	18
3. Krypton sampling and measurement	23
3.1. Krypton-85 in the environment	23
3.2. Sampling networks and source location	26
3.3. Krypton measurement technologies	28
3.3.1. Radiometry	28
3.3.2. Atom trap trace analysis	29
3.3.2.1. Optical cooling basics	29
3.3.2.2. Creating metastable states	29
3.3.2.3. Atom trap trace analysis capabilities	30
3.4. Prior krypton separation methods	30
3.4.1. German Federal Office for Radiation Protection	30
3.4.2. University of Bern	31
3.4.3. Yokochi	32
3.4.4. Yang	33
3.4.5. Tu	33
3.4.6. Yokochi 2016	33
3.5. Adsorbents for Krypton	34
3.5.1. Zeolite molecular sieves	34
3.5.2. Activated charcoal	34

3.5.3.	Novel materials	37
3.5.3.1.	Metal organic frameworks	37
3.5.4.	Ideal adsorbent for krypton separation	38
4.	Constructing an automated krypton separation line	39
4.1.	Requirements for krypton separation	39
4.1.1.	Sample size	39
4.1.2.	Sample purity	40
4.1.3.	Automation	40
4.1.4.	Flexibility and upgrades	41
4.1.5.	Duration and sample throughput rate	41
4.1.6.	Design goals	41
4.2.	Development of separation line elements	42
4.2.1.	Sample entry	42
4.2.1.1.	Desiccation	42
4.2.1.2.	Dust protection	43
4.2.1.3.	Injection	43
4.2.2.	Air sampling bags	46
4.2.3.	Surveillance via quadrupole mass spectrometry	47
4.2.3.1.	Comparison with thermal conductivity detector	47
4.2.3.2.	Monitoring the gas stream	47
4.2.3.3.	Capillary connection	49
4.2.4.	Chromatographic column	51
4.2.4.1.	Adsorbent comparison at room temperature	53
4.2.4.2.	Selective krypton freezing	53
4.2.4.3.	Thawing experiments	53
4.2.4.4.	Carrier gas	58
4.2.4.5.	Separation without fine temperature regulation	58
4.2.4.6.	Choice of column	64
4.2.5.	Flow control	64
4.2.6.	Temperature control	65
4.2.6.1.	Options	65
4.2.6.2.	Implementation	65
4.2.7.	Getter	68
4.2.7.1.	Choice of getter	68
4.2.7.2.	Purification experiments	70
4.2.8.	Purified sample container	72
4.3.	Krypton separation line	73
4.3.1.	Final layout of the krypton separation line"	73
4.3.2.	Control, automation and monitoring	78
4.3.2.1.	Manual control	78

4.3.2.2.	Automation and logging	78
4.3.2.3.	Evaluation	79
4.3.3.	General separation procedure	80
4.3.4.	Optimisation of the separation procedure	80
4.3.4.1.	MS4A troubles	80
4.3.4.2.	Stability of results and error propagation	81
4.3.4.3.	AC1 temperature and timing	83
4.3.4.4.	Pause before heating	85
4.3.4.5.	AC1 end temperature	85
4.3.4.6.	AC2 temperature	87
4.3.4.7.	Sample size	88
4.3.4.8.	AC2 capture timing	88
4.3.4.9.	Sample concentration	89
4.3.4.10.	Transfer to krypton container	89
4.3.4.11.	Cross-contamination	91
4.3.4.12.	Sample purity	92
4.3.5.	Final separation procedure	92
4.3.6.	Routine operation	95
5.	Evaluation of separation performance	96
5.1.	Ambient air sample	96
5.1.1.	Separation procedure	97
5.1.2.	Measurement procedure	98
5.1.3.	Yield	99
5.1.4.	Evaluation	99
5.2.	Enriched samples, Series 1	99
5.2.1.	Separation	100
5.2.2.	Measurement	100
5.2.3.	Yield	100
5.2.3.1.	Memory effect	102
5.2.4.	Evaluation	102
5.3.	Enriched samples, Series 2	103
5.3.1.	Separation	103
5.3.2.	Measurement	105
5.3.3.	Yield	105
5.3.4.	Re-evaluation based on the composition of the standard gas	105
5.4.	Overall performance of the krypton separation line	107
6.	Conclusions	109
7.	Outlook	110

Bibliography	110
A. Final separation procedure	118
Acknowledgements	121
Eidesstattliche Versicherung (Declaration on oath)	122

1. Introduction

1.1. History of krypton-85 measurement

Krypton-85 is mostly emitted by anthropogenic sources. Similar to the xenon isotopes relevant to nuclear test tracing and verification purposes, it is produced in minuscule amounts by the spontaneous fission of naturally occurring uranium-238 (England and Rider, 1994; Hebel, 2010), but this amount is negligible compared to other sources. The interaction of cosmic rays with stable krypton contributes a small amount to the global inventory. It has first been introduced into the atmosphere in a large scale by industrialised nuclear activities, specifically the production of fissile material and subsequent detonation of the first nuclear weapons during the Manhattan Project. For this reason, older samples free from Kr-85 contamination are frequently referred to as “pre-bomb” krypton in the scientific community.

The role of Kr-85 as a byproduct of nuclear fission and especially plutonium production has been known since the very beginning of the nuclear arms race between the United States and the Soviet Union. In 1951, an American mission dubbed “Operation Bluenose” saw the collection of atmospheric air samples to measure the krypton-85 content and estimate the size of the Russian plutonium stockpile (Avenhaus et al., 2006). Ideally, one would estimate the size of a fissile material stockpile based on the capacity of a state’s nuclear fuel cycle, especially reactors and reprocessing plants and their times of operation. If these parameters are not well known, one may resort to compiling an inventory of known Kr-85 sources, compare these releases to the atmospheric concentration, and estimate the amount of fissile materials whose production may account for the deviation (von Hippel et al., 1986).

While most of the krypton-85 produced is emitted into the atmosphere, the isotope has some commercial uses, mainly as an ionizer to reduce the conductivity in discharge lamps, electron tubes and similar appliances. The other major field of use is leak detection, where krypton seeping through microscopic cracks can be detected using radiometric imaging.

The continued accumulation of krypton in the atmosphere has also caused alarm. Since the nineteen-sixties, when a steep rise in nuclear power production during the following decades was anticipated, scientists warned of the radiation hazard posed by a rising krypton concentration, and even pondered the effects of an increased atmospheric conductivity on the frequency of thunderstorms (Harrison and ApSimon,

Isotope	neutron energy	fission yield [%]	cumulative yield [%]
U-235	thermal	0.027	0.285
	fission	0.000	0.275
U-238	thermal	—	—
	fission	0.000	0.149
Pu-239	thermal	0.016	0.128
	fission	0.000	0.125
Th-232	thermal	—	—
	fission	0.000	0.829

Table 1.1.: The Kr-85 yields from induced fission reactions of common fissile isotopes, as compiled by England and Rider (1994).

1994). Today, nuclear energy is stagnant, and plutonium not widely used as a nuclear fuel. Incidentally, the global krypton concentration is seemingly stabilising at a level not considered hazardous (see Section 3.1).

Since a few decades, krypton-85 has attracted the attention of the environmental sciences, and is seen as a valuable tool for dating groundwater (Purtschert et al., 2009). Also, its use as a tracer in hydrology and the atmospheric sciences is considered. All of these applications rely on a well defined, historical inventory of Kr-85, which is constantly being improved (Winger et al., 2005; Ahlswede et al., 2013).

The effort to use Kr-85 for quantifying and even tracing covert plutonium production is also continued and is the major motivation behind the work presented in this thesis.

1.2. Production of krypton-85

Krypton-85 is produced in nuclear reactors as a fission product of either uranium or plutonium. All major fissile materials will produce some amount of krypton-85, so it occurs in all burnup and breeding operations and cannot be avoided by choosing some specific fuel. The majority of Kr-85 is no direct product of induced fission, but a product of successive beta decay of precursor fission products. The Kr-85 yields of the most important fission processes are listed in Table 1.1.

For example, 0.28 % of thermal neutron induced fission reactions of U-235 will eventually produce a Kr-85 atom, 10 % of which are direct fission products. Per gram of U-235 burned in a reactor, that is 15 GBq of Kr-85.

Kr-85 will accumulate either in fuel rods or in irradiated targets and remain there during storage, which usually takes years except for operations aimed at producing

short lived isotopes, mostly for medical purposes. Fuel from reactors for plutonium production commonly has a lower burnup, and needs less storage time before it can be reprocessed safely. According to UNSCEAR (1982), less than 1 % of the contained noble gases leak from the assembly before it is opened up for reprocessing.

Ultimately, the amount of krypton-85 released from plutonium production amounts to about 10–40 TBq/kg, depending on the plutonium burnup (up to 50 TBq/kg) and storage time (up to 15 years) according to calculations by Schoeppner and Glaser (2016).

There is a large backlog of fuel stored worldwide, and despite the low demand for MOX fuel in the nuclear energy market, La Hague in France is still separating about 5–10 t of plutonium per year (IPFM, 2015), and Sellafield in the United Kingdom also conducts separation campaigns irregularly.

The standard method for nuclear reprocessing is the PUREX process (“Plutonium Uranium Redox EXtraction”). It is an aqueous technique in which plutonium and uranium are recovered from fuel elements by chopping and dissolving them in nitric acid. At this point, any enclosed gases such as krypton are released, mainly into the gaseous phase, with only a minor amount being solved in the aqueous phase. Afterwards, organic solvents including tributyl phosphate (TBP) precipitate uranium and plutonium complexes, which in turn are separated using ferrous sulphamate.

Retaining the large quantities of Kr-85 released in this process is technically challenging, as the noble gas cannot be chemically contained in a solid or liquid compound, but must be absorbed using cryogenic techniques. While the short-lived isotopes can be reduced significantly by delaying emission, krypton-85 would have to be stored much longer. One must therefore assume that at some point, all of the krypton produced has to be emitted into the atmosphere if the plutonium is being separated (Ross et al., 2009; Ross, 2010).

1.3. Potential for krypton-85 in treaty verification

As an inevitable by-product of plutonium production, krypton-85 has the potential to be used for the verification of international treaties concerning the production of nuclear weapons and their fissile material components.

The Comprehensive Test Ban Treaty (CTBT) is aimed at outlawing nuclear test explosions. It has not yet entered into force, but the attached Provisional Technical Secretariat has already established an International Monitoring System (IMS) to detect and localise nuclear explosions. Although explicitly not employing krypton measurements, the network has set a highly successful example of using measurements of radioactive noble gases for uncovering illicit nuclear activities by doing atmospheric transport modelling for backtracking suspicious radionuclide signals and correlating them with seismic events.

1.3.1. The Non-Proliferation Treaty

IMS xenon measurements have been regarded as a model for new verification techniques for the Treaty on the Non-Proliferation of Nuclear Weapons (NPT). The NPT has been the most important instrument in the regulation of nuclear weapons since its entry into force in 1970. It bans the development, production, ownership and use of nuclear weapons to all members except the five designated Nuclear Weapon States in return for assisting the Non Nuclear Weapon States in their nuclear programmes and, without any given timeframe, taking steps towards nuclear disarmament.

To enforce the NPT, the International Atomic Energy Organisation (IAEA) was tasked with operating a regime of Safeguards establishing a mutual trust that any given state's nuclear programme is not military in nature. This is done by regularly conducting announced inspections of nuclear facilities using techniques such as visual inspection, tagging, sealing, routine measurements and inventory checking (IAEA, 1972). Usually, these measures are conducted in the least intrusive manner in order not to disturb operations, and are detailed in a Safeguards Agreement between the IAEA and each individual state party.

This system was shaken up in the early 1990s when the United Nations Special Commission (UNSCOM), which was created by the United Nations after the Gulf War to ensure Iraqi compliance with the destruction of biological, chemical and missile weapons, uncovered a nuclear weapons programme that had been built up outside the existing Safeguards regime. In response, the IAEA pursued an extension of traditional Safeguards in order to provide capabilities for detecting illicit nuclear activities, which took the form of Additional Protocols (AP), extensions of the Safeguards Agreements signed by each state party. They may contain a number of measures including short notice (i.e. 24 hours in advance) complementary access and intrusive sampling measures, so called environmental samples, even outside declared nuclear facilities (IAEA, 1997). At the time of writing, AP have been signed by about half of the NPT member states.

Most of the environmental samples taken today are swipe samples, taken inside nuclear facilities using standardised kits. During the 1000 inspection visits conducted per year, about 800 swipes are taken and analysed in a laboratory part of the Network of Analytical Laboratories. Swipe samples are location specific samples, the only kind currently permitted under the AP. An implementation of so called wide-area environmental sampling would have to be approved by the Board of Governors, like any other novel measurement method.

Air samples for krypton-85 measurement could be used as either location specific or wide-area environmental sampling, which makes them politically controversial. Still, routine Kr-85 samples have the potential of providing valuable information on potential covert plutonium production, if they can be implemented in a way that is compatible with inspection activities: using small samples that are easy to obtain and

transport by a single person, and can be archived for later analysis.

For this reason, a number of projects have been investigating and improving Kr-85 sampling and measurement to these ends. The IAEA Novel Technologies Project has placed a major focus on Kr-85, inciting research and funding studies (Whichello et al., 2010). Projects, many of which were conducted at the Centre for Science and Peace Research, University of Hamburg, have researched all building blocks for a Safeguards routine centred on Kr-85, starting with the source terms, background and atmospheric dispersal (Ross et al., 2009; Ross, 2010), detection networks and source location (Klingberg et al., 2011), global krypton inventories (Winger et al., 2005; Ahlswede et al., 2009, 2013), sampling machinery, sample purification (this thesis), and, most importantly, a precise, high throughput measurement method using atom trap trace analysis (Daerr et al., 2011; Kohler et al., 2014). All of these projects have been building upon invaluable research by other groups, more of which is presented in Section 3.

The vision is to provide an instrument where a simple air sample of 1 L can be taken, brought to a certified laboratory, and processed and measured with high precision within a few hours.

1.3.2. Other treaties

Of course, a simple but effective Kr-85 measurement capability may also find use in other treaties concerning nuclear proliferation.

The Fissile Material Cut-off Treaty (FMCT) is a proposed treaty to limit the production of weapons-usable fissile materials. Proposals have also included monitoring sensitive facilities in nuclear weapon states using non-intrusive methods such as satellite imagery. As it is directly tied to plutonium production, Kr-85 could be a valuable tool in demonstrating FMCT compliance by monitoring the operational status of facilities and uncovering undeclared facilities. Since 1995, the Conference on Disarmament (CD) has a mandate to negotiate such a treaty, but a political stalemate has hampered any progress on the matter.

Avenhaus et al. (2006) have proposed a role for Kr-85 in the verification of a Middle East Nuclear Weapon Free Zone (MENWFZ), to increase mutual trust between states parties even when not all of them are subject to IAEA Safeguards.

2. Theory of gas separation

2.1. Adsorption

In the process of adsorption, an adsorbate is drawn to and held on an adsorbent by attractive forces.

2.1.1. Adsorption isotherms

The amount of gas that is adsorbed in equilibrium on a specific adsorbent is fundamentally a function of pressure and temperature. For a fixed temperature, this function is called isotherm and is a fundamental property of the adsorption process for a specific adsorbate-adsorbent pair. These isotherms can be derived experimentally or theoretically. The main reference for the information in this Chapter is Yang (2003).

2.1.1.1. Langmuir isotherm

The most fundamental approach to model adsorption is the Langmuir equation, which describes the kinetics of a monolayer adsorbed on an ideal surface where each adsorbate particle has one adsorption site where it stays until it is released, uninfluenced by neighbouring sites.

The fraction of occupied adsorption sites is

$$\theta = \frac{n}{n_{max}}$$

Particles are adsorbed at a rate that is proportional to the rate r at which they strike the surface. According to the Hertz-Knudsen equation:

$$r = \frac{p}{\sqrt{2\pi mRT}} \quad (2.1)$$

with pressure p , molecular weight m , universal gas constant R and Temperature T . Adsorption only takes place on free adsorption sites, so the rate of adsorption is

$$\frac{dN_{ad}}{dt} = k_{ad} \cdot r \cdot (1 - \theta) \quad (2.2)$$

with the sticking coefficient k_{ad} describing the likelihood of adsorption upon contact with an empty site. Analogously, the desorption rate is

$$\frac{dN_{de}}{dt} = k_{de} \cdot \theta \quad (2.3)$$

where k_{de} is the rate constant for desorption.

In equilibrium, Equations 2.2 and 2.3 yield the Langmuir isotherm:

$$\theta = \frac{K_L p}{1 + K_L p} \quad (2.4)$$

$$K_L = \frac{k_{ad}}{k_{de}} \cdot \frac{1}{\sqrt{2\pi mRT}}$$

where K_L is the Langmuir Constant. Figure 2.1 shows the resulting adsorption isotherms. For small pressures, θ is a linear function of pressure:

$$n = n_{max}\theta = n_{max} \frac{K_L p}{1 + K_L p} \xrightarrow{K_L p \ll 1} H p$$

$$H = n_{max} K_L$$

As this relation is highly reminiscent of Henry's Law, H is commonly called the Henry constant.

2.1.1.2. BET isotherm

Brunauer et al. (1938) have developed an extension of the Langmuir theory for a flat, homogeneous surface taking into account layered adsorption. Each layer is behaving according to the Langmuir equation and the adsorbate is treated as a liquid. Only the upper layer is in equilibrium with the vapour phase. The resulting BET isotherms are:

$$\theta = \frac{n}{n_{max}} = \frac{K_{BET} \cdot \frac{p}{p_L}}{\left(1 - \frac{p}{p_L}\right) \cdot \left[1 - \left(1 - K_{BET}\right) \cdot \frac{p}{p_L}\right]} \quad (2.5)$$

where p_L is the pressure of the liquid phase, $\frac{p}{p_L}$ is called the relative pressure, K_{BET} is the BET constant and n_{max} is the coverage of one monolayer. The resulting isotherms are shown in Figure 2.2. There is no saturation limit in BET isotherms, as layers can be infinitely stacked. If $\frac{p}{p_L}$ approaches unity, an infinite amount is adsorbed. For small pressures, multilayers are almost nonexistent and the BET isotherms behave linearly with the Henry constant

$$H = \frac{n_{max} K_{BET}}{p_L}$$

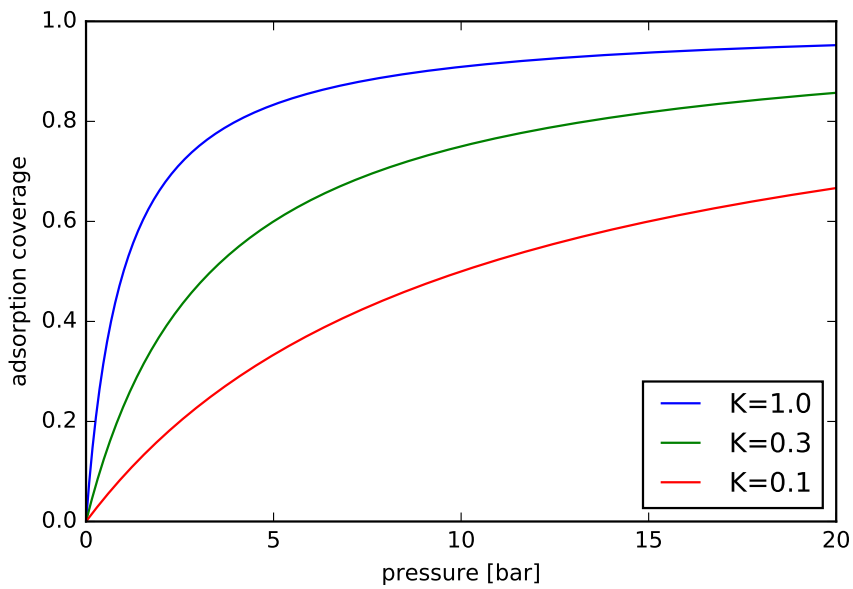


Figure 2.1.: Adsorption isotherms for different Langmuir Constants K , according to Equation 2.4.

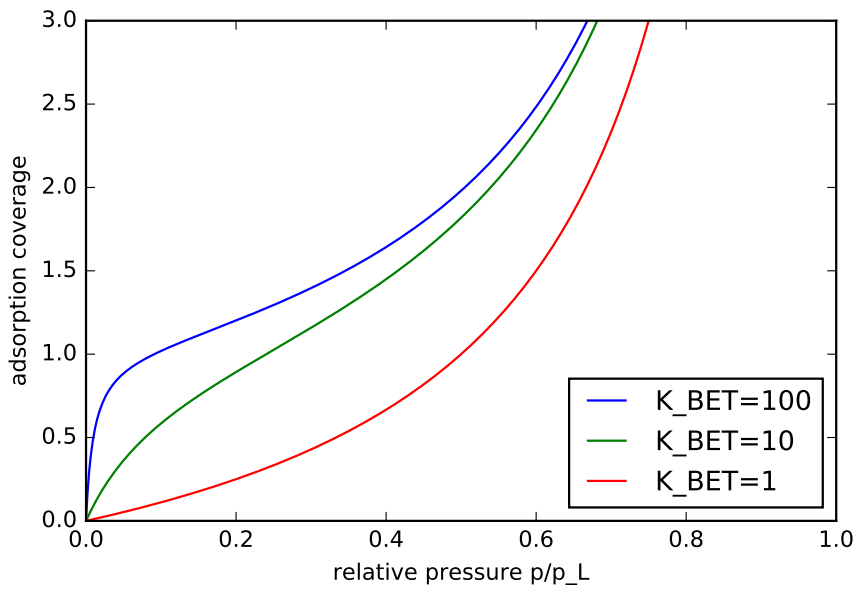


Figure 2.2.: BET adsorption isotherms according to Equation 2.5 for different BET constants K_{BET} .

K_{BET} is a function of the heat of adsorption ΔH_{ads} and the heat of condensation ΔH_{liq} :

$$K_{BET} \approx \left(\frac{\Delta H_{ads} - \Delta H_{liq}}{RT} \right)$$

Therefore, usually $K_{BET} \gg 1$ because $\Delta H_{ads} \gg \Delta H_{liq}$.

The BET equation is often used to determine the surface area of porous substances. Equation 2.5 can be rearranged so that

$$\frac{p}{n(p_L - p)} = \underbrace{\frac{1}{n_{max}K_{BET}}}_{intercept} + \underbrace{\left(\frac{K_{BET} - 1}{n_{max}K_{BET}} \right)}_{slope} \frac{p}{p_L}$$

which is a linear function of $\frac{p}{p_L}$. By fitting experimental data to this equation, a linear plot can be obtained and its slope and intercept used to determine n_{max} and K_{BET} . The surface area of the substance can be determined as

$$A = n_{max} \cdot N_A \cdot a_m$$

for Avogadro number N_A and molecular projected area a_m , which is specific for each adsorbate.

2.1.2. Adsorption forces

The adsorption process is governed by a number of forces depending on the interactions between the adsorbate and adsorbens, and interactions between adsorbate particles. The potential of physical adsorption is the result of a number of energy potentials and can be expressed as

$$\Phi = (\Phi_D + \Phi_R) + \Phi_P + \Phi_{FD} + \Phi_{FQ}$$

resulting from the dispersive and repulsive terms Φ_D and Φ_R , the polarisation energy Φ_P , the dipole energy Φ_{FD} , and the quadrupole energy Φ_{FQ} .

The terms Φ_D and Φ_R are nonspecific and occur in every sorbate-sorbent interaction. They are dominated by van-der-Waals interactions and a close range Pauli repulsion force and are well described using a Lennard-Jones potential of the form

$$\Phi_D + \Phi_R = \Phi_{LJ} = 4\epsilon \left(\left(\frac{\sigma}{r} \right)^6 - \left(\frac{\sigma}{r} \right)^{12} \right) \quad (2.6)$$

where ϵ is the depth of the potential well, σ is the distance at which the potential is zero, and r is the distance between adsorbens and adsorbate. Adsorption on activated

charcoal is dominated by this potential, whereas in zeolites electrostatic interactions often dominate. Figure 2.3 contains a generic diagram of the resulting potential.

The polarisation or inductive energy Φ_P results from a polar surface which induces a dipole in the adsorbate. It can be described as

$$\Phi_P = -\frac{1}{2}\alpha E^2 = \frac{\alpha q^2}{2r^4 (4\pi\epsilon_0)}$$

with the electric field E , the adsorbate's static polarisability α , the electronic charge q of the adsorbent surface, the vacuum permittivity ϵ_0 and distance r .

Dipole interactions occur if the adsorbate has a permanent dipole, whereas quadrupolar moments occur in adsorbates which are not spherical. The potentials of the dipole and quadrupole field interactions are

$$\Phi_{FD} = -E\mu \cos \theta = -\frac{q\mu \cos \theta}{r^2 (4\pi\epsilon_0)}$$

$$\Phi_{FQ} = \frac{1}{2}QE = -\frac{Qq (3 \cos^2 \theta - 1)}{4r^3 (4\pi\epsilon_0)}$$

where μ is the permanent dipole moment, θ is the angle between field gradient and the dipole or quadrupole and Q is the linear quadrupole moment. While none of the regular air constituents have dipoles, the molecules N_2 , O_2 and CO_2 possess quadrupole moments.

Activated charcoal is lacking any electrostatic surface effects, therefore the binding strength is generally lower than for polar materials, as seen in Table 2.1. This usually means that a lower temperature is required for effective adsorption. Another consequence is that large, heavy atoms like Kr or Xe are affected more strongly than smaller molecules due to their larger polarisability. Charcoal is therefore well suited to separate Kr and Xe from N_2 and O_2 .

2.2. Chromatography

In chromatography, gases are running along columns containing adsorbents, usually driven by an inert carrier. The technique employed in this thesis is gas-solid chromatography, that is chromatography of a gas running through a column of solid adsorbent, but the theoretical principles also hold for fluid-solid chromatography.

The main mechanism behind chromatographic separation is the adsorption of part of the solute onto the adsorbent in the column. For any given combination of adsorbate, adsorbent, temperature and pressure, there is an equilibrium in which part of the adsorbate is in the stationary phase. This equilibrium cannot last as the mobile

Adsorbent	Adsorbate	$-\Phi$	$-(\Phi_D + \Phi_R + \Phi_P)$	$-(\Phi_{FD} + \Phi_{FQ})$
Charcoal	Ne	0.74	0.73	.0
	Ar	2.12	1.84	.0
	Kr	2.8	2.48	.0
	Xe	3.7	3.1	.0
Na-X	N ₂	6.5	3.10	3.4
	CO ₂	12.5	4.20	7.98
	H ₂ O	17.9	2.65	31.3

Table 2.1.: Energies of adsorption for different combinations of adsorbens (activated charcoal, molecular sieve Na-X) and adsorbate, compiled by Yang (2003).

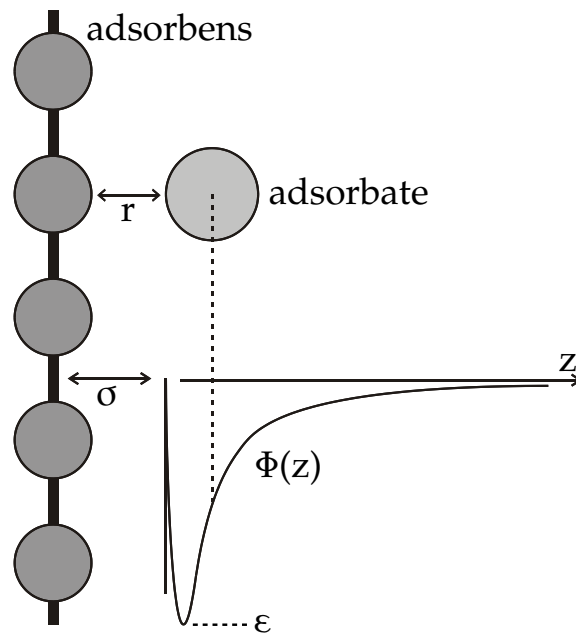


Figure 2.3.: Generic physical adsorption potential Φ according to equation 2.6. This Lennard-Jones type potential is typical for neutral atom adsorbates which predominantly interact (Simgen, 2003).

phase is moved along the column by two processes: diffusion, which moves the gas in all directions, and advection driven by the carrier gas, which is constantly flowing in one direction.

Depending on the equilibrium, gas species will travel at different speeds. If the speed difference is sufficient, gases which start at the same point in the column eventually do not overlap any more. At the same time, the gas peaks are broadened because the gaseous phase leaves the adsorbed phase behind. Diffusion is also a factor in peak broadening. These effects have to be balanced in a way that avoids peak overlap by choosing appropriate parameters for the separation, in order to obtain a peak of high purity.

The process of chromatography can be parametrised using the model of theoretical plates, which can be applied to numerous separation processes that are mainly governed by equilibrium conditions. The column is considered as separated into N discrete layers or theoretical plates of height equivalent H so that

$$N = \frac{L}{H}$$

in a column of length L . This height equivalent H of a theoretical plate is a measure for the efficiency of a separation column, with smaller H being more efficient and therefore requiring a shorter column to achieve the same effect. To accommodate band broadening, a sufficiently large number of plates is required in a column. If a Gaussian peak shape of variance σ^2 is assumed, this is the case when

$$H = \frac{\sigma^2}{L}$$

resulting in the required minimum number of plates

$$N = \frac{L^2}{\sigma^2}$$

The average speed u of a peak can be expressed as a function of the time t required to traverse the column:

$$u = \frac{L}{t}$$

Analogous to the spacial standard deviation σ of the peak, a temporal standard deviation τ can be determined:

$$\tau = \frac{\sigma}{u}$$

The resulting number of theoretical plates is

$$N = \frac{t^2}{\tau^2} = 16 \left(\frac{t}{W} \right)^2$$

for the temporal full width at half maximum $W = 4\tau$ of the peak. By measuring the retention time and temporal peak width, the number of theoretical plates in a column can be determined experimentally.

For any two peaks, the *resolution* R of a column is defined as

$$R = \frac{t_2 - t_1}{\frac{W_2 + W_1}{2}} = \frac{2 \cdot \Delta t}{W_1 + W_2}$$

A value of $R = 1$ corresponds to a separation of 4σ , or 94 %. If $R < 1$, the peaks are not clearly separated. In this case, the column can be characterised by stating the *separative power* or *selectivity* δ , which is found by connecting the two peak maxima with a line, and regarding the point where the two peaks intersect: the height of the interconnecting line above the base line at that point is G , and the height of the interconnecting line above the peak intersection is F . Now, the separative power is defined as

$$\delta = \frac{F}{G}$$

For a complete separation, $F = G$ and $\delta = 100\%$.

To achieve a good separative power, broadening of the peaks must be limited. The main contributions to broadening are *eddy diffusion*¹ caused by the column's packing introducing multiple non-ideal paths along the column, *longitudinal diffusion*, and *mass transfer kinetics* to account for the non-ideal mass transfer between the gaseous and adsorbed phase. These are parametrised in the Van Deemter equation

$$H = A + \frac{B}{u} + Cu \quad (2.7)$$

for the carrier gas's linear velocity u , eddy diffusion parameter A , longitudinal diffusion coefficient B and mass transfer coefficient C . For each column, there is a carrier flow speed

$$u = \sqrt{\frac{B}{C}}$$

where H reaches its minimum, indicating that the chromatography column works most efficiently for that speed, as indicated in Figure 2.4.

A , B and C depend on particle size and shape of the adsorbent, and mobile phase viscosity and diffusion coefficient of the adsorbate, as well as temperature and saturation. In general, H increases for higher temperatures. Measured values are very specific and, for activated charcoal, are in the range of several mm to cm. For example, Munakata et al. (1999) has determined a plate height of about 1 cm for an activated charcoal column of 2.5 cm diameter at room temperature.

¹i.e. turbulent diffusion

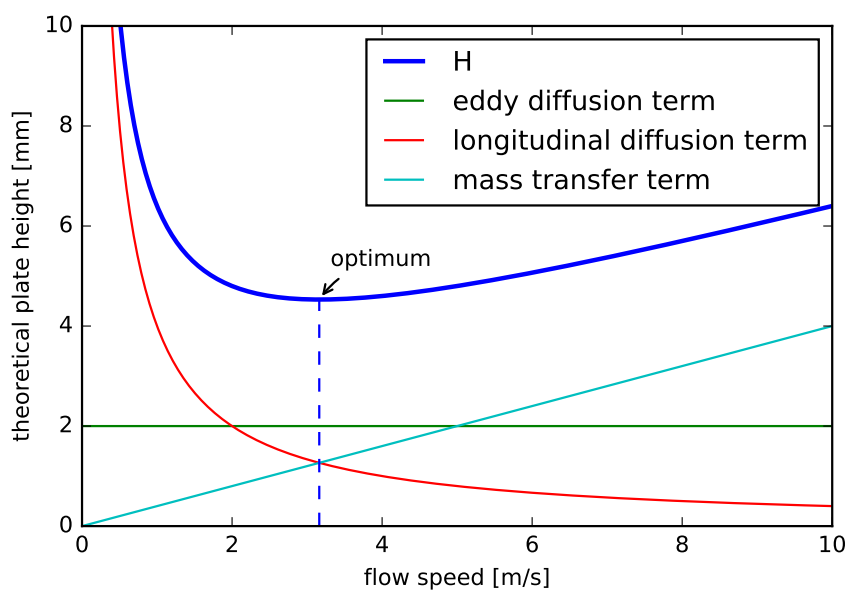


Figure 2.4.: Theoretical plate height H resulting from the Van Deemter equation (Equation 2.7), and the contributing effects. Note that there is an optimal carrier flow speed for a column where the plate height reaches its minimum.

3. Krypton sampling and measurement

3.1. Krypton-85 in the environment

Ever since the advent of nuclear engineering, Kr-85 has been emitted into the atmosphere. Since it does not react chemically, nor dissolve well in water (see Figure 3.1) or wash out with the rain, radioactive decay with a half life of 10.74 years is the only significant sink. As a result, the atmospheric Kr-85 concentration has been steadily increasing since 1945.

In the following decades, numerous measurements of the atmospheric background all over the world have been published (Stockburger et al., 1977; Cimbák and Povinec, 1985; Wilhelmová et al., 1986; Sartorius et al., 2002; Connan et al., 2014).

The most comprehensive continuous measurement campaign is that of the German Federal Office for Radiation Protection (BfS), which employs a world wide network collecting weekly samples, including stations in East Asia and the southern hemisphere. Figure 3.2 shows how the atmospheric concentration has continually increased, stagnated in the 2000s, and seems on the rise again at the time of writing.

The average concentration of Kr-85 is well understood. Winger et al. (2005) have compiled an exhaustive list of known reprocessing facility emissions from 1945–2000, encompassing 10,600 PBq of releases of which 4,800 PBq remain. Monthly emissions from La Hague, the largest emitter by far, are published regularly, while emissions from Russian plants are more uncertain. The releases were fed into an ECHAM4 atmospheric transport model and found in good agreement with the measured background, although the northern hemisphere was systematically overestimated, and the southern hemisphere shows measurement spikes which cannot be attributed to known sources and might originate in isotope production. Agreement is especially good in the US, Japan and southern hemisphere, less so in Europe, where the signal fluctuation is high due to the vicinity of the La Hague and Sellafield reprocessing plants, and the coarse model resolution of $3.75^\circ \times 3.75^\circ$.

Ross (2010) has continued investigations into the global background using the more sophisticated ECHAM5 model and a better resolution. Particular attention has been paid to interhemispheric transport, which is delayed by an interhemispheric exchange

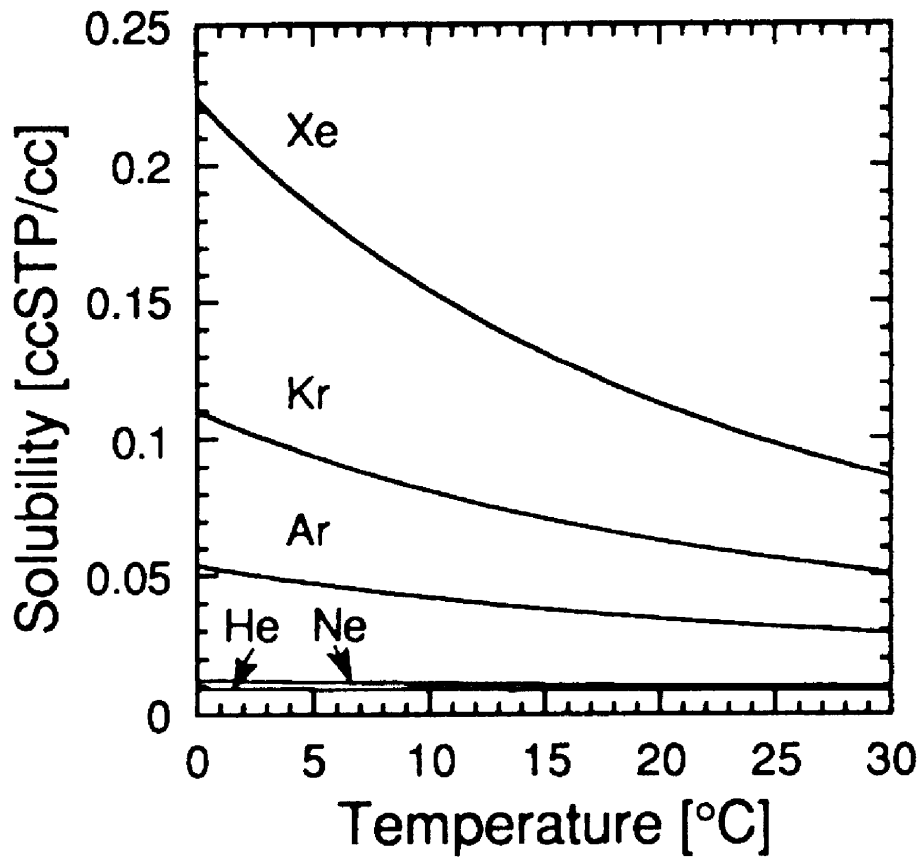


Figure 3.1.: Temperature dependence of the noble gas solubilities in distilled water (Stute and Schlosser, 1993).

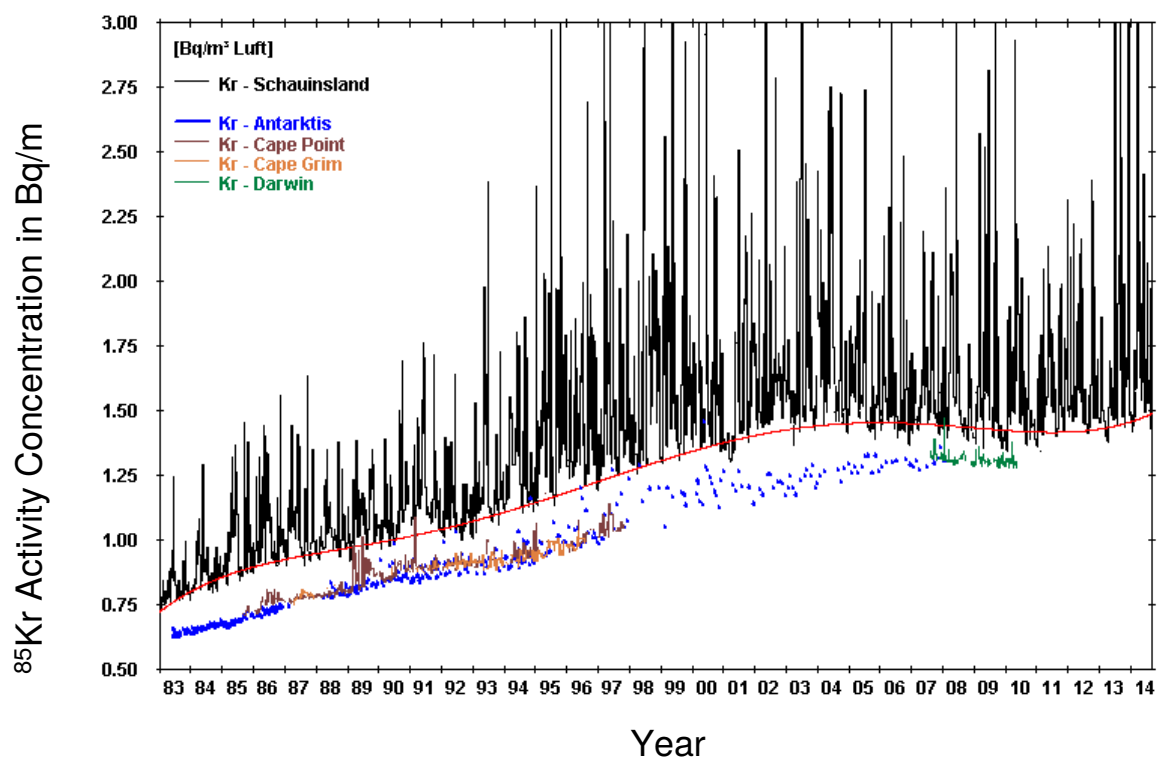


Figure 3.2.: Krypton-85 weekly measurements from 1983–2014 from several sampling stations operated by the German Federal Office for Radiation Protection, compiled by Schlosser and Klingberg (2014).

Source	amount [PBq]
Nuclear weapons Tests	111–185
Chernobyl (1986)	35
Fukushima (2011)	45
Natural	0.0009
Nuclear Reprocessing	~4750
Overall	~5000

Table 3.1.: Atmospheric inventory of krypton-85 from different sources in 2014, corrected for decay (Schlosser and Klingberg, 2014)

time of 10.5 months, meaning that the concentration in the southern hemisphere is lagging behind the northern hemisphere where most emitters are located, but is more smooth and stable. One important result of this work is a better understanding of the background variability in each region of the world, which is fundamental for a sound interpretation of Kr-85 measurements, be they for verification or environmental research purposes.

Efforts to build a comprehensive emission database of Kr-85 have been continued by Ahlswede et al. (2013), arriving at an atmospheric inventory of 5,500 PBq as of 2013. The major contributions originate from reprocessing, but other emissions have also been included. Isotope production facilities contribute up to 50 TBq/a, the largest emitters being “MDS Nordion” in Chalk River, Canada and “Institut des Radioéléments” in Fleurus, Belgium according to Saey (2009). The contribution of nuclear power reactors is rather small with 0.46 GBq/MW totalling in 0.39 TBq/a, the largest contributor being 17.2 TBq from the boiling water reactor “Dresden Nuclear Power Plant” in Illinois, USA. A breakdown of the sources of the current Kr-85 inventory is presented in Table 3.1.

3.2. Sampling networks and source location

When not isolated from the atmosphere, krypton will inadvertently disperse and spread beyond its point of origin. The long half-life of Kr-85 means that any atmospheric krypton detection may be polluted by other sources, potentially thousands of kilometres away. For this reason, any sample, be it intended for surveying the short or long range, has to undergo some considerations regarding attribution.

For on-site environmental sampling inside a facility or chimney yielding an extreme concentration, this may be trivial because only a local source is plausible, but commonly, air transport models are required with according degrees of sophistication.

For short ranges up to 50 km, simple Gaussian dispersion models can be applied, which calculate the concentration and point of touchdown simply based on chimney height, wind direction and atmospheric stability (Turner, 1970).

The application of Gaussian dispersion schemes for nuclear emissions has often been motivated by radiation protection and civil protection as well as research into atmospheric transport models. For example, Ferber et al. (1977) have monitored Kr-85 plumes emitted from the “National Reactor Testing Station” in Idaho, United States, using a network of 13 stations and collecting 2500 samples and compared the results with predictions from simple diffusion models. Although less samples were detected above background than was expected based on the models, emission clouds were detectable and it was concluded that Kr-85 was an excellent tracer within 100 km of the source, but barely affected the long distance concentrations in the midwest United States, about 1500–2500 km from the source. Still, some detections occurred up to 1000 km away.

A more recent investigation of near field detectability of krypton was conducted by Connan et al. (2013, 2014) for the reprocessing plant in La Hague, France. Emissions were so large that up to 20 km from the source, real-time measurements using gas proportional counters were possible, with concentrations reaching 500 Bq/(m³·min); samples further from the source were collected by their DIAPEG sampling system in 20 L bags. The discharge periods were known and lasted 30–45 minutes each. Both HYSPLIT and Gaussian plume models by Briggs (1973, 1985) were compared with the measurement results, which had been underestimated by the theoretical models. In particular, Kr-85 was detected very close, less than 500 m, to the source, which was unexpected on account of the 100 m stack height.

Emission measurements to systematically research Kr-85 for verification purposes have been conducted by Kalinowski et al. (2004) downwind of the Karlsruhe reprocessing plant (WAK) during a reprocessing campaign, with measurement stations up to 130 km away. Based on the resulting source-receptor sensitivity, they conclude that, given the local background variation, a plutonium production of 2 g per week is only detectable at a distance less than 1 km, while at 130 km, production rates larger than 1000 g per week are detectable.

Ross et al. (2009); Ross (2010) have conducted a much broader theoretical examination of detection probabilities for hypothetical emitters across the world using the HYSPLIT atmospheric transport model. They are assuming the production of one significant quantity of plutonium (8 kg) within 1 year, reprocessed in 50 dissolution campaigns, which is a realistic emission scheme for a covert weapons usable material production. The resulting emission of 3.2 TBq is well detectable in a catch-the-plume scenario within 24 hours, but almost impossible after 72 hours. In the follow up study, Klingberg et al. (2011) investigate the locatability of an emitter using small sampling networks of up to 5 stations, set up to monitor specific regions. In the chosen scen-

arios, the emitter could be located with a precision of less than 350 km in most cases. The overall conclusion is that while the capabilities of Kr-85 detection for safeguards have been underestimated by earlier reports such as IAEA-STR-351 (2006), a standing worldwide network of monitoring stations is indeed not feasible. Mid range surveillance of a region, on the other hand, could be effective, especially for repeated emissions.

A similar study has been conducted by Schoeppner and Glaser (2016), comparing the hypothetical emissions of processing plants of varying sizes and locations and comparing their effect with the background variability. Their results are compatible with the previous studies, concluding that Kr-85 emissions of any size will be detectable for 4 weeks at most. Regular batch emissions were assumed, although the emission profile only had a small effect. In most cases, the impact of the additional sources is much smaller than the deviation caused by regular reprocessing, and detection is somewhat feasible in the southern hemisphere, difficult in the northern hemisphere, and almost impossible in Europe.

All cited studies point to the fact that the attribution of Kr-85 emissions faces two major obstacles: a long half life which makes backtracking more difficult than for shorter lived radioisotopes, and a fluctuating background from civil sources which in some cases even precludes detection. These difficulties may be mitigated by reducing or better characterising background emissions, for example through a voluntary or mandatory declaration of emissions. As of yet, no major study has investigated the effect this might have on detection probability. However, it is likely that even given such in-depth knowledge of the background, a global sampling network of sufficient density is prohibitively expensive.

Kr-85 is therefore best suited for local, environmental grab sampling and catch-the-plume scenarios. Due to its volatility, it may also fill a role for “off-site on-site” sampling where for security reasons inspectors may not enter a facility, but are allowed to take samples in the vicinity to verify that no reprocessing is taking place. This could be accomplished even more effectively by small, local sampling networks surrounding a facility or region. For these tasks, a cheap and robust sampling method using small air samples is ideal.

3.3. Krypton measurement technologies

3.3.1. Radiometry

Krypton-85 has predominantly been measured radiometrically. It decays predominantly (99.57 %) through β -decay up to 687 keV, the average energy being 251 keV, without γ -emission. 0.43 % of atoms undergo β -decay with a maximum of 173 keV, followed by a 514 keV γ -emission (Levins et al., 1977).

Due to the long half-life of Kr-85, a certain amount is required for radiometric measurement. This is the case when one has direct access to the exhaust streams of a nuclear facility, which can be measured inline using high purity Ge gamma counters to measure the 514 keV line (Connan et al., 2014). To aid this process, the krypton can be concentrated by running the off gas through a delay track, e.g. a cooled, activated charcoal column.

To analyse trace concentrations of Kr-85, a larger amount of krypton needs to be collected and concentrated using sampling and preparation methods like those discussed in Section 3.4. For efficient detection of the more abundant β -decay path, the krypton should be mixed into a scintillation medium and introduced into a detector. This is commonly done by mixing the krypton with a counting gas, e. g. methane (Stockburger et al., 1977; Loosli et al., 1999). Momoshima et al. (2010) are solving the krypton in p-xylene with 0.4 % 2,5-diphenyloazole and mixing it with a liquid scintillator.

In any case, several μL of krypton are required to measure the atmospheric concentration of Kr-85 within several days in a low-background laboratory.

3.3.2. Atom trap trace analysis

A new method for measuring trace amounts of krypton-85 is atom trap trace analysis: krypton atoms are cooled and captured using magneto-optical traps in varying setups, and counted by detecting their fluorescence. The feasibility of trapping krypton atoms was first demonstrated by Chen et al. (1999).

3.3.2.1. Optical cooling basics

The main process at work is called “Doppler cooling”, in which a laser is aimed at an atom which corresponds in wavelength to an electronic transition of that atom, but is slightly detuned towards a higher wavelength. If the atom travels towards the laser, it is able to absorb a photon due to the Doppler Effect, transitioning to the higher energy state and also receiving the momentum of that photon. When the atom drops back to the base state, it emits a photon in a random direction, and can be excited again. The atom is slowed down because it receives a net momentum opposite to its direction of movement (Metcalf and van der Straten, 1999).

3.3.2.2. Creating metastable states

As the ground state of the krypton atom is not suitable for laser cooling techniques using available laser wavelengths, they must be excited to the $5s[3/2]_2$ metastable state, which has a half life of 40 s.

Most atom trap trace analysis implementations achieve this metastable state by generating a radio-frequency driven plasma to produce a diverging beam of excited atoms. One drawback is the production of ionised atoms in the plasma which are implanted into the walls of the vacuum chamber, leading to cross contamination which can only be mitigated by flushing the vacuum chamber with xenon for 36 hours (Jiang et al., 2012).

Currently optical excitation schemes are in development which do not produce ions and are therefore not subject to the aforementioned cross contamination, and have the potential to achieve smaller sample sizes and faster processing times. Daerr et al. (2011) have developed a vacuum ultraviolet lamp which is able to excite krypton atoms into the required states. Kohler et al. (2014) have successfully demonstrated its use for Kr-84 and Kr-83 in their atom trap trace analysis.

3.3.2.3. Atom trap trace analysis capabilities

The cooling and trapping mechanisms used in atom trap trace analysis are highly selective and therefore resistant to interference by other isotopes or elements. At the moment, 5–10 μL are sufficient for measurement, but pending improvements in the excitation schemes will enable the analysis of much smaller samples. Currently, one measurement takes about 2 days, but improved memory effect correction methods will improve this number, and optical excitation has the potential to eliminate memory effect altogether and allow for measurement within a few hours.

3.4. Prior krypton separation methods

Several existing krypton separation facilities are introduced in this section, and compared regarding their capabilities.

3.4.1. German Federal Office for Radiation Protection

The German Federal Office for Radiation Protection (BfS) is collecting approximately 600 samples per year using a well established procedure with a sample loss rate of less than 1 % (Sartorius et al., 2002).

Most samples are weekly samples taken using a large (1000 mL) activated charcoal adsorber submerged in liquid nitrogen. For one week, ambient air is pumped through the adsorber at a low pressure of 500 mbar to prevent excessive O_2 and N_2 accumulation. After one week and 10 m^3 of sampled air, the column is thawed to remove water, CO_2 , N_2 and O_2 and heated to desorb the Kr into a 1 L aluminum minican which is sent to the laboratory in Freiburg, Germany for measurement.

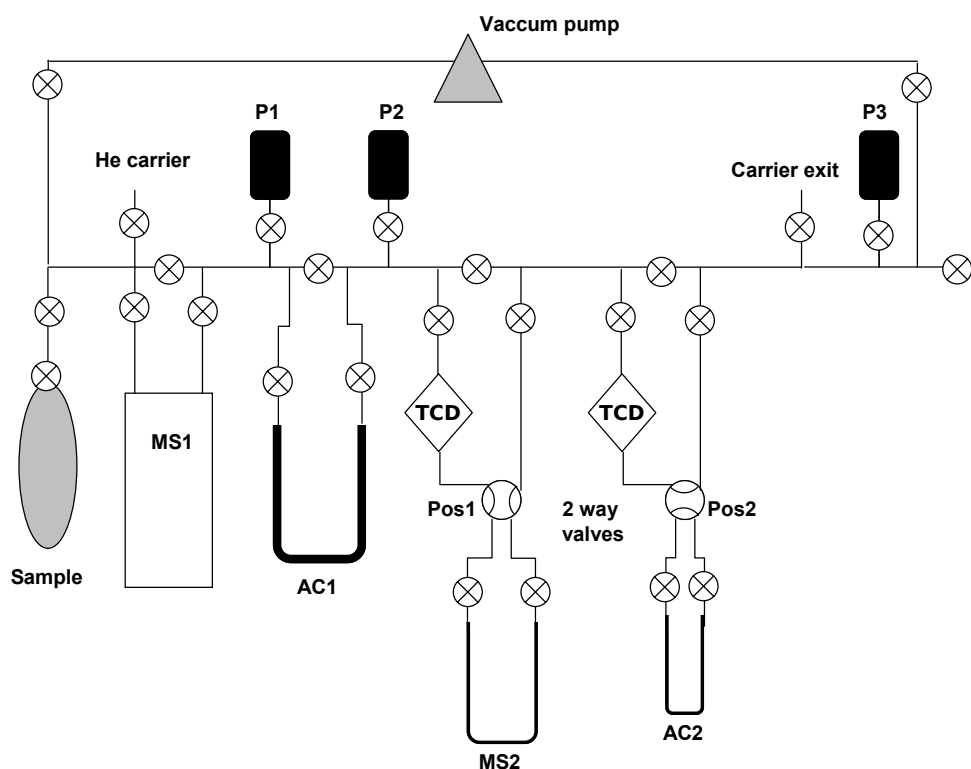


Figure 3.3.: The EFA (Edelgas Fraktionierungs-Anlage; *german*: Noble Gas Separation Facility) used at Uni Bern for separating the krypton fraction from gas samples (Purtschert et al., 2009).

In the laboratory, more CO₂ and H₂O are removed using alkali-wet columns and silica gel before gas chromatography is initiated using a methane carrier gas and two columns, one charcoal and one molecular sieve (Stockburger et al., 1977).

The finished sample is then measured using β -counting, and its volume determined using a gas chromatograph. The xenon content is also extracted and measured.

3.4.2. University of Bern

The “Edelgas-Fraktionierungs-Anlage” (noble gas separation facility, “EFA”) at the University of Bern is used for the routine separation of krypton from air or water samples with varying composition. It is portrayed in detail because it served as a conceptual basis for the development of the separation line in this thesis. Its layout is shown in Figure 3.3.

Before entering the EFA, ground water samples have to undergo degassing and pass a copper-lined furnace to reduce the elevated methane content. Afterwards, the sample is connected to the EFA in a rigid container. It is then passing molecular sieve

MS1 for desiccation and drawn onto the large 77 K charcoal trap AC1 while pumping on the far end. The entrance of AC1 is then closed and cooling is removed for a short time, thereby releasing much of the N₂ without losing much krypton. After cooling it back down, the process is repeated.

Now, a He carrier stream is established, running through AC1 as it is thawed to room temperature again, and the effluent carrier stream is monitored using a thermal conductivity detector. Two large peaks can be observed passing the thermal conductivity detector, N₂ and Ar. At this point, the carrier is redirected through 5 Å molecular sieve column MS2, which is also cooled. The Kr peak is now passing the thermal conductivity detector, too small to be visible, and frozen on MS2.

The same process is repeated to move the sample from MS2 to the final charcoal trap AC2. Passing through MS2 will separate the remaining sample into three peaks, Ar, Kr and CH₄, which are clearly visible in the second thermal conductivity detector.

AC2 is then disconnected and carried over to a gas chromatograph containing another 5 Å molecular sieve column as a last separation step, and to determine the yield by integrating the Kr peak. The purified sample is now mixed with counting gas and filled into a counting tube for radiometric measurement.

The separation yield of the EFA depends on the sample volume. For 10 L or more, an experienced operator will achieve a yield of around 75 %. When the author of this thesis visited Bern University, several attempts have been made at separating a 1 L sample using the same procedure, but no detectable yield was achieved. A sample of 3.3 L has resulted in a yield of 29 %, with an estimated purity of 7 %.

3.4.3. Yokochi

A purification method directly aimed at preparing samples for atom trap trace analysis has been developed by Yokochi et al. (2008).

It starts off by cryogenic distillation, compressing the sample into a container at liquid nitrogen temperature and then pumping the gaseous phase out of the container for some time. The vacuum pressure of Kr is lower than that of the other air components, so the sample is enriched considerably. Afterwards, the residual sample is boiled and sent into an activated charcoal trap at 77 K. From there, a He carrier is used to send it through an activated charcoal column, 6 mm by 180 cm, at room temperature to separate Kr and CH₄ from the rest of the sample. Next, the sample passes a 5 Å molecular sieve column to separate Kr and CH₄ by monitoring the output on a quadrupole mass spectrometer and sending the Kr peak to a final charcoal trap. Now the sample is released by heating the trap and exposing it to a titanium sponge getter to remove the remaining N₂ and O₂ impurities.

This method works for a sample size of 5–125 L of air, providing a 90 % yield with 98 % purity, achieved within 6 hours, although 4.5 hours are also feasible if a reduced

yield is acceptable. Due to the cryogenic distillation, gases extracted from water can be used without prior treatment.

3.4.4. Yang

Yang et al. (2015) employ a method very similar to that of Yokochi et al. (2008) for even smaller gas samples, also aimed at sample preparation for atom trap trace analysis. They are starting of with the same cryogenic distillation process, before using a He carrier to move the sample through a furnace for removing N₂, O₂ and hydrocarbons, then a 2 m long 5 Å molecular sieve column and catch it in a trap. To remove the remaining impurities, mainly N₂, the sample can be recirculated and pass the chromatography column several times.

The yield of this system is reported at 90 % for 20 L samples, and 73 % for 1 L. The exact purity is not stated, but a constant contamination of 0.5 µL of Ar is observed, probably due to a leak from ambient air.

3.4.5. Tu

In the setup by Tu et al. (2014), the air sample is also condensed into a frozen charcoal trap. After pumping out the bulk of gaseous nitrogen and oxygen from the trap, constraining the flow with a mass flow controller, a 10 L air sample is reduced to about 0.1 L. If the residue is large due to a high CH₄ content, it is passed through a CuO furnace. Otherwise, the trap will be heated and the sample is expanded into a volume containing a titanium getter for further purification. Then, after freezing it onto another charcoal trap, it undergoes chromatography in a 2 m 5 Å molecular sieve column using a He carrier, which may be repeated by recirculating the gas.

The process takes 3–4 hours and the reported yield is 90–97 %, measured indirectly using a quadrupole mass spectrometer, even for samples as small as 1 L. A constant Ar amount of 0.5 µL is contained just as described by Yang et al. (2015), but Tu et al. (2014) attribute this to the Ar tail in the Kr peak during chromatography.

3.4.6. Yokochi 2016

Parallel to this thesis, Yokochi (2016) has refined the method introduced in Yokochi et al. (2008) to be faster and applicable to smaller gas samples. The main component of the separation is a single activated charcoal column at 138 K responsible for capture, desorption and chromatography of the air sample. Afterwards, two optional separation columns and a getter are used to further purify the sample depending on its anticipated composition. Within 75 minutes excluding regeneration, > 90 % yield and 99 % purity are achieved for sample sizes ranging from 1.2 – 26.8 L. We will see

that this process is very similar to the one established in this thesis, albeit slightly more complex and not automated.

3.5. Adsorbents for Krypton

Adsorbents are usually porous materials with a high internal surface area on which adsorption can take place. They are characterised by the size and distribution of micropores (ca. 1 nm) which form the bulk of the surface, mesopores (ca. 10 nm) and macropores (> 50 nm) which enable a fast transport of the adsorbate in and out of the adsorbent. Zeolite molecular sieves and activated charcoal are the most common adsorbents for gas chromatography. While being selective towards different gas species, none of these adsorbents will alter the isotopic ratios of heavy noble gases (Bernatowicz and Podosek, 1986).

3.5.1. Zeolite molecular sieves

Molecular sieves are porous materials with a relatively uniform pore size. There are numerous types commercially available, mostly used for filtering gases and fluids by adsorption of specific components, but also for chromatography. A common material are zeolites, a group of aluminosilicate minerals which occur naturally in numerous forms but can also be synthesised with varying properties.

Two types are of particular interest for krypton purification. Molecular sieve with a 4 Å pore diameter is well suited for desiccating the gas stream by adsorbing H₂O, CO₂ and several smaller hydrocarbons, although not methane. It is heat resistant and can be regenerated using high temperatures.

5 Å molecular sieve is suited for chromatography or air components. The heats of adsorption for zeolites increase in the order Ar < O₂ < Kr < N₂ ≈ CH₄ < CO₂, which is not to say that gases are separated in that order, as separative power also depends on temperature as illustrated in Figure 3.4. Using a 5 Å sieve, Kr can easily be separated from CH₄, but is difficult to separate from N₂, especially when the latter is abundant.

3.5.2. Activated charcoal

Activated charcoal is produced from organic materials like coal, turf or nutshells by gaseous or chemical activation resulting in most components except the carbon being removed. The activation process forms a pore network of differing properties depending on the method, determining properties like porosity, pore size distribution and surface per volume.

Pore sizes are usually less uniform than in inorganic molecular sieves, with the majority of pores in the range of a few Å (Figure 3.5). Within these small pores, the

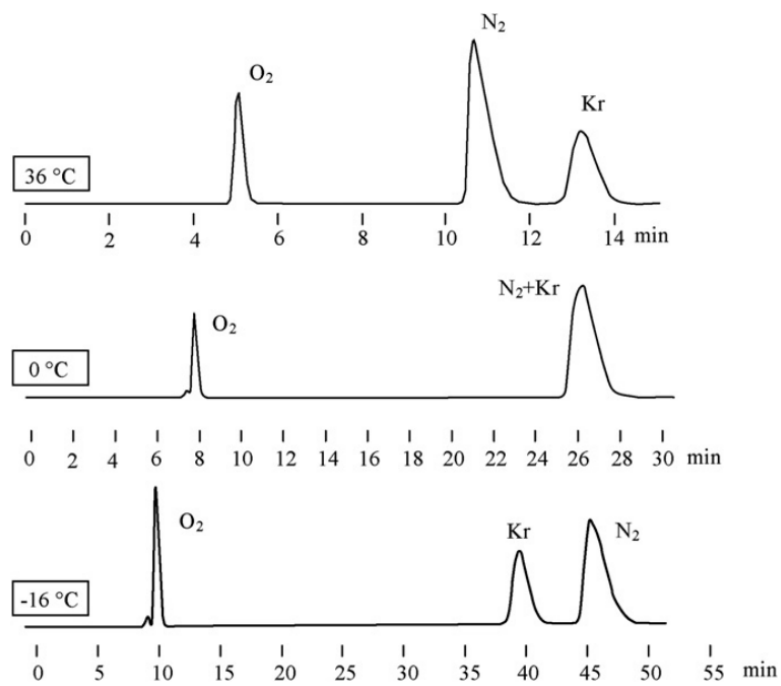


Figure 3.4.: Chromatographic separation of oxygen, nitrogen and Krypton on a column containing 30–60-mesh molecular sieve 5 Å at different temperatures (Moshima et al., 2010).

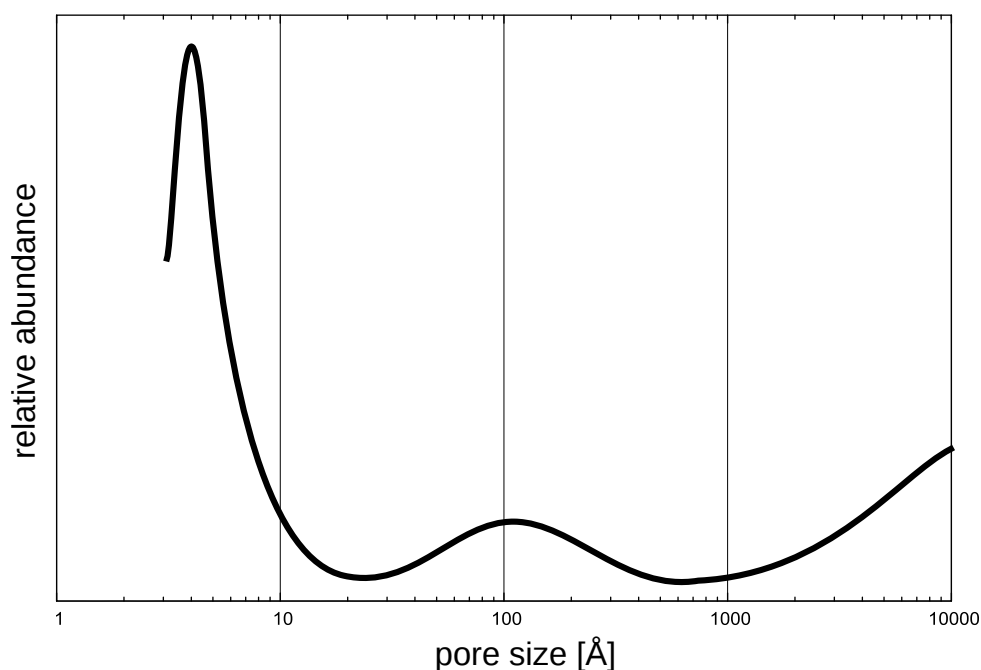


Figure 3.5.: Relative pore size distribution of one type of activated charcoal (Simgen, 2003).

adsorbate atoms are subject to attractive forces from two or more walls at once, which makes them the primary sites for adsorption while the larger pores serve as an entry path.

Activated charcoal adsorbents often adhere to the Gurvitsch Rule, which states that the maximum amount, expressed in equivalent liquid volume, adsorbed by a porous adsorbent is independent of the adsorptive. Exceptions can be due to a sieving effect where pore sizes are too small for some molecules to penetrate. There are more complex cases such as water, which tends to occupy a lower maximum micropore volume despite being a relatively small molecule (Carrott, 1995).

One subset of activated charcoals are carbon molecular sieves, commonly defined by their molecular sieving properties due to a much smaller average pore size. Whereas activated charcoals separate adsorbents based on their differing adsorption equilibria, the separation in carbon molecular sieves is mostly governed by differing rates of adsorption (Mieville and Robinson, 2010). This makes them particularly suitable for pressure swing adsorption, which is a major commercial application of carbon molecular sieves for nitrogen separation from air, mainly useful for bulk quantities and not suited for small sample sizes of high purity.

The adsorption in charcoal is governed by van-der-Waals interactions only, and dipole interactions will not help to separate gas species with similar molecular weights,

such as N₂/O₂ and Ar. Kr, however, is strongly selected over all other air components except CH₄, whose adsorption characteristics on charcoal are similar at all temperatures.

A multitude of different types of activated charcoal are commercially available, offering a variation of adsorption characteristics. Comparisons as conducted by Munkata et al. (1999, 2000, 2006, 2008) suggest that krypton adsorption properties do not differ strongly between investigated products.

3.5.3. Novel materials

Adsorbents play a key role in many industrial processes, and novel sorbents are in particular demand by the energy industry to purify or store fuels.

For example, super-activated carbon and activated carbon fibers are being investigated for vehicular storage of methane fuel, and π -complexion sorbents¹ for purification of fuels intended for fuel cells (Yang, 2003).

3.5.3.1. Metal organic frameworks

Candidates for H₂ storage are carbon nanotubes and metal organic frameworks, which have some potential for Kr retention, as do periodic mesoporous organosilica. Conclusive experimental data regarding krypton sorption was only found for metal organic frameworks.

Metal organic frameworks are a novel class of porous materials consisting of metal ions or clusters linked by organic polymers. These materials possess a very large surface area (up to 6000 m²/g) and can be synthesised to offer diverse properties, in particular pore sizes and adsorption properties. At the moment, they are primarily considered for storage purposes, for example in hydrogen tanks. There has been research into their properties regarding noble gas adsorption (Fischer, 2011), hinting at a large adsorption capacity, especially for metal organic frameworks possessing an increased amount of metal sites such as NiDOBDC². Thallapally et al. (2012) have investigated this material and found a superior selectivity of Xe over Kr compared to activated carbon, but not for Kr over nitrogen. Other studies regarding metal organic frameworks for noble gas purification were not available at the time of writing.

When separating krypton for atom trap trace analysis, xenon impurities are small and not an issue, so it is not yet clear whether a metal organic framework is available that performs superior to activated charcoal and zeolite for this task. The investigation of metal organic frameworks is beyond the scope of this work, but the field is advancing quickly and may offer adsorbents of interest in the future.

¹such as Cu(I)Y, AgY for sulfur removal from gasoline; CuCl/ γ -Al₂O₃, CuY, AgY for CO removal from H₂ (Yang, 2003)

²Nickel nitrate with the organic linker 2,5-dihydroxyterephthalic acid.

3.5.4. Ideal adsorbent for krypton separation

Based on these considerations, activated charcoal is the superior adsorbent for the task at hand. It separates Kr from all other air components except CH₄, which is not abundant in air samples and can be removed using a getter or a separate 5 Å molecular sieve column.

4. Constructing an automated krypton separation line

In this Chapter, the development cycle of the krypton separation line “Krypton-Abtrennungs-Anlage (KAA)” is described in detail. After outlining design requirements in Section 4.1, the reasoning and development behind the different components are presented in Section 4.2. The resulting set-up, separation routine and experiments to improve its performance make up Section 4.3. Actual evaluation and performance characterisation of the separation line follow in Chapter 5.

4.1. Requirements for krypton separation

The krypton separation facility is intended for the routine preparation of samples for the atom trap trace analysis developed in the same laboratory¹, resulting in some particular requirements.

4.1.1. Sample size

The atom trap trace analysis is intended to process high purity krypton samples of about 1 μL , however the required volume for an effective measurement is not yet known. The corresponding amount of 1 L of atmospheric air is well suited for routine sampling in the field. While 100 % extraction efficiency from this target sample volume will be pursued from the beginning, the separation procedure should allow for larger sample volumes to provide headroom in case either the extraction or measurement procedure turns out less efficient than anticipated.

To account for the small sample size, one design goal is to keep the separation line compact and avoid unnecessary steps, especially freezing and thawing. A small overall volume reduces the potential for krypton loss.

¹For a detailed description of the atom trap trace analysis technique, please refer to Section 3.3.2.

4.1.2. Sample purity

While the magneto optical trap itself is tolerant of a considerable degree of sample impurities (Yang et al., 2015), the optical excitation scheme employed at the University of Hamburg's atom trap trace analysis imposes some additional limitations.

A novel type of vacuum ultra violet (VUV) lamp is used to excite krypton atoms into the metastable state required for cooling. The transmission windows are made of magnesium fluoride (MgF_2), which is subject to continuous decline of transmissivity caused by the formation of colour centres during use as well as adsorption of water, oxygen, carbon dioxide and hydrocarbons, particularly methane (Daerr et al., 2011; Kohler, 2011). Steps were taken in the VUV lamp's design to minimize contamination of the lamp gas, but a krypton sample contaminated with water, oxygen or hydrocarbons may still cause an accelerated deterioration. To avoid a regular replacement of the MgF_2 windows, the krypton sample should be thoroughly rid of any reactive components, whereas an elevated content of noble gases such as argon or helium is not problematic. In fact, an atom trap trace analysis is still possible with considerable Ar content (Yang et al., 2015).

4.1.3. Automation

Another important requirement is the automation of the separation in order to save personnel and allow for a high sample throughput. Apart from the selection of appropriate components, this has some implications on the separation procedure itself.

As laid out in Section 3.4, existing noble gas separation techniques often require human operators to precisely regulate parameters or perform certain actions dependent on their own observations and experience, resulting in complex instructions which can be difficult to implement in an automated procedure, covering all eventualities during every step. Instead, the procedure should be robust enough to work despite varying circumstances such as sample size and composition, moisture, ambient temperature, and other parameters which may influence the duration of each step in the separation.

Consequently, all conditional instructions should be kept simple to be easily updated without the need to write complex programming subroutines whenever a step in the separation is to be changed.

Previous separation methods do employ the precise manual handling of metering valves to some degree. High performance automated metering valves are expensive and require a complex technical implementation to operate compared to valves only supporting a binary on/off setting, so the separation procedure should be implemented using mainly the latter.

Finally, the automation is to be implemented in the National Instruments LabView environment, which is an established standard in industry and research and provides

a multitude of interfaces to integrate most available hardware.

4.1.4. Flexibility and upgrades

Despite being intended for routine sample processing, the apparatus will also be under frequent development until final, so a modular design is key to remodelling, optimising configurations and performing experiments. Beyond the scope of this work, the separation line may also be used for processing samples with a composition notably different from air, for example from ground water, and must allow for necessary additions.

To provide enough information for evaluation and redesign, all accessible parameters and measurement data should be collected and logged for every sample, if only as state of health parameters or for later diagnosis.

4.1.5. Duration and sample throughput rate

Automation alone will save considerable working time in the laboratory. In addition, the separation will have to keep pace with the time required for one atom trap trace analysis measurement. The vacuum ultra violet excitation mechanism will eliminate memory effect in the vacuum chamber, and the current projection is that one sample will require a measurement time of 3–4 hours. While this is achieved in existing measurement methods such as Yokochi et al. (2008), a complete separation cycle notably includes regeneration of all traps, getters and chromatography columns. This requires baking the parts for some time until all residual gases are removed, as well as cooling everything to prepare for the next sample, which can take hours especially for large reservoirs of charcoal.

The target duration of the whole procedure will be two hours: one hour for separation, and another hour for regeneration. Ideally, this will enable the continuous supply of two atom trap trace analysis facilities running in parallel.

4.1.6. Design goals

The preceding considerations arrive at the following design goals, which will be frequently referenced in the following sections:

- allow for sample sizes ranging from 1–5 L
- achieve sufficient yield to provide 1 μL of krypton for measurement
- minimise the number of dead volumes to avoid krypton loss
- completely eliminate H_2O , O_2 , CO_2 and hydrocarbons

- automate the procedure as much as possible
- enable easy reprogramming
- implement modular design
- record state of health parameters
- reduce the time of one separation cycle below 2 hours

4.2. Development of separation line elements

While based on previous krypton extraction methods, the krypton separation line and its major components have been developed from the ground up. This section describes the most important features of the separation line, as well as the reasoning and experiments leading to their realisation.

In case a component's role is unclear, the reader is advised to first study the complete layout of the separation line in Section 4.3.1.

4.2.1. Sample entry

This section discusses which sample container and method is suitable for inserting the air sample into the separation line and freeze it onto the separation column which also functions as a cryotrap.

4.2.1.1. Desiccation

When using cryotrap for chromatography, it is important to dry the sample to avoid water ice accumulating blocking the entry of the column.

Freeze drying Drying can be performed using a freezing trap before the actual charcoal cryotrap. Such a trap must operate at a temperature low enough to freeze the water, but high enough to avoid the adsorption of krypton. In an experiment, a stainless steel vessel submerged in liquid nitrogen (77 K) was adsorbing krypton almost completely, which agrees with experiments conducted by Lott (2001).

A freezing trap can also be cooled using dry ice submerged in ethanol to reach a temperature of 195 K, where no krypton is adsorbed. Thermoelectric cooling methods are also an option.

Despite not requiring a precise temperature control, the fact that the temperature needs to be controlled at all makes freeze drying cumbersome when compared to room temperature drying agents.

Molecular sieve One suitable drying agent is a zeolite molecular sieve with a pore size of 4 Å (MS4A). It will adsorb water, but also CO₂ at room temperature while not retaining noble gases like krypton. It can also easily be regenerated by baking.

To build such a trap, a stainless steel vessel of 250 cm³ has been filled with MS4A and wrapped with heating wires and aluminium foil. This high volume enables to process a number of samples before requiring regeneration. Regeneration itself is a time consuming process, the trap is bulky and takes some time to heat up to 300 °C, and much longer to cool down again, requiring a heating cycle of at least 2 hours before the trap can be used again. This can be done overnight after processing samples throughout the day.

This trap is successfully used in the final separation line.

4.2.1.2. Dust protection

It was found out that the MS4A was emitting dust that had damaged some of the valves by burrowing into the PCTFE stem tip. To avoid this in the future, sintered metal filters with a pore size of 0.5 µm have been introduced at both ends of the MS4A volume. This provides for an enhanced flow resistance, which has its benefits (see Section 4.2.4), but also makes it more difficult to evacuate a large gas volume: whereas small gases like Helium are evacuated quickly, completely removing an atmosphere of N₂ from the vessel takes several minutes (see Figure 4.1).

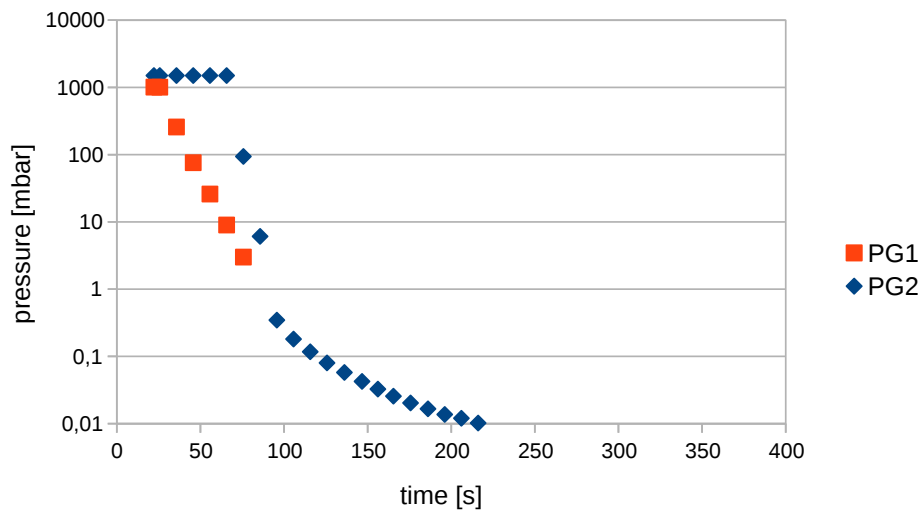
4.2.1.3. Injection

The first step of the separation procedure is the injection of the sample into the separation line. In the EFA at University of Bern and similar experiments, this is done by attaching a fixed volume sample container, such as a steel bottle, to the separation line and opening a charcoal cryotrap cooled to 77 K, while pumping on the far side of the trap. The vacuum will draw the sample in, which, entering the trap, will be adsorbed.

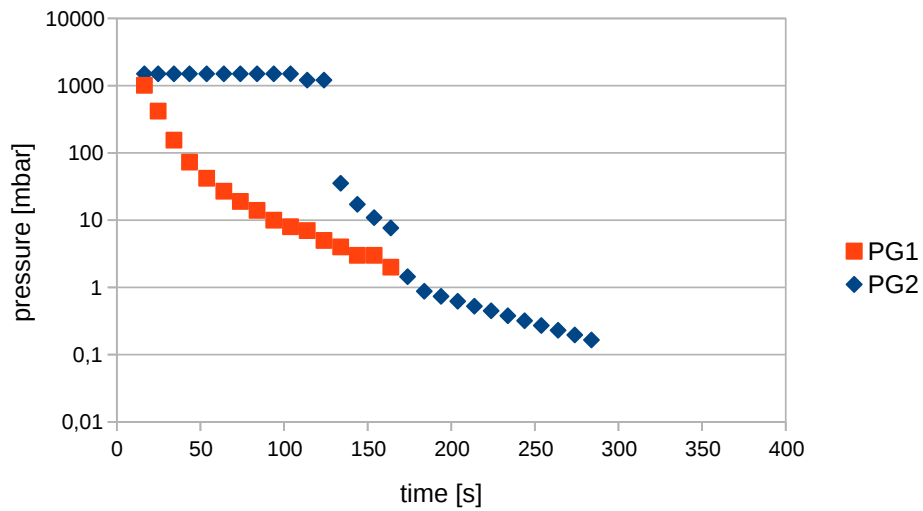
The above method works for large cryotrap with a low flow resistance, but shows its limits when using a narrow, high resistance trap such as the 6 mm chromatographic charcoal column described in Section 4.2.4. When the remaining sample pressure falls below 50 mbar, the gradient is not sufficient to drive the gas onto the charcoal within a reasonable amount of time, which is shown in Figure 4.2, corresponding to a 5 % sample loss, which would be unacceptable. For the EFA, the pressure falls below 10 mbar within 20 minutes, corresponding to 99 % of a sample.

In this section, several measures to avoid this loss are examined.

Container flushing When the pressure has dropped, the container could be flooded with helium and then evacuated again. Depending on how much the pressure is



(a) Pressure reduction when pumping pure helium.



(b) Pressure reduction when pumping pure nitrogen.

Figure 4.1.: The gas pressure reduction when trying to evacuate different gases from the MS4A moisture trap of the krypton separation line for several minutes. For pressures above 1 mbar, the membrane gauge (PG1) is more accurate than the pirani gauge (PG2). The evacuation speed is inhibited by the flow release from the molecular sieve pores, but also the sintered metal filters.

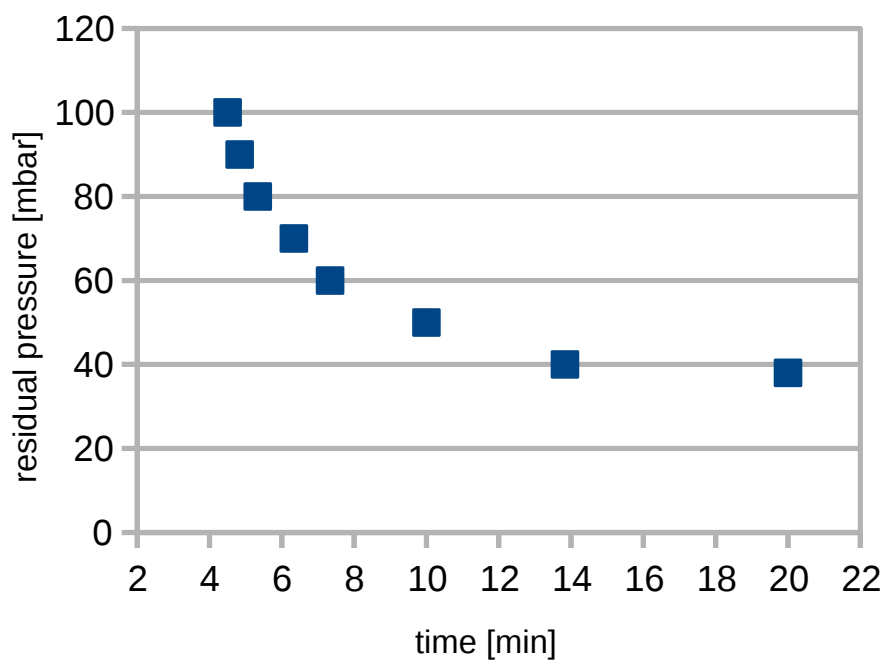


Figure 4.2.: When drawing a nitrogen sample from a fixed volume onto a 6 mm activated carbon trap, the residual pressure will not reach zero due to the decreasing pressure gradient and high flow resistance.

lowered, the procedure has to be repeated a number of times to completely flush out the remaining sample. A good compromise between number of flushes and pumping time per flush can be determined experimentally.

Alternatively, a pass-through container with an inlet and an outlet can be used. That way, the helium carrier can be used to flush the sample directly onto the cryotrap. This procedure was tested using a 250 cm³ vessel filled with argon and a quadrupole mass spectrometer to detect how quickly the Ar content of the exit stream would be depleted. The result was promising, as with a He flow of 0.5 L/min, 99 % of the Ar was purged from the vessel within 30 seconds. To further reduce the flushing time, an inlay may be constructed to parallelise the current and reduce turbulence, similar to a catalytic converter. These measures, however, would yield a very complex and specialised sampling vessel.

Compressor pump A pump between sampling container and cryotrap could be used to compress the sample, forcing it onto the trap. This method was successfully tested with a Pfeiffer MVP 015-4 diaphragm pump². Rotary pumps in which the sample comes in contact with oil are not advised, as the sample may be contaminated with hydrocarbons.

Sampling bags Another practical solution is the use of sampling bags instead of rigid containers, letting the ambient pressure force the sample into the cryotrap. This method is technically the least complex and compatible with efforts at the ZNF to use bags for its automated sampling unit.

Although most of the initial experiments were conducted using an inline vessel and compressor pump, the final separation line is employing sampling bags as described in Section 4.2.2.

4.2.2. Air sampling bags

Air samples at the ZNF are contained in custom-made compound foil bags with a self-sealing coupling. These bags are lightweight and sufficiently airtight for storing samples for several weeks or months (Göring, 2014).

Other sampling containers can be connected. If the container is not compressible, the sample intake will have to be modified to account for the sinking sample pressure slowing the sample intake down.

²This type of pump is actually not designed as a compressor. A flow limiter was employed to avoid building up a pressure above 1 atm at the pump exit.

4.2.3. Surveillance via quadrupole mass spectrometry

A Pfeiffer QMA220 quadrupole mass spectrometer is used to monitor all experiments, as well as the ongoing separation procedure, and is also handy for rest gas analysis in order to diagnose leaks and residue in the vacuum system as it is being constructed.

4.2.3.1. Comparison with thermal conductivity detector

Another common instrument for monitoring chromatography columns is the thermal conductivity detector, which will not discriminate but only show the amount of gas leaving the column at any given time. The principal advantage of a quadrupole mass spectrometer is the ability to discriminate between gas components, enabling to identify whether a peak consists solely of a certain gas species or has others overlapping. Very small peaks of certain species may also be visible in a quadrupole mass spectrometer, but not observed above the baseline of a thermal conductivity detector.

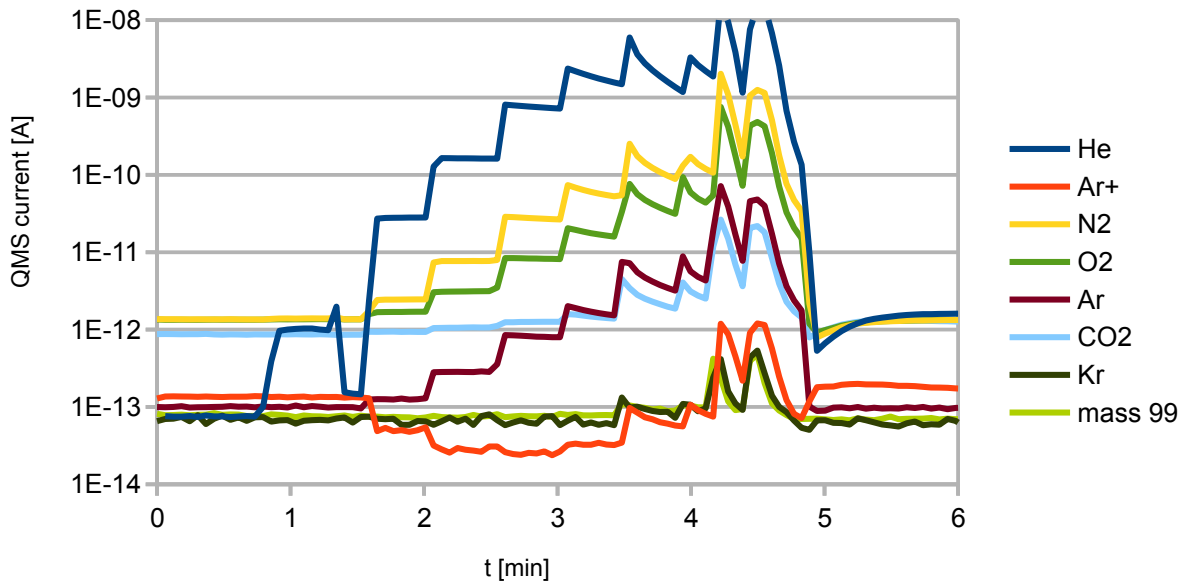
Measurements in a quadrupole mass spectrometer are generally less robust and reproducible: the results depend on the temperature and degradation of the filament used to ionise the gas components, which are constantly changing. For a precise measurement, the quadrupole mass spectrometer must be warmed up for hours and calibrated every time. More importantly, for high pressures, the signals for the different gas species are not independent, as is demonstrated in Figure 4.3. This shows that while the quadrupole mass spectrometer currents provide useful hints as to what species are present in the gas stream, they do not allow for precise, quantitative measurements.

4.2.3.2. Monitoring the gas stream

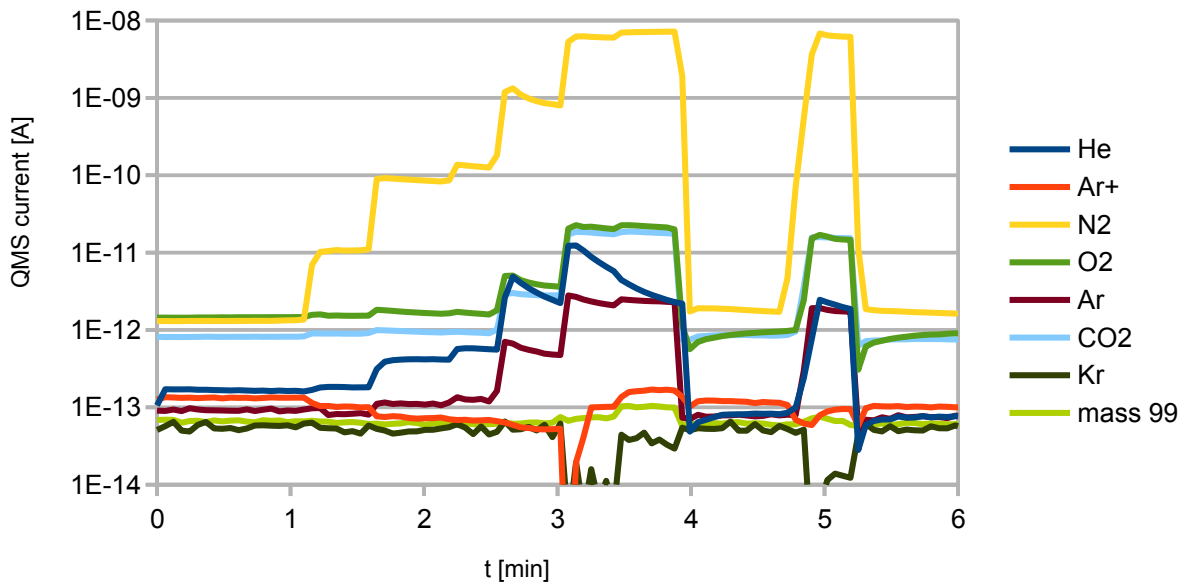
Quadrupole mass spectrometers generally offer two main modes of data preparation. In “multiple ion detection” mode (MID), the currents detected for each mass are detected directly and displayed in units of Ampere. The signal strength is attenuated by the background pressure in the measurement volume as well as the ionisation properties of the respective gas species, thus it does not correctly project the absolute amount and ratios.

The “multiple concentration detection” mode (MCD) uses a gas specific calibration matrix (GSC) to derive the actual composition of the gas. For added precision, and to account for the problem of mass peaks containing components from several species, several peaks per species can be included in the gas specific calibration matrix, such as the double ionisation peak³ accompanying each mass. An multiple concentration

³A quadrupole mass spectrometer does not directly measure mass, but rather the mass-charge-ratio of each ion. A fraction of the ionised molecules will carry two (or more) charges, and accordingly detected as if it had half (or less) the mass.



(a) Fluctuations induced by a varying He concentration.



(b) Fluctuations induced by a varying N₂ concentration.

Figure 4.3.: Background-induced fluctuations of partial pressure during quadrupole mass spectrometer measurement. Mass 99 is definitely not present in the quadrupole mass spectrometer chamber and measured to test whether the effect is inherent to the quadrupole mass spectrometer.

detection is only accurate when performed under similar conditions as the calibration, especially concerning the pressure and composition of the gas.

For monitoring the continuous gas stream of a chromatographic procedure, an multiple ion detection measurement is more suitable where the operator can directly observe the fluctuations of each species. In this thesis, all chromatographs logged to illustrate the separation procedures are multiple ion detection measurements.

4.2.3.3. Capillary connection

The gas stream will contain a pressure above atmosphere during the separation, whereas in a quadrupole mass spectrometer chamber the pressure must not exceed 10^{-4} mbar. This is ensured by connecting separation line and quadrupole mass spectrometer with a capillary, referred to as *differential pump*.

Two types of capillaries are widely available and suitable for this purpose. Capillaries made from quartz glass are most commonly used. In the krypton separation line, a stainless steel capillary with an inner diameter of 100 μm is employed. Quartz capillaries are available in smaller diameters and have a smaller error in inner diameter, and are relatively easy to cut using razors. Steel capillaries, on the other hand, have an inner diameter variation of up to 10 %, but are less brittle, can be connected to leak tight $1/16''$ Swagelok fittings and are resistant to high temperatures occurring during baking.

Capillary length The high inner diameter requires the stainless steel capillary to be relatively long in order to achieve the required pressure reduction factor of 10^9 (i. e. from $1.5 \cdot 10^3$ mbar to 10^{-5} mbar). The required length has been approximated using the law of Hagen-Poiseuille (Jousten et al., 2006):

$$\dot{V} = \frac{\pi r^4 \Delta p}{8\eta l}$$

where \dot{V} is the volumetric flow rate, r is the radius, η is the dynamic fluid viscosity⁴, Δp is the pressure difference and l is the length of the capillary. For a compressible ideal gas, for which the volumetric flow rate is not constant along the capillary, a corrected flow rate can be derived:

$$\dot{V} = \frac{\pi r^4}{16\eta l} \left(\frac{p_i^2 - p_o^2}{p_o^2} \right) \quad (4.1)$$

with pressures p_i and p_o on each end of the capillary (Jousten et al., 2006). With the help of Equation 4.1, the required length of the capillary can be approximated by

⁴For air: 18.6 $\mu\text{Pa}\cdot\text{s}$ at 300K (Lide, 2005)

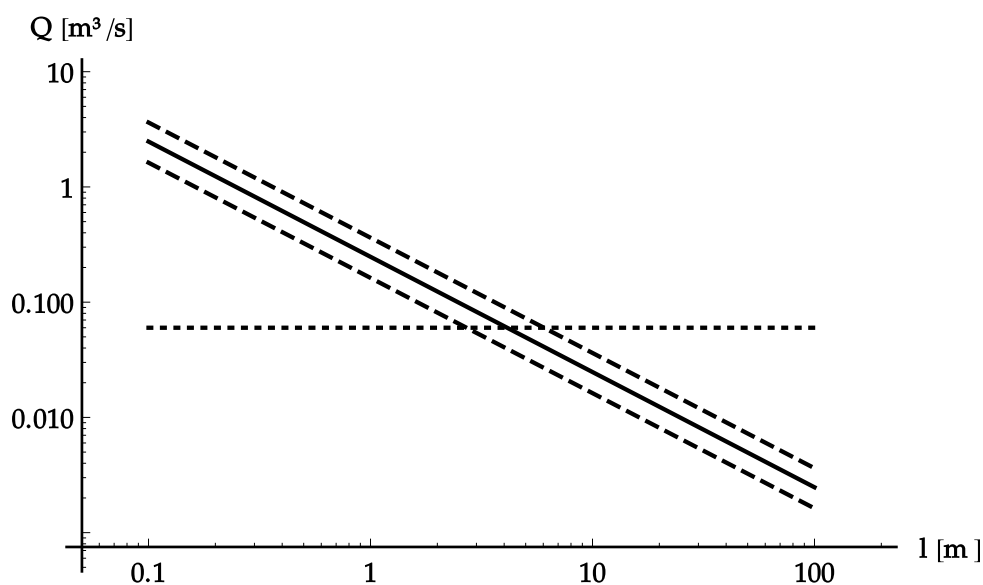


Figure 4.4.: Volume flux (solid line) through a capillary with an inner diameter of 100 μm , with a pressure of $5 \cdot 10^{-5}$ mbar on one side and atmospheric pressure on the other side. The dotted line shows the maximum pumping speed of a Pfeiffer Vacuum HiPace 80 turbo pump. The dashed lines show the volume flux for a change of 10 % in inner diameter, which reflects the capillary's specifications. According to this graph, a minimum capillary length of 3–6 m is required to ensure the target pressure of $5 \cdot 10^{-5}$ mbar.

inserting atmospheric pressure and the maximum allowed pressure in the quadrupole mass spectrometer chamber, and solving the equation for the pumping speed of the turbo pump used, which is around 60 L/s depending on the gas species (Pfeiffer, 2012). The result is plotted in Figure 4.4 and shows that a capillary length of about 4.1 m is required, or 2.7–6.0 m if the capillary is 10 % narrower or wider than 100 μm .

This result is confirmed in practice, with a length of 6 m currently employed in the separation line, connecting the quadrupole mass spectrometer chamber with a port close to the exit of activated charcoal trap AC1.

The chosen capillary length is a compromise between guaranteeing a sufficiently low pressure in the quadrupole mass spectrometer chamber in order not to wear out or damage the ionisation filament, and being able to analyse gas streams of lower pressure. There are only 4 orders of magnitude between the maximum pressure and the detection threshold of the Faraday cup detector. Using a secondary electron multiplier allows for detection of lower partial pressure, but also requires an ambient pressure below 10^{-6} mbar. Switching between detectors is not advisable, as it complicates the automatic separation procedure due to detector warmup times.

Reaction time A pressure change on the far side of the capillary does not propagate instantly to the quadrupole mass spectrometer. To assess this, the response of the argon signal was measured when switching the far end of the capillary from an argon to an air environment, both at atmospheric pressure. The response time was clocked at 2.4 s, which is sufficient for real time surveillance.

The reaction time is much higher if the pressure in the separation line, including the carrier gas, is low: for a pressure of 10 mbar, an experiment has shown that it can take 5 minutes for the pressure on the far side of the capillary to reach equilibrium. During the separation, however, the carrier gas is always present.

Dead volumes Any dead volumes between separation line and quadrupole mass spectrometer are problematic when gas cannot escape quickly, as high pressure gas volumes caught within will dominate the gas stream reaching the quadrupole mass spectrometer, effectively superseding the signal from the separation line. For example, the capillary might be connected to the line via a valve. When that valve is closed under high pressure, that pressure will remain in the dead volume of the valve. Emptying the volume through the capillary will take a long time during which the quadrupole mass spectrometer will continue to show the same signal as was present the last time the valve was open.

Having a valve on the quadrupole mass spectrometer side is also difficult, because the dead volume will accumulate high pressure when the valve is closed. When opened, the valve will flood the quadrupole mass spectrometer chamber with a sudden surge of gas, possibly exceeding the allowed pressure and damaging components.

Consequently, valves on both sides of the capillary should be avoided or at least not actuated during the separation procedure. Even then manual valves are advised as they can be opened gradually if necessary.

As an additional measure, special connectors⁵ have been acquired to connect the capillary as closely to the separation line as possible.

4.2.4. Chromatographic column

Four columns of different properties have been constructed to gain practice and conduct initial testing. The specifications are detailed in Table 4.1. Two different adsorbents were used: activated charcoal with a bulk density of 0.4 g/cm³, and 5 Å molecular sieve Li-LSX supplied by Zeochem AG. One of the columns is shown in Figure 4.5.

⁵Swagelok SS-6M0-3-6M-1

Table 4.1.: Columns/traps built and used for the chromatography experiments. They are filled with activated charcoal (AC) and 5 Å molecular sieve (Li-LSX) respectively. All columns are made from 6 mm stainless steel pipe and stuffed using steel wool.

N ^o	type	amount [g]	length [cm]	max flow [cm ³ /min]
1	AC	5	60	100
2	Li-LSX	5	75	453
3	AC	10	180	50
4	Li-LSX	10	150	250



Figure 4.5.: “Trap No3”, consisting of 180 cm stainless steel tube with 4 mm inner diameter, loaded with 10 g of activated charcoal. This trap will be used in the final separation line and labelled “AC1”.

4.2.4.1. Adsorbent comparison at room temperature

To compare the performance of the adsorbents at room temperature, a test gas (80 % N₂, 19 % Ar, 1 % Kr) was introduced into a 250 cm³ “parking volume” and flushed through the column with a helium carrier, while pumping at the end of the line. The He was introduced directly with the maximum pressure of 1.3 bar.

The results are shown in Figures 4.6 and 4.7. Activated charcoal separates the N₂-Ar and Kr fractions much better than zeolite, and a longer column with more adsorbent has a better separation capability.

The different retention times are not only caused by the column lengths, but also by the different flow coefficients and their effect on the carrier flow rate. This effect is much more pronounced in the activated charcoal columns which have a high flow resistance.

Note that the gases are not completely separated at room temperature, and the gas stream still contains a considerable amount of N₂ and Ar when the Kr breaks through. This is caused by the fact that the sample volume is much larger than the volume of the traps (less than 5–20 cm³).

For comparison, a separation run by Yokochi et al. (2008) is shown in Figure 4.8, using a slightly longer activated charcoal column and achieves a slightly stronger separation.

4.2.4.2. Selective krypton freezing

In this experiment, it was tested whether the traps will selectively retain all krypton that is introduced in a continuous flow. To this end, a test gas⁶ is continually introduced into the chromatography column held at 77 K.

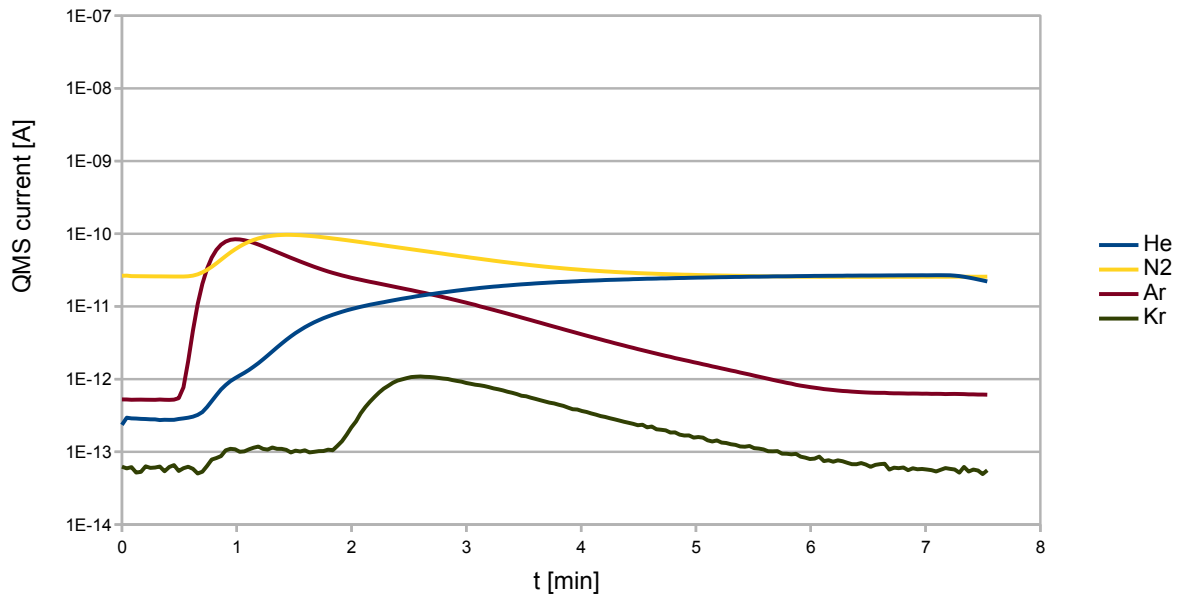
One exemplary result is shown in Figure 4.9. As expected, Ar and N₂ start seeping from the end of the column shortly after starting the experiment. In columns packed with molecular sieve, krypton would eventually pass the column despite the low temperature. For charcoal columns, this was not observed, nevertheless they retain a large amount of non-krypton gases that are released upon thawing.

This shows that, as expected, selective freezing of krypton on the columns was not feasible, and temperature shifts and chromatography are required to improve selectivity.

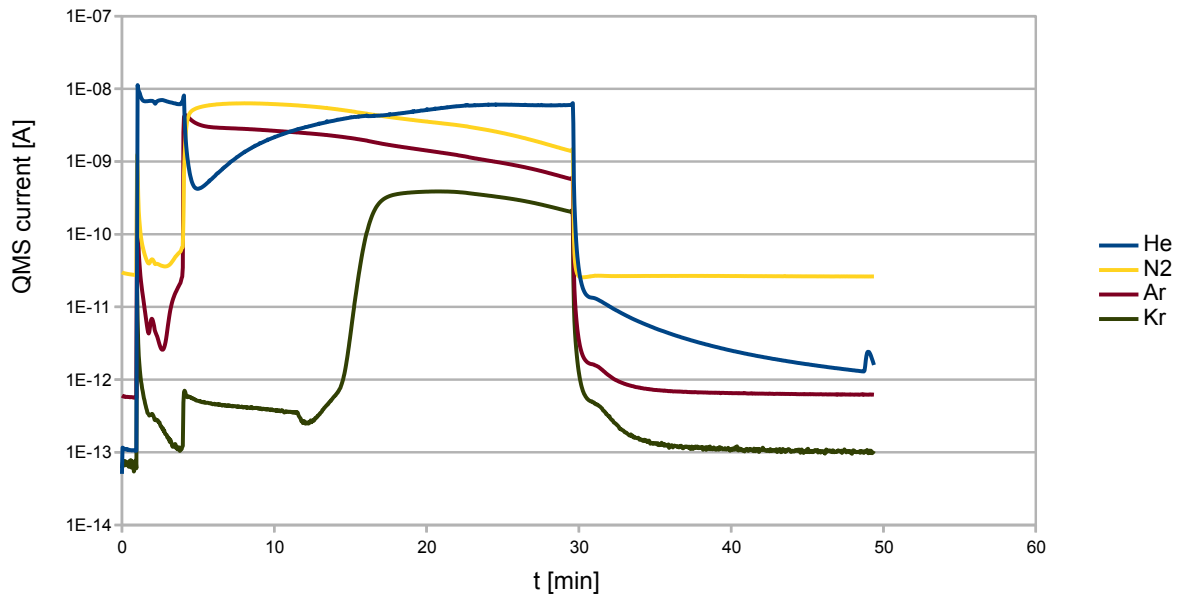
4.2.4.3. Thawing experiments

An effective procedure to achieve pre-enrichment of a sample is to freeze it onto the initial portion of a column, set up a carrier gas stream and heat the column to the

⁶Composition: 80 % N₂, 19 % Ar, 1 % Kr

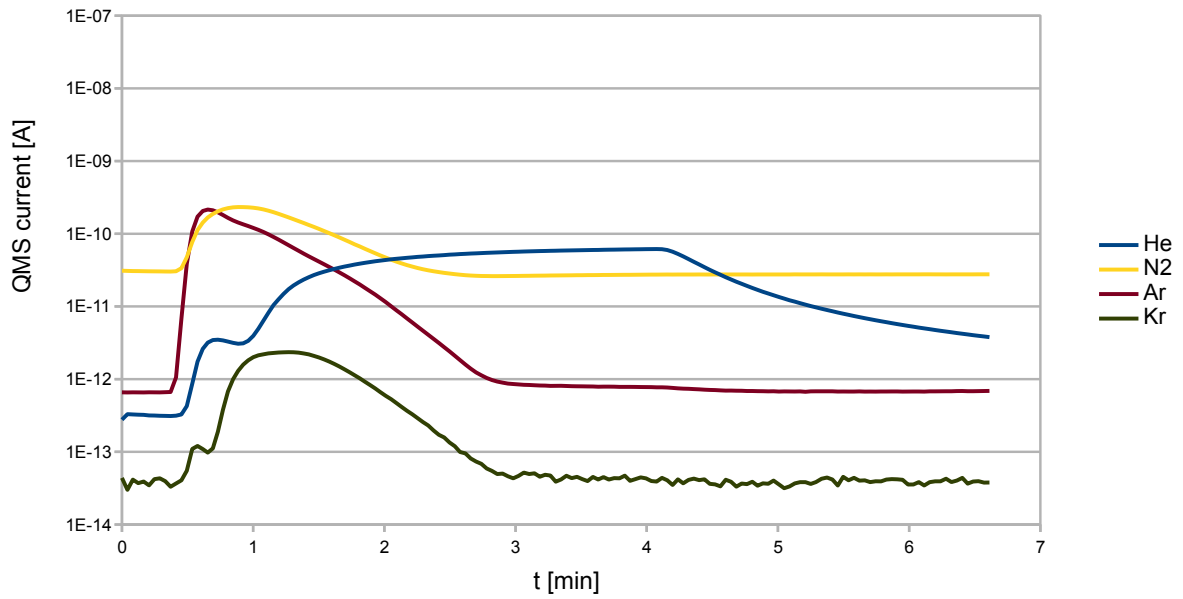


(a) No. 1: 5 g activated charcoal

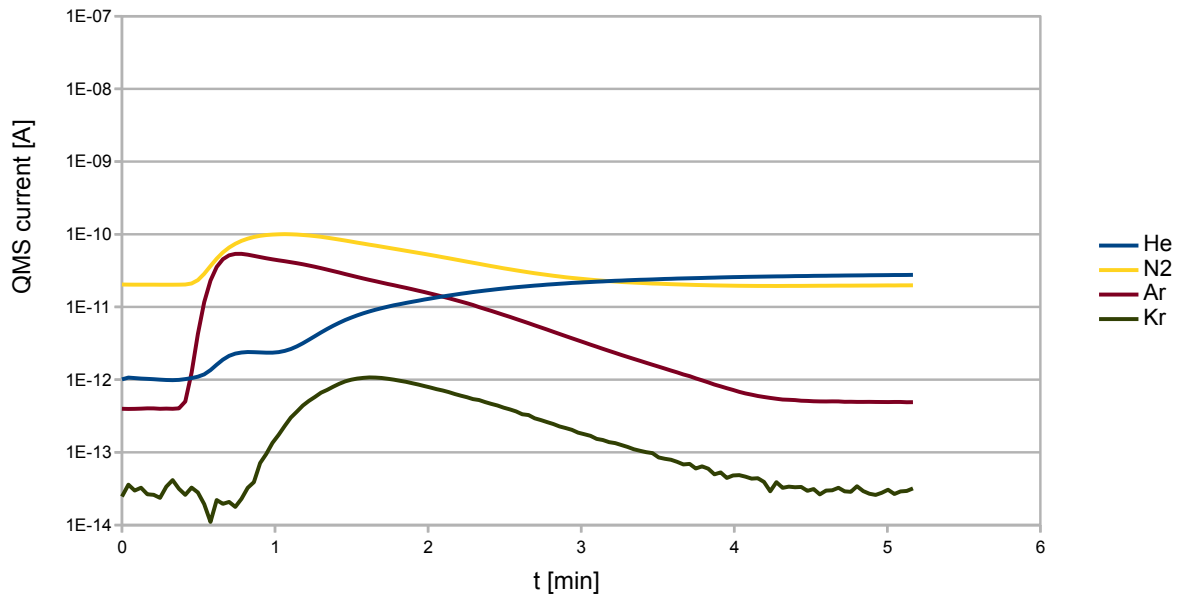


(b) No. 3: 10 g activated charcoal

Figure 4.6.: Breakthrough experiments: using He to flush 1 L of N₂-Ar-Kr mixture through charcoal chromatography columns at room temperature. Traps are specified in Table 4.1.



(a) No. 2: 5 g Li-LSX 5 Å molecular sieve



(b) No. 4: 10 g Li-LSX 5 Å molecular sieve

Figure 4.7.: Breakthrough experiments: using He to flush 1 L of N₂-Ar-Kr mixture through molecular sieve chromatography columns at room temperature. Traps are specified in Table 4.1.

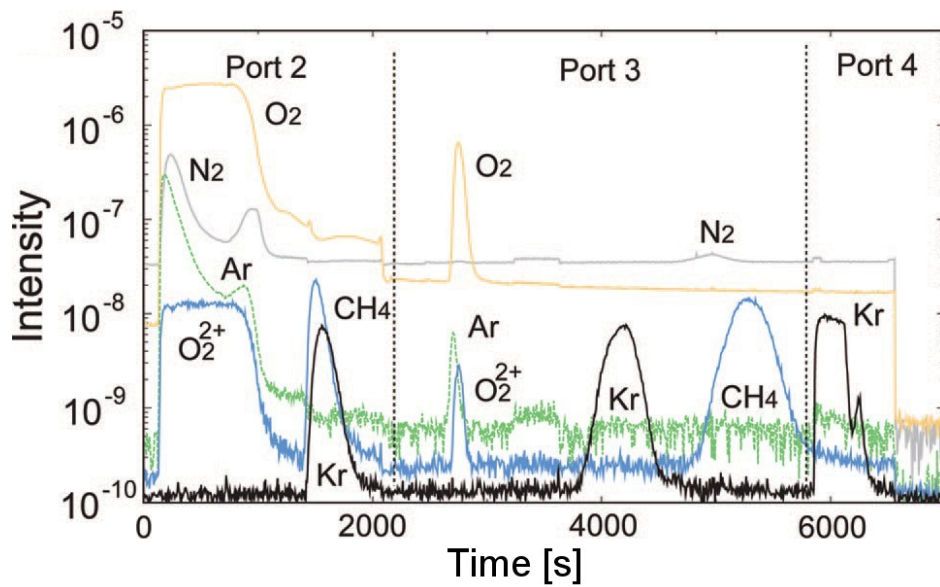


Figure 4.8.: Breakthrough of air sample components through the activated charcoal column (»Port 2«) and molecular sieve column (»Port 3«) in the separation procedure by Yokochi et al. (2008). Compare with Figure 4.6b.

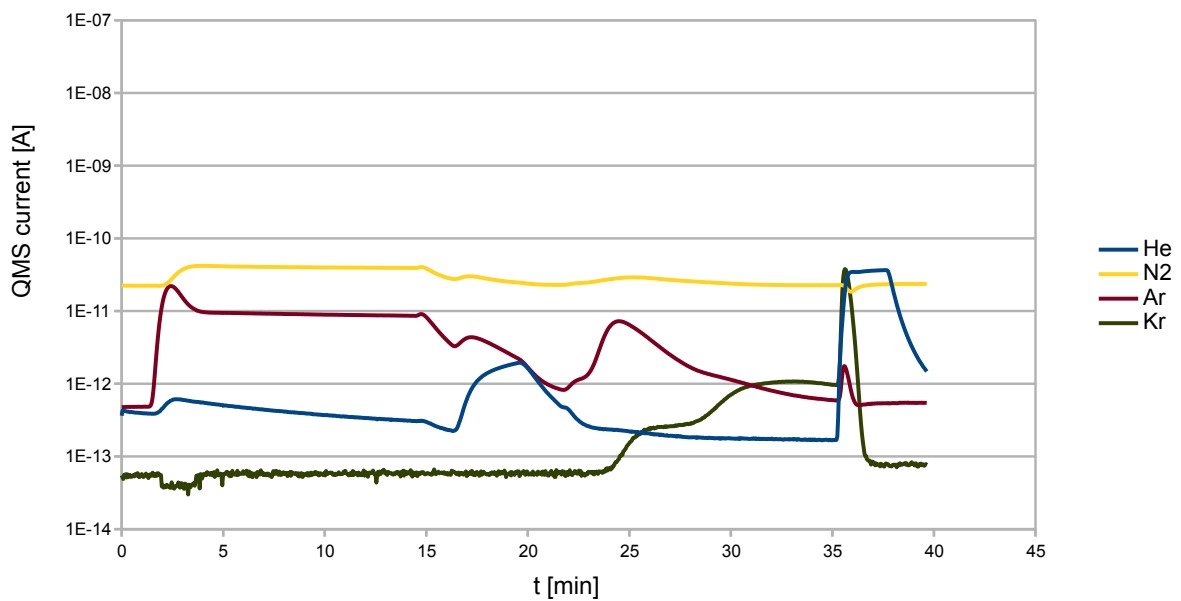


Figure 4.9.: Capacity test for Column 4, cooled with liquid nitrogen. Cooling is removed and thawing starts at 21.5 minutes.

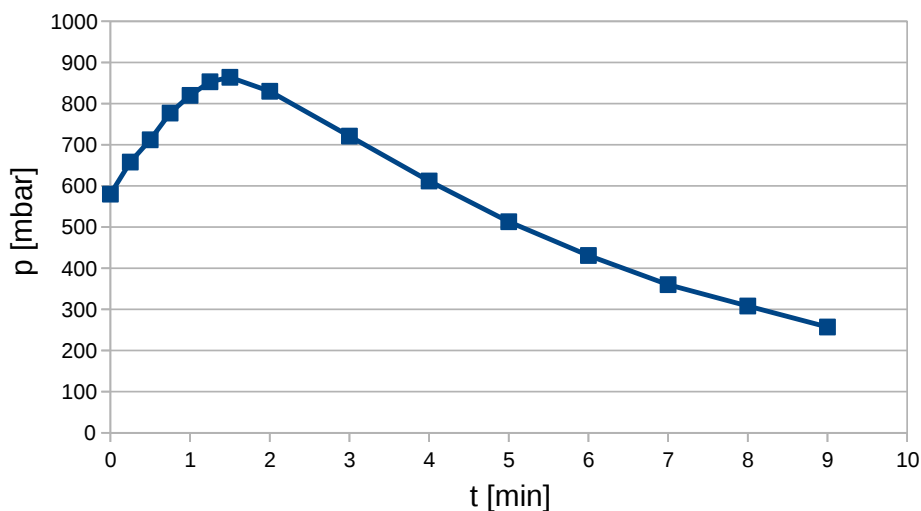


Figure 4.10.: Pressure increase in the separation line when thawing a 6 mm gauge activated charcoal column which previously adsorbed 1 L of nitrogen.

temperature required for chromatography, which also serves the purpose of having the complete sample start its run from a single point.

A problem can be encountered when thawing the column and a large amount of gas, mainly N_2 , is suddenly released at once. When the gas encounters a high flow resistance in the column, it may push against the carrier and flow back into the volume before the column, causing a suboptimal separation as explained in Section 4.2.4.1.

The dynamic of this effect was tested using one of the 6 mm activated charcoal traps, by adsorbing a sample at 77 K and then removing the cooling. Figure 4.10 shows that the pressure is highest around 1.5 minute of thawing, and that levels are safe again after about 5 minutes. During thawing, the entry side of the column can be closed to avoid part of the sample leaving the trap in the wrong direction, at the disadvantage of not having any tracer flow during thawing.

In the Bern EFA, several such thawing procedures are performed to rid the sample of part of its excess N_2 . Presumably, this is the part of the procedure responsible for most of the Kr loss, as the strong burst of N_2 forces Kr out of the trap even before the temperature is high enough for Kr to evaporate on its own. This is less of a problem for a long column such as the one employed at the krypton separation line because the Kr will have to travel a long way through the column before exiting. Still the Kr should stay bunched together as long as possible to exploit the full separation power of the column and obtain a narrow krypton peak, so an explosive desorption of N_2 should be avoided.

For the krypton separation line, a hybrid approach is adopted in which the thawing

is slowed down, while not closing off the column entry and having a tracer flow. This way, the evaporating N₂ can be transported towards the end of the line by the carrier while the Kr has time to settle again due to the low temperature. Eventually the krypton completely evaporates, along with the remaining N₂ and Ar, and undergoes chromatography.

4.2.4.4. Carrier gas

As a carrier gas, helium is chosen. Being a noble gas, it is inert and will not interact chemically and alter components of the sample or separation line. It also stays gaseous at low temperatures.

Some krypton separation efforts employ methane as a carrier, mainly due to the fact that it can also be used as a counting gas for radiometric determination of Kr-85 content. For atom trap trace analysis, no counting gas is necessary, but contamination with methane should be avoided.

One question is the required purity⁷ of the He carrier. The EFA at Uni Bern is using 5.0 purity He for samples ranging from 10–50 L. Small samples may require a higher purity. Assuming a flow rate of 80 cm³/min, a 5.0 purity and a typical composition of impurities⁸, up to 5 µL of N₂ can be accumulated in a 20 minute separation step, five times the amount of a 1 µL Kr sample. This can be alleviated by employing a getter (Section 4.2.7) and purchasing cleaner helium. A purity of 6.0 was chosen as a compromise.

The carrier flow speed is either limited by a flow controller or by the density of the chromatography columns. In the final design (see Section 4.3.1), the flow controller will limit the flow to around 66 cm³/min. When column AC2 is attached, that will limit the flow to 50 cm³/min. Similar applications in other laboratories operate at similar speeds: the EFA in Bern is set⁹ to 76 cm³/min, albeit with a much larger column diameter.

4.2.4.5. Separation without fine temperature regulation

Before implementing fine temperature control, a number of experiments have been conducted to achieve a good separation of small krypton samples without fine temperature control, solely using direct contact with liquid nitrogen for cooling and room

⁷For gases, purity is commonly given in the form of a grade consisting of two numbers separated by a colon, the first number denoting the number of “nines” in the percentage of the actual purity, the second number denoting the last digit of said percentage. Thus, a purity of “6.5” would actually be a 99.99995 % purity. In other words, the notation “x.y” expresses a purity of $P = 1 - 10^{-x} + y \times 10^{-(x+1)}$

⁸N₂, H₂O, O₂ ≤ 3 ppm; hydrocarbons ≤ 0.2 ppm (Linde, 2008)

⁹own measurement using an Agilent ADM-1000 diaphragm flow meter

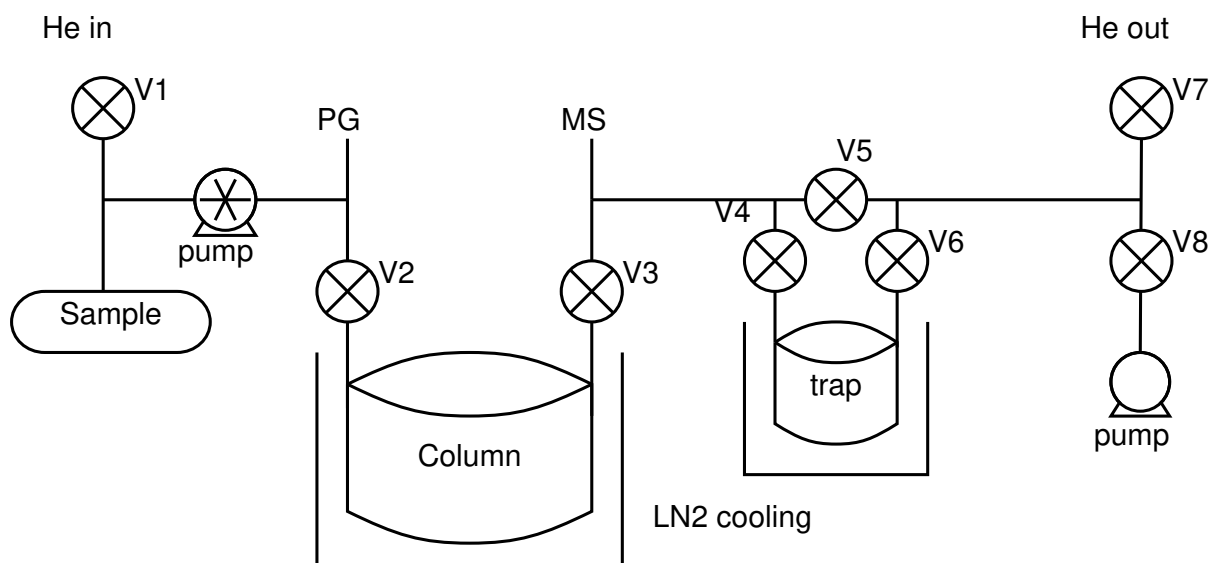
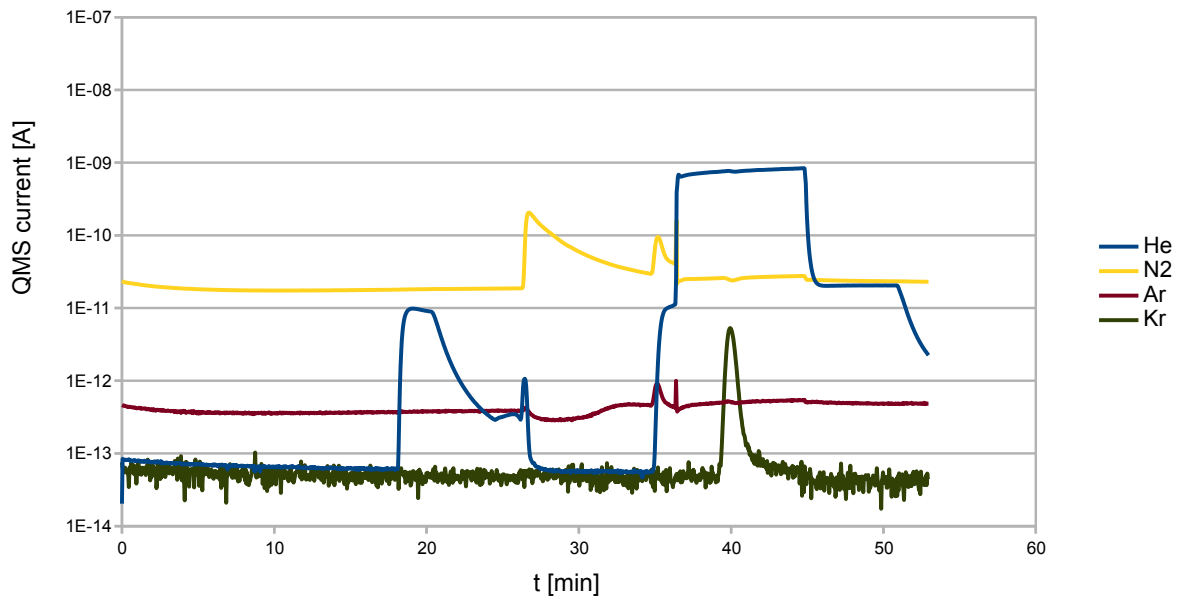


Figure 4.11.: Sketch of the setup used for the chromatographic separation experiment described in Section 4.2.4.5, including pressure gauge (PG), quadrupole mass spectrometer (MS) and valves (V1–8).

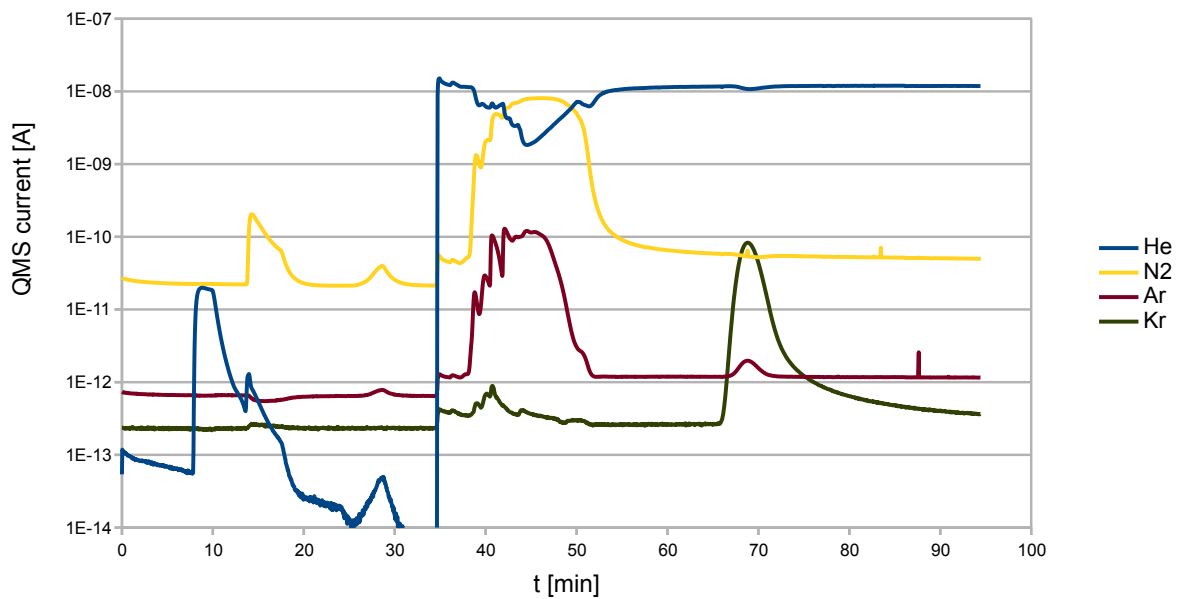
temperature for heating. The experimental setup is shown in Figure 4.11, using the activated charcoal column N^o 3 described in Table 4.1 attached to the Bern EFA, whose “AC2” trap is used for storing and transferring the sample. Two exemplary separation methods for this setup have been examined, methods A and B.

Method A: fast This Method requires only 45 minutes. The pressure is monitored by the pressure gauge (PG) and must not rise above the carrier pressure to avoid sample seepage into the volume before the column. The resulting quadrupole mass spectrometer chromatogram is shown in Figure 4.12a. The sequence is as follows:

1. The sample is pumped onto the column; V2, V3, V5, V8 are open. [minutes 0–18]
2. V1 is opened to flush the remaining sample into the column using a He carrier. [minutes 18–25]
3. V2 is closed and cooling removed from the column. The column will retain all the Kr at this point. [minutes 26–32]
4. V2 is opened again, until the initial N₂ and Ar peaks are over.

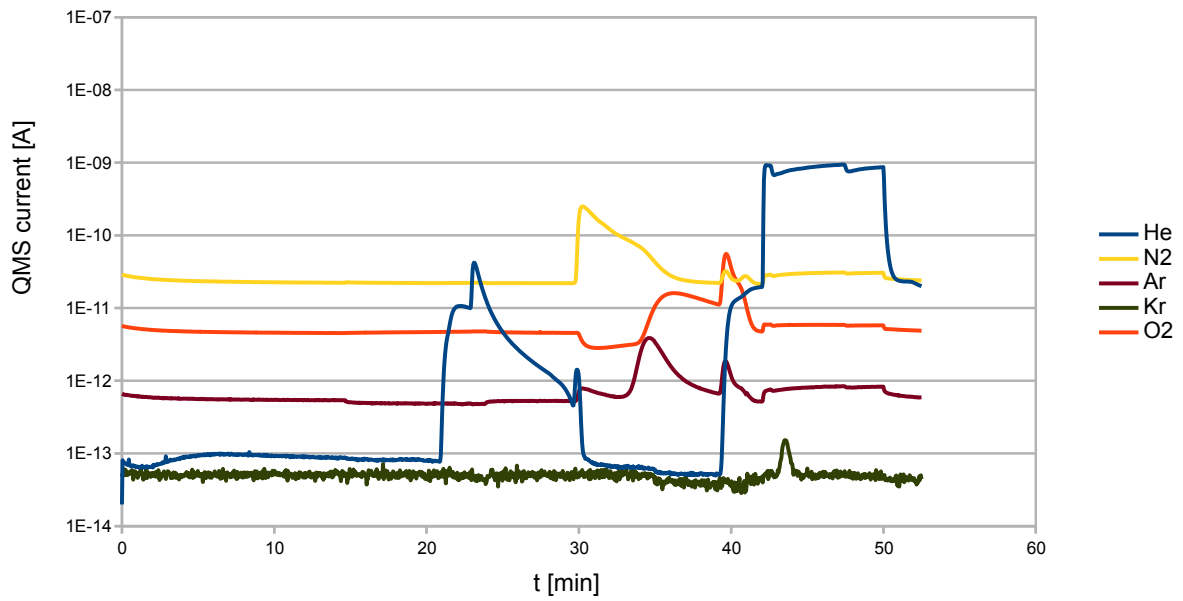


(a) Separation method A, as detailed in Section 4.2.4.5.

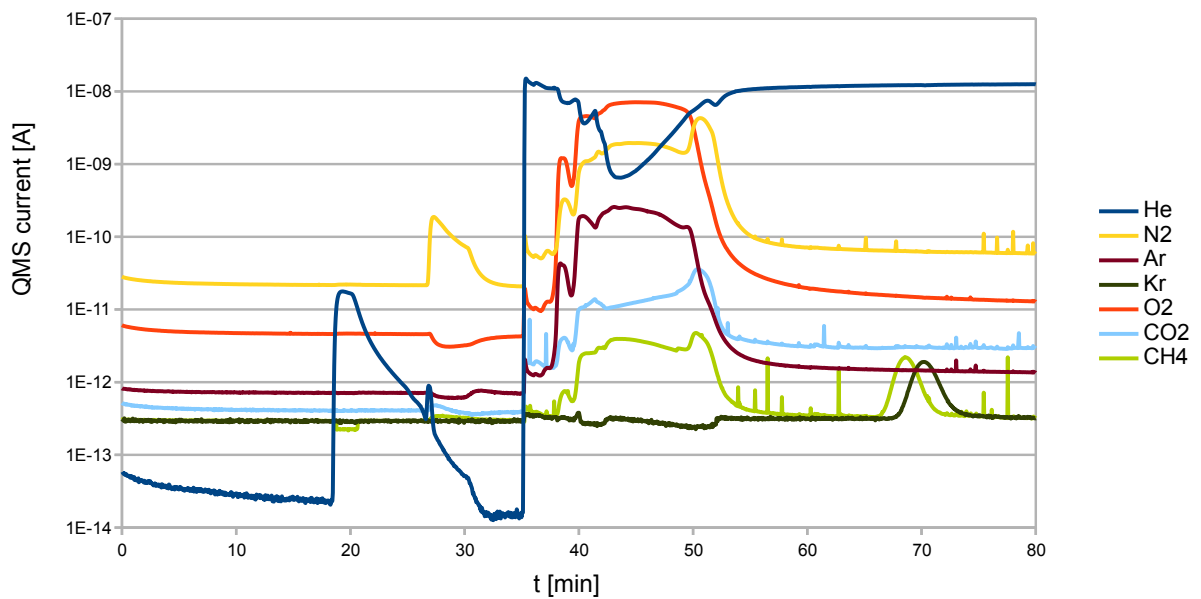


(b) Separation method B, as detailed in Section 4.2.4.5.

Figure 4.12.: Separation procedures applied to a N₂/Ar/Kr (80/19/1) test gas, shown via quadrupole mass spectrometer surveillance. Both methods use Column 3 (activated charcoal).



(a) Separation method A, as detailed in Section 4.2.4.5.



(b) Separation method B, as detailed in Section 4.2.4.5.

Figure 4.13.: Separation procedures applied to air, shown via quadrupole mass spectrometer surveillance. Both methods use Column 3 (activated charcoal).

5. The flow is directed through the trap to capture the He peak for 10 Minutes. [minutes 36–46].
6. The trap is removed for counting the sample volume in the gas chromatograph, or measuring the sample composition in the quadrupole mass spectrometer.

Method B: slow This method introduces an additional thawing cycle to rid excess N₂, similar to the standard EFA procedure in Section 3.4, and the final thawing is conducted in a He carrier stream. The resulting quadrupole mass spectrometer chromatogram is shown in Figure 4.12b. The sequence is as follows:

1. The sample is pumped onto the column; V2, V3, V5, V8 are open. [minutes 0–8]
2. V1 is opened to flush the remaining sample into the column using a He carrier. [minutes 8–10]
3. V2 is closed and cooling removed from the column. [minutes 12–17]
4. The column is cooled again for 5 minutes. [minutes 18–23]
5. Steps 3–4 can be repeated if desired. [minutes 25–35]
6. He carrier gas is directed through the frozen column. V1, V2, V3, V5, and the exit vent V7 are open, V8 closed. Only the carrier pressure, which is slightly higher than the external pressure, is driving the flow rate. [minutes 35–65]
7. After the N₂ and Ar peaks have passed, the flow is directed through the trap to capture the He peak for 10 Minutes. [minutes 65–85]
8. The trap is removed for counting the sample volume in the gas chromatograph, or measuring the sample composition in the quadrupole mass spectrometer.

Yield and purity optimisation After developing the Methods A and B using a 1 % Kr test gas, the methods have been evaluated quantitatively using a test gas containing 51 ppm Kr, measuring the yield with the gas chromatograph and evaluation software used in the EFA procedure. Each method has been repeated several times. The results are displayed in Table 4.2 auf Seite 64.

Method A is producing the higher yield, close to 50 %, while Method B is producing a much better purity, up to 50 %. The purity values using Method A are erratic, ranging from 13 – 44 %.

The methods have been applied to actual air, see Figure 4.13, in which the Kr peaks were clearly visible in the quadrupole mass spectrometer and well shaped. The Kr and CH₄ fractions are clearly visible in Figure 4.13b at around 70 minutes; due to a calibration error, no CH₄ signal is available for the other experiments.

Yield The yield of Method A is close to 50 %. Compared to the EFA procedure applied to a small sample volume¹⁰ of 3.3 L, this is a definite improvement.

The yield of Method B is much lower than that of Method A. Over the course of all experiments, a greater number of thawing processes generally led to a lower yield. This may be due to Kr being flushed out of the column by the quickly boiling and expanding N₂, especially Kr that is trapped in an N₂ matrix instead of being directly adsorbed on the activated charcoal.

The following steps can be taken to improve the yield:

- Reduce the impact of thawing,
 - either by decreasing the number of thawing steps,
 - slowing down the thawing procedure to allow any stirred Kr to settle
 - operate at a temperature higher than that of liquid nitrogen to reduce N₂ uptake in the first place.
- Heating of traps to desorb more of the remaining Kr.

Purity In Method A, most of the thawing procedure is performed without a carrier, meaning that impurities remain at the start of the column until the carrier gas is introduced.

Method B yields a much higher purity as the column is thawing in the carrier stream, flushing away impurities while the Kr is still retained by the low temperatures. This positive effect may have been countered by the numerous thawing procedures, each of which moves some of the Kr down the column, broadening the peak which leads to additional N₂ and Ar adsorption while it is captured on the trap. Using pure air samples, the purity is much smaller, which is to be expected as the amount of remaining impurities per sample volume is not affected by the Kr concentration.

The purities of up to 50 % correspond to an enrichment factor of 10⁴ in just one separation step. Normally, an enrichment factor of ~10 per gas chromatography separation step is expected (Collon et al., 2000).

Lessons learned for an enhanced separation procedure Using this simple procedure, there seems to be a general tradeoff between yield and purity. The methods examined provide a suitable basis for a separation procedure for small sample volumes, but at this point it is unclear which one is the more suitable template.

The most likely reason for the low yield observed is the dispersal of krypton by the strong nitrogen flow during thawing. A refined temperature control has the potential to avoid this and improve yield, and a getter will help to further enhance the purity.

¹⁰3.3 L is the smallest sample where EFA produced a measurable yield

Table 4.2.: Results of several separation experiments. Methods A and B are shown in Figures 4.12a and 4.12b. The table denotes the amount of krypton separated (Kr) as well as the amount that was present in the air sample (Kr_{target}).

N ^o	Date	method	yield [%]	purity [%]	Kr [μ l]	Kr _{target} [μ l]
5	13-06-23-1	A	42	20	21.41	51.0
6	13-06-23-2	A	48	13	24.45	51.0
7	13-06-24-1	A	43	44	21.86	51.0
3	13-06-22-1	B	27	45	13.68	51.0
4	13-06-22-2	B	16	48	8.34	51.0
8	13-06-24-2	B	12	1	0.12	1.0
	13-06-28-1	EFA (3.3L)	29	7	0.95	3.3

4.2.4.6. Choice of column

Based on these experiments, conforming with experience from prior krypton separation methods and in line with the reasoning presented in Section 3.5.4, the 2 m activated charcoal column displays properties suitable for this application and is used directly in the final separation line.

4.2.5. Flow control

A calorimetric mass flow meter/controller¹¹ is implemented to monitor and control the flow of the carrier gas. This type of flow meter is relatively independent of ambient pressure and temperature, but results must be corrected for specific heat when the observed gas differs from air (Ewing and Ramberg, 1984; MKS Instruments, 1996).

To account for the age of the flow controller, calibration factors have been determined experimentally: for air at 80 cm³/min, the correction factor is 1.087. For He, the correction factor is 1.651.

The accuracy of the flow meter is quoted at ± 0.5 % full scale (MKS Instruments, 1996), but in practice, the uncertainty for the volumes derived via integrating the flow were around 1 %. This value is used as the uncertainty for all volumes determined in this thesis using the flow controller. The uncertainties due to outside temperature and pressure variation are negligible in comparison, and a correction for STP is not necessary.

¹¹MKS 1359C Masster-Flo™

4.2.6. Temperature control

4.2.6.1. Options

Three basic mechanisms are available for controlling the temperature of the activated carbon traps.

Liquid cooling The column is submerged in a liquid, most commonly liquid nitrogen or a solution of dry ice and ethanol. Due to convection and direct contact of the coolant, the cooling effect is fast. Convection also keeps the temperature homogeneous and close to the boiling point.

If temperatures between room temperature and coolant temperature are desired, some form of heating must be introduced, which requires a lot of energy and drains the coolant quickly, perhaps even requiring a refill.

Liquid cooling may be automated by physically adding and removing coolant, be it by pumping or by lowering the trap into a coolant basin, requiring suitable pumps or mechanical moving parts.

Thermoelectric cooling Peltier elements allow for a precise temperature control, which was utilised for gas separation by Lott (2001), with small samples in the order of microlitres. Implementation for chromatography is difficult because a much more powerful peltier element is necessary and needs to be adapted to the complex geometry of a column.

Gas cooling A more promising option has been implemented for argon separation by Riedmann (2011). In a closed chamber, several columns are suspended above a basin of liquid nitrogen with the air being constantly stirred by a fan to achieve a homogeneous temperature distribution. The columns are directly heated by an electrical current of 60 A and wired to a temperature controller, with a target temperature of 193 K, which is reached after about 30 minutes of cooling.

The gaseous coolant will act much slower than liquid due to low thermal conductivity, meaning less energy and coolant are consumed once the target temperature is reached. Compromises between both methods are feasible: Riedmann (2011) is bringing the columns in contact with liquid nitrogen to kickstart the cooling process.

4.2.6.2. Implementation

To regulate the trap temperatures in the separation line, a gas cooling scheme has been developed. The traps are wrapped with heating wire and aluminium foil to spread the temperature evenly, and then kept above a pool of liquid nitrogen, with a fan constantly dispersing the air around the trap.

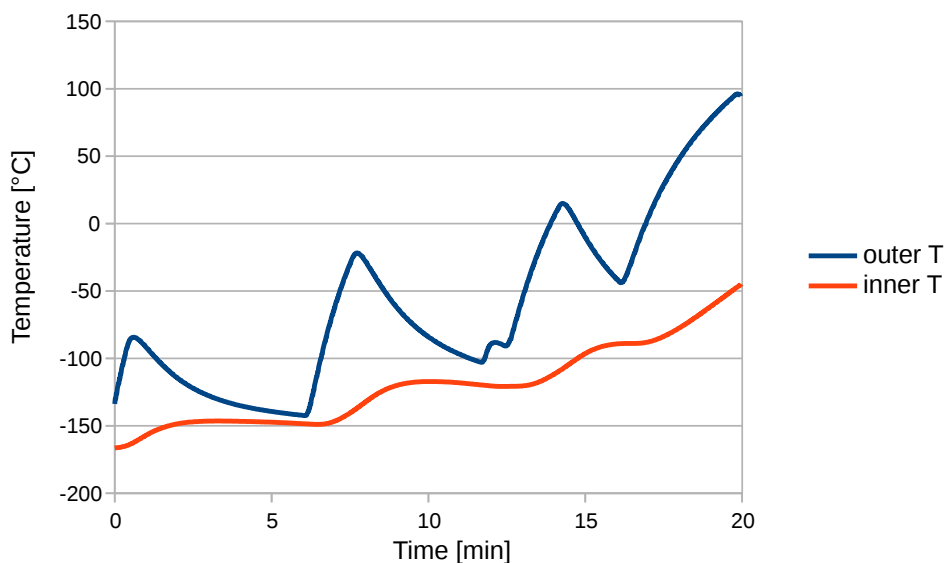


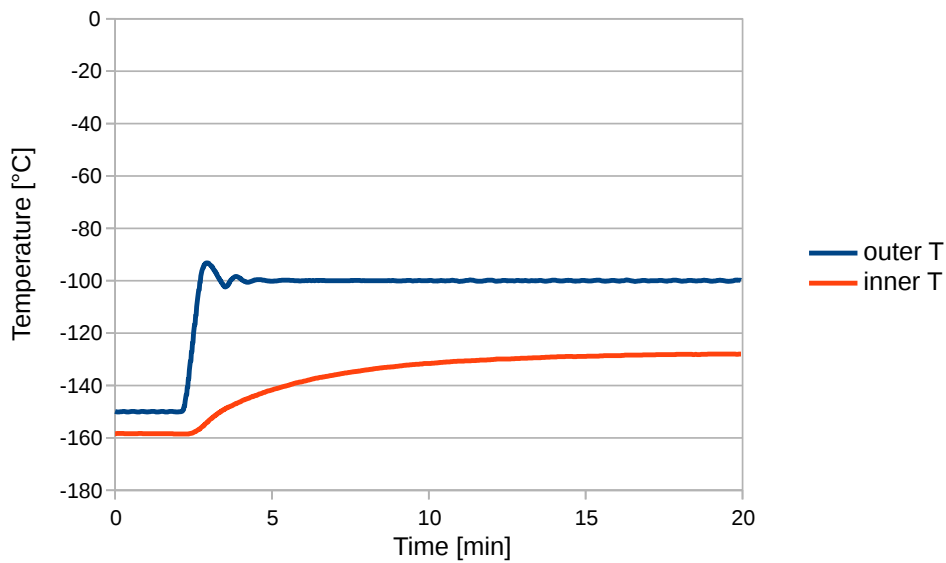
Figure 4.14.: Inner and outer temperature of the trap coil AC1 when using PID regulation to control the *inner* temperature. Even for small jumps in target temperature, the values differ up to 100 °C as the PID controller tries to raise the inner temperature as quickly as possible.

A specialised heating wire¹² is employed. For technical reasons, the rigid wire could only be wrapped on the outside of the charcoal trap coil. To test the ramifications of this geometry, temperature sensors have been placed both on the outside and inside of the coil to monitor the heat distribution. The intended behaviour is an even temperature distribution with inside and outside temperature not differing. A PID controller is used to regulate the temperature. In its first configuration, the inner temperature was regulated, resulting in a suboptimal heat distribution, seen in Figure 4.14, due to the slow distribution of heat from the outside of the coil to the inside. In case of such an uneven distribution, it is hard to estimate the exact temperature of the activated charcoal packing within the column.

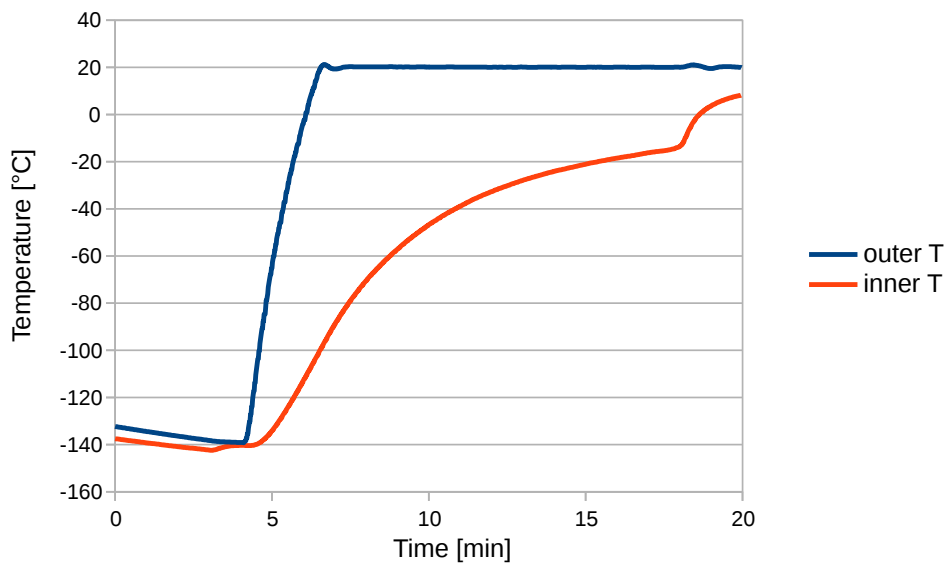
Uneven temperature distribution in combination with large amounts of nitrogen present on the column can even lead to krypton loss when the set temperature is very low, see Figure 4.16.

To achieve a more homogeneous temperature, the PID controller was configured to regulate the outer temperature instead. With the temperature sensor in close proximity to the heating wire, the outside temperature can be finely regulated (see Figure 4.15). This does not defeat the fact that sudden temperature increases are not possible while maintaining a homogeneous temperature. In practice, this is acceptable because a slow heating curve is required to avoid pressure buildup (see Sec-

¹²HORST GmbH KF00330, 42VAC 220W, magnesium oxide isolation



(a) A sudden change of set temperature by 50 °C.



(b) A sudden change of set temperature by 150 °C. The sudden rise of the inner temperature is caused by the liquid nitrogen running out.

Figure 4.15.: Inner and outer temperature of the trap coil AC1 when using PID regulation to control the *outer* temperature. After 10 minutes, the temperature difference between outside and inside of the trap is about 30 °C (4.15a) and 45 °C (4.15b) respectively.

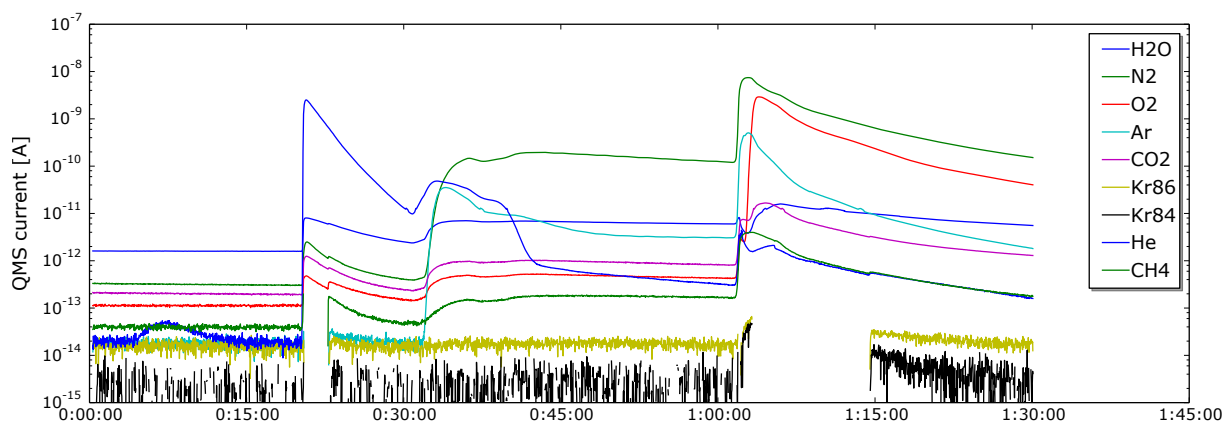


Figure 4.16.: Experiment with a 1 L air sample frozen in AC1 at $-150\text{ }^{\circ}\text{C}$. After pushing with He after about 20 minutes, gas components exit the column. Using the initial heater, the temperature is raised to $-100\text{ }^{\circ}\text{C}$ after about 1 hour. Observe how a burst of gas is released, including some Kr.

tion 4.2.4.3). A suitable heating curve has been determined experimentally and is plotted in Figure 4.17.

At a later point, the inner volume of the coil was closed off with aluminium foil to achieve an even more homogeneous temperature distribution, and the temperature curve adapted accordingly. Table 4.3 shows the settings for the temperature controller to increase the temperature of AC1 from $-120\text{ }^{\circ}\text{C}$ to $40\text{ }^{\circ}\text{C}$ within 8 minutes: heating starts slowly and accelerates after the initial surge of released nitrogen. For higher initial temperatures, the first part of the curve is simply omitted, thereby using faster heating from the onset.

The dewars must be sufficiently large as to provide enough cooling for the whole separation procedure. When an isolating lid is applied, liquid nitrogen is lost at a rate of 1 L/h.

4.2.7. Getter

4.2.7.1. Choice of getter

Attaching a volume filled with getter material to a separation line can be difficult to handle because of the very small volume of the purified sample, which has to be evacuated after gettering. An inline getter enables to skip this step and achieve purification faster and with less sample loss. Still, a compromise must be struck between getter volume and efficiency. For the initial purification experiments detailed in the following section, a Mini XL by NuPure Corporation has been used. This small getter includes a heating unit providing variable temperatures up to $550\text{ }^{\circ}\text{C}$. Larger

Table 4.3.: Temperature settings to heat trap AC1 from -120 °C to 40 °C within 8 minutes. This is sufficiently slow to increase the adsorbent temperature homogenically as well as to avoid an N₂ pressure buildup that pushes sample content out of the entry side of AC1.

time [min:s]	T [°C]
00:00	-120
00:30	-115
01:00	-110
01:30	-105
02:00	-100
02:30	-95
03:00	-90
03:30	-85
04:00	-80
04:30	-70
05:00	-60
05:30	-50
06:00	-40
06:30	-20
07:00	0
07:30	40

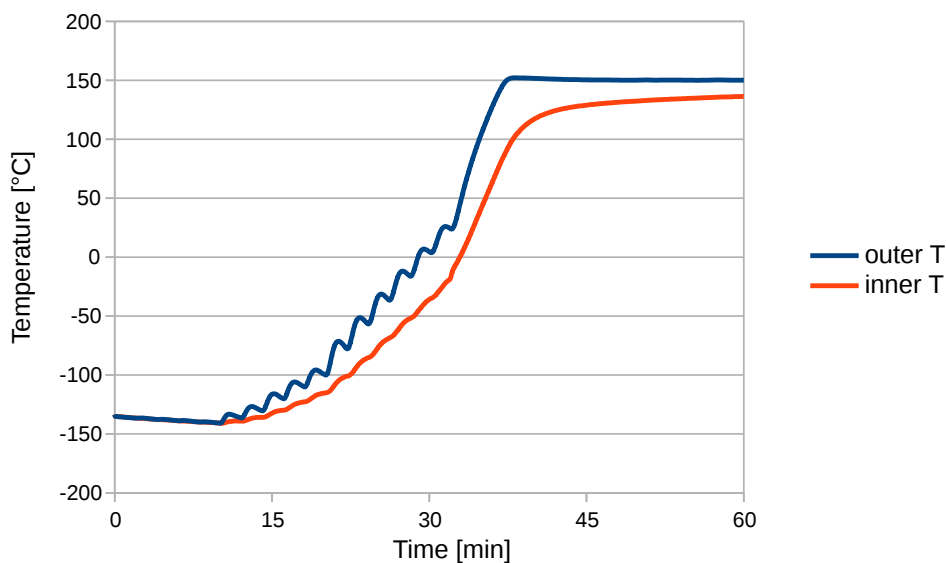


Figure 4.17.: Inner and outer temperature of the trap coil AC1 when heating the trap from -150 °C to +150 °C within 20 minutes. The temperature difference between inner and outer walls never exceeds 50 °C.

models are available in case the performance is lacking.

4.2.7.2. Purification experiments

The getter requires a flow rate below 200 cm³/min, which works well with the charcoal column AC1 restricting the helium flow rate to 50 cm³/min. As a result, the gas chromatography and gettering steps could be performed in one go without an additional trap in between.

To test the getter, it was placed in a line with two activated charcoal traps. Trap 1 contained the sample, which was flushed through the getter into Trap 2. Afterwards, Trap 2 was disconnected and taken to the quadrupole mass spectrometer for analysis. The test gas (85 % N₂, 5 % Ar, 10 % Kr) was made to conform to a particularly impure sample after the first chromatography step. The getter was operated at 450 °C.

Results The experiment was set up as seen in Figure 4.18, results are laid down in Table 4.4.

In the first few samples, the N₂ content was reduced by a factor of 10 using two different flow rates, a promising result. The Ar/Kr ratio in samples 130702-1 and 130702-3 should be 1/2, which suggests that the Kr recovery was not effective. This was corrected by additional heating of Trap 1 from sample 130703-1 on. Sample 130703-2 shows a recline in gettering quality.

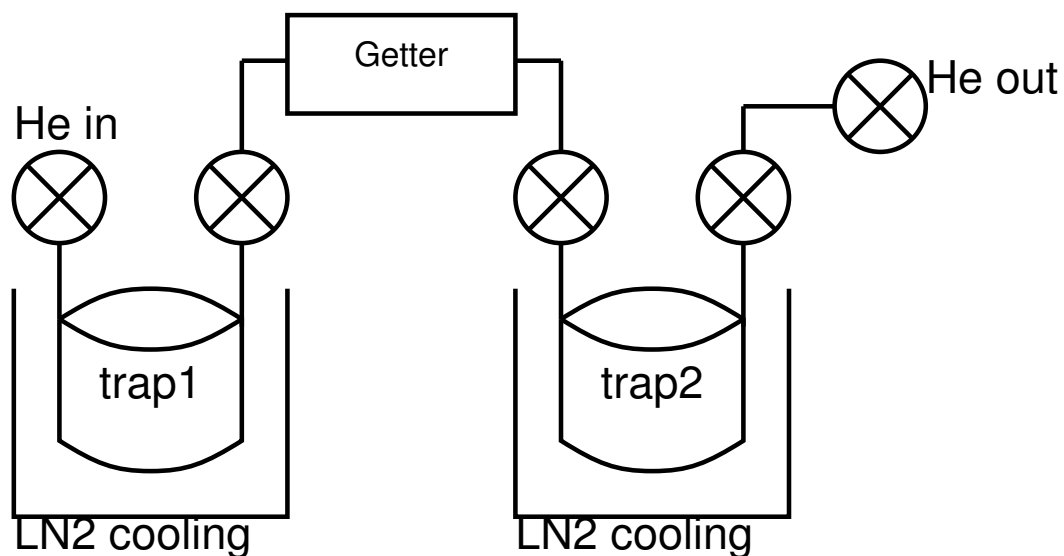


Figure 4.18.: Setup for testing the NuPure Mini XL getter.

Table 4.4.: Results of treating a test gas with a NuPure MiniXL getter. Each sample was 0.5 cm³, and transported through the getter using a He carrier at 1.3 bar and 25 cm³/min. The results were measured via quadrupole mass spectrometer. Sample 130704-4 was processed without a carrier.

	N ₂ [%]	Ar [%]	Kr [%]	heat	He flow [cm ³ /min]
<i>Test gas</i>	85	5	10		
130702-1	9	39	52	no	30
130702-3	9	42	49	no	20
130703-1	5	35	64	yes	20
130703-2	17	25	58	yes	20
130704-4	75	13	12	yes	0 (20)
130704-5	92	4	4	yes	20
130704-6	15	38	47	yes	20

Table 4.5.: Lifetime capacity of the NuPure Mini XL getter for different impurities. It contains 37.5 g of getter material.

	Capacity	
	weight [%]	volume [std L]
N ₂	3.0	0.9
O ₂	12.0	3.1
CH ₄	1.5	0.4
CO ₂	1.5	0.4

For 130704-4, the sample was slowly let into the getter without a carrier to achieve a longer exposure to the getter material. The results were particularly bad, and did not improve with the next sample, which was using the carrier again. The lifetime capacity of the getter, which allows for 2000 samples of 0.5 cm³, has definitely not been reached (see Table 4.5). In a later experiment on the same day, the result improved again (130704-6), after the getter had time to regenerate.

Discussion The results have been shared and discussed with the getter manufacturer. Getters are commonly used for cleaning gas streams that are already very pure, and not tested in conditions where the impurities make up a significant amount of the stream. In the experiment, the He flow was 50 cm³/min, amounting to an effective average purity of 99.9 %, probably never less than 90 % at any given time.

For the getter to operate effectively, the rate of arrival of impurities at the surface needs to be lower than the rate of diffusion of impurities into the getter material. This explains the sudden decline in results: the high impurity of the sample without a carrier was too much for the getter to handle, blocking the uptake of impurities for a time. After a period of regeneration, results improved again.

Performance can be improved by operating the getter at a higher temperature of 550 °C, and regenerating the getter at 350 °C overnight. The actual air samples that will be processed in the final separation line will be about 100 times smaller, reducing the performance requirements for the getter.

4.2.8. Purified sample container

A container vessel is required to store the purified sample and transfer it to measurement.

The vessel constructed for this purpose consists of a 1/8" stainless steel tube with a length of 15 cm which is soldered shut on one end and connected to a high per-

formance bellow valve¹³ with the other. It is connected to the entry side of the valve, which has the lower dead volume, making for an overall volume of about 0.6 cm³.

Krypton can be drawn into the container by submerging the tube in liquid nitrogen, and expelled by heating the tube with a hot-air gun. It is sufficiently long to stay submerged in coolant for an extended amount of time, even when the nitrogen-level is sinking due to evaporation.

A few cubic millimetres of activated charcoal are contained within to facilitate krypton adsorption. To keep charcoal particles from entering the valve, a circular stainless steel frit¹⁴ with an outer diameter of 1/16" and a pore width of 0.5 µm has been inserted loosely, and is kept in the tube by the compressed Swagelok fitting.

The vessel is connected to the extraction line via Swagelok VCR® fittings, with the body on the vessel side, and using a stainless steel gasket. This metal-to-metal stainless steel sealing is sufficiently leak tight and durable for repeated reattachment.

This sample container was employed not only for storage and transfer within the laboratory, but also for transport to other laboratories, without any indication of leakage.

4.3. Krypton separation line

4.3.1. Final layout of the krypton separation line"

The layout of the krypton separation line ("Krypton-Abtrennungs-Anlage") is shown in Figure 4.19 and Figure 4.20. Most functional elements of the separation line are described in detail in Section 4.2, including any reasoning and testing leading to their implementation.

The krypton separation line is constructed from 6 mm OD stainless steel tubing with a 4 mm ID, and fixed to a single aluminium strut profile bar. All elements are connected using Swagelok fittings, making the krypton separation line modular. All elements can be disconnected, and whole parts of the assembly moved along the bar without disassembling them, so elements can easily be added and switched around.

Pressure gauges The line contains three pressure gauges: two active Piezo gauges¹⁵, PG1 and PG3, are used for monitoring operational pressure at both ends of the line. A Pirani gauge, PG2, is employed at the end of the line to monitor pressures below 1 mbar, which is mainly important to assess the quality of vacuum in the system.

An additional gauge, PGQ, is used to measure the pressure in the compartment containing the quadrupole mass spectrometer.

¹³Swagelok SS-2H

¹⁴Valco .5FR1-10, sold by Macherey-Nagel GmbH & Co. KG

¹⁵Pfeiffer CPT 200, can measure up to 2000 mbar independent of gas type.

ZNF Krypton Separation v.3.7

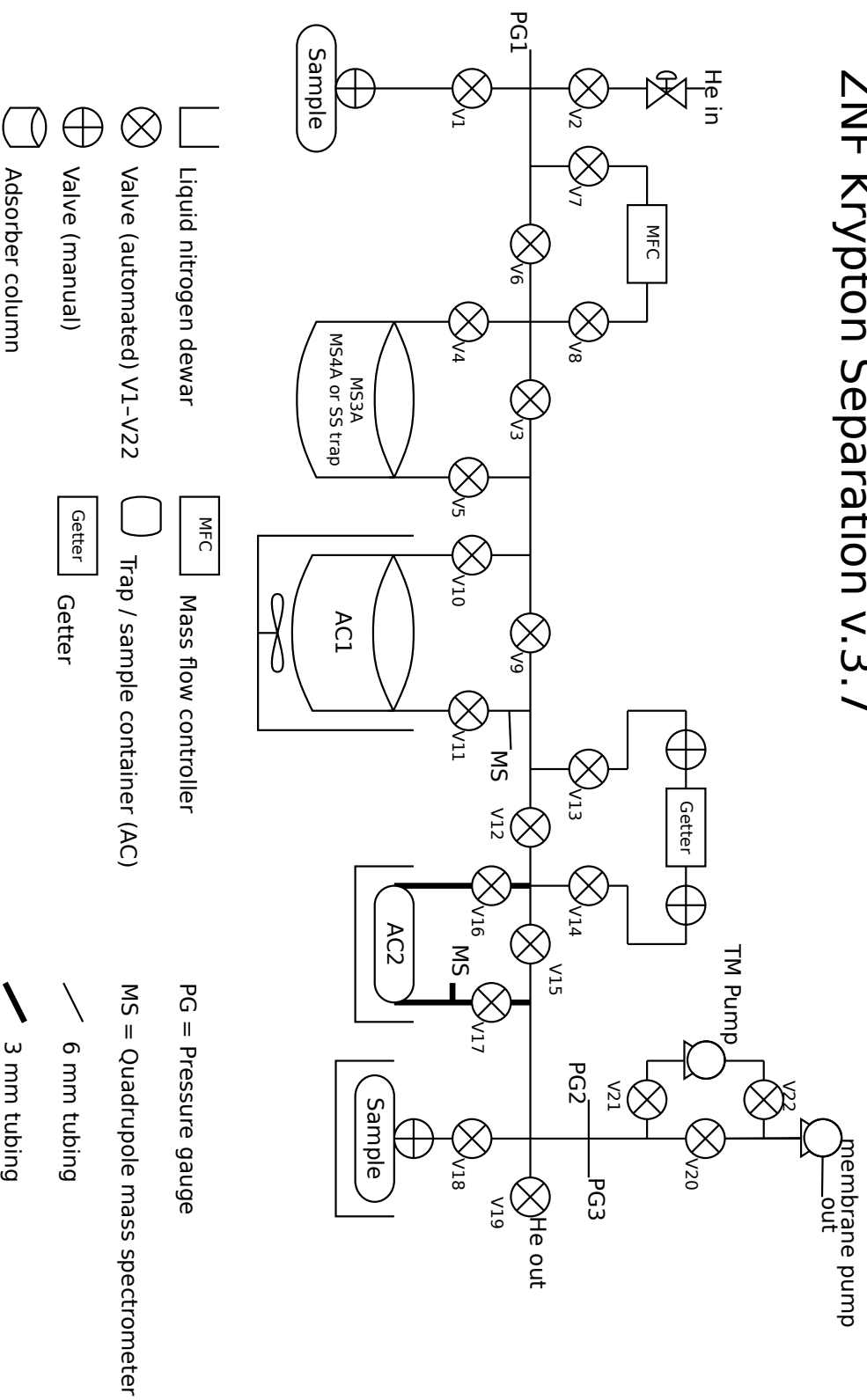


Figure 4.19.: The final layout of the Krypton separation line, the “Krypton-Abtrennungs-Anlage (KAA)”.

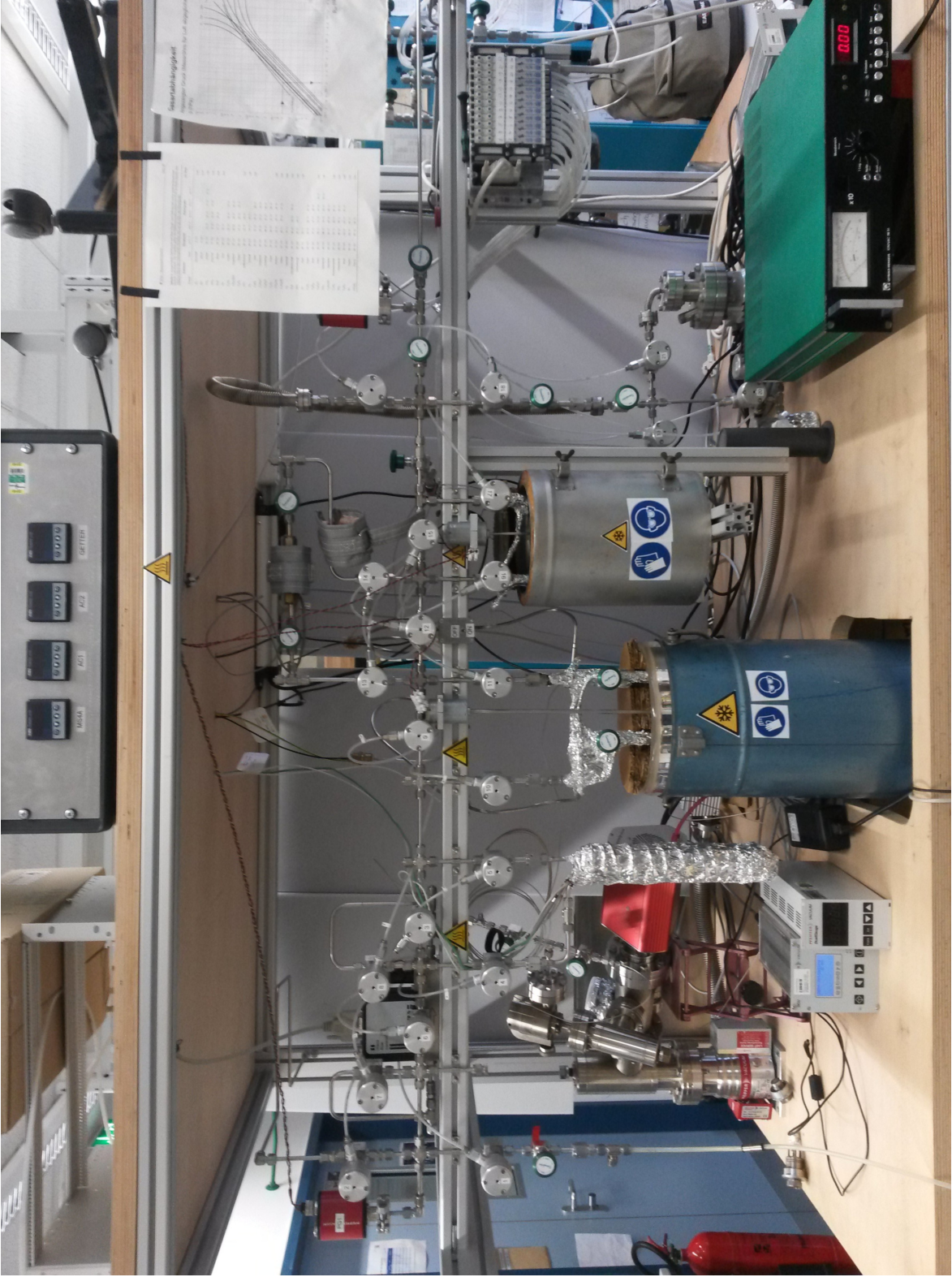


Figure 4.20.: The krypton separation line "Krypton-Abtrennungs-Anlage (KAA)" at the University of Hamburg.

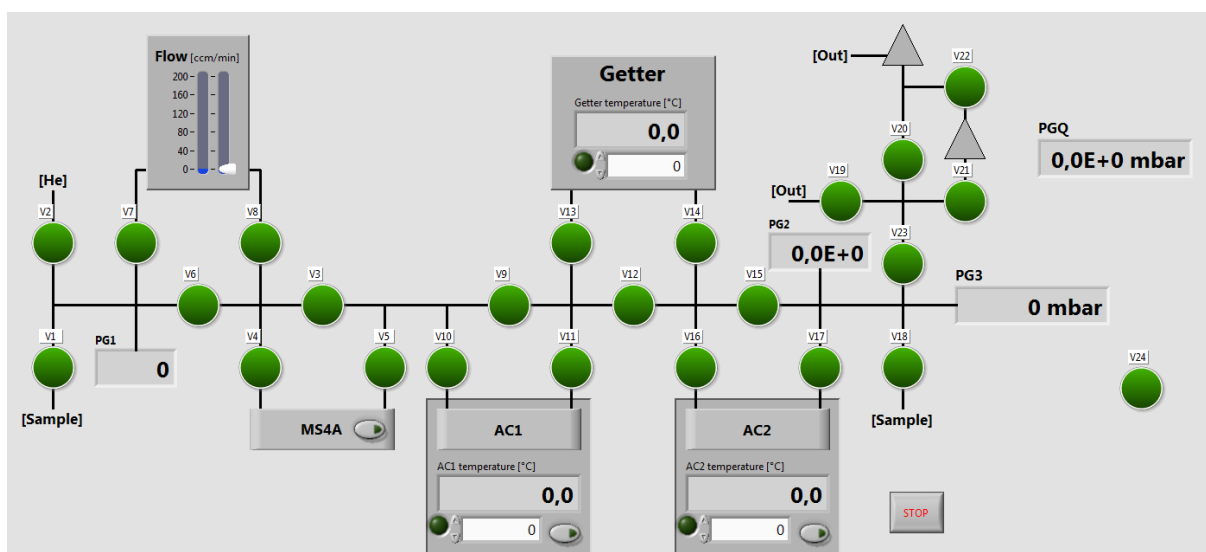


Figure 4.21.: Virtual interface of the krypton separation line as implemented in LabView, allowing manual control of all components. The green lights signify valve status and are interactive. Helium flow as well as temperatures can be monitored and set.

Helium The helium is introduced via valve V2 and has a constant pressure of about 1500 mbar.

Pumps Two pumps are cooperating in the krypton separation line. A diaphragm pump (Pfeiffer MVP 015-4) is used as a roughing pump to remove large gas amounts. It is rugged enough to cope with the higher pressures of up to 2000 mbar that can arise during routine operation, and brings the pressure down to 0.5 mbar when operating smoothly.

Optionally, a turbopump (Pfeiffer HiPace 80) is used to achieve lower pressures and clean the system of residual gas. It is constantly running and can be connected by closing valve V20 and opening valves V21 and V22, but only when the residual pressure in the separation line is below 2 mbar as higher pressures can cause the pump to overheat and shut down. The diaphragm pump doubles as booster for the turbopump.

Both pumps are virtually free of inline lubricants and therefore do not exude carbohydrates, which is a major requirement at the atom trap trace analysis laboratory.

4.3.2. Control, automation and monitoring

The krypton separation line is controlled using the National Instruments LabView 2013 framework, which facilitates collecting data from a multitude of different sources and protocols and bundling these resources in a single interface. The code is modular and easily adapted.

In LabView, programs take the form of virtual instruments (VI), each of which has an interface presenting relevant information and controls to the user.

The main data sources are serial RS-232 and RS-485 protocols (for digital pressure gauges PG1 and PG3 and temperature controllers) and the Pfeiffer serial protocol (for the Pfeiffer DualGauge controller which integrates analogue sensors PG2 and PGQ), all of which are connected using USB-serial-adapters.

A number of analogue signals are managed by an Arduino Mega microcontroller, which can be operated in LabView using the LYNX framework and firmware. These include the input and output of the flow controller and the self-developed solid state switches and relay switches for controlling the cooling fans and valves.

4.3.2.1. Manual control

All functions are implemented in the control interface¹⁶ shown in Figure 4.21, which is used for manual control of the krypton separation line and all of its components. The only exception is the quadrupole mass spectrometer, which is controlled separately by its own driver software.

4.3.2.2. Automation and logging

The automation is implemented in a separate automation interface¹⁷. It will parse instructions for the separation procedure and pass them to the control interface, which in turn controls the krypton separation line. While the automation interface is running, the user still has full control over the control interface and may intervene at any time. The automation interface is shown in Figure 4.22.

It also records all parameters which are displayed in the control interface and saves a complete log of all system parameters while it is running, including pressures, temperatures and valve states. The log files are human readable text files automatically deposited in folders according to date.

¹⁶Filename: "KAA.vi"

¹⁷Filename: "KAA-Controller.vi"

4.3.2.3. Evaluation

All separation runs and other experiments can be evaluated based on the data collected by automatic logging.

A software implemented in the Python 3 programming language will, when called, parse any given log file and calculate a result. For a regular separation experiment, this result is the Kr-84 peak area in A·s (Ampere-seconds), not the peak height.

This value is usually not a meaningful measure of the actual separation performance, as it depends on a number of variables such as the pressure in the quadrupole mass spectrometer chamber, filament temperature and age, which have varied in the course of several months in which the experiments have been conducted. The peak area can be used to compare the relative efficiency of separation runs, especially when the runs are consecutive and parameters are varied systematically.

Evaluation script The evaluation script¹⁸ is used to evaluate a separation run.

The evaluation encompasses the following steps:

1. Calculate the average quadrupole mass spectrometer current for mass 84 in minutes 6–10 of the separation run. This background is subtracted from the mass 84 current so the signal is positive at all times. This is preferable to simply subtract the lowest measurement value, which can vary from sample to sample. This and the next step are necessary mainly to facilitate automated peak correction.
2. To correct for fluctuations in the signal caused by pressure fluctuations, the signal for mass 87 is subtracted from the mass 84 signal. Mass 87 was chosen as a blank because there is usually no such gas species present, and it is close enough to mass 84 to react similarly to background effects.
3. On the corrected signal, a rough peak detection is performed, and the peak closest to the expected detection time of krypton is identified. This is necessary as even with background correction, the krypton peak is not always the maximum of the overall mass 84 signal. By default, the peak is expected at 50 minutes, but if for whatever reason¹⁹ the script selects the wrong peak, the user can forward a different time value instead when the peak can be identified by visual inspection of the signal.
4. A Gaussian is fitted to the detected peak, which is a good approximation for the average gas peak exiting from a chromatography column, according to experi-

¹⁸Filename: "KAA.py"

¹⁹As experiments with many different parameters and retention times are performed, it is difficult to write a peak detection function which foresees all eventualities.

ence and theoretical plate theory (see Section 2.2). By default, the fit is marked in the chromatogram.

5. The Gaussian is integrated to obtain the approximate peak area in Ampere-seconds. A baseline is calculated to account for the remaining background.

Based on the integrated flow, the approximate volume of the air sample is also calculated.

Visualisation script The visualisation script²⁰ is used to parse log data and show selected signals in a graph, intended for easy visualisation and analysis of parameters and measurement values. One example can be seen in Figure 4.25 auf Seite 84.

4.3.3. General separation procedure

The krypton separation line is laid out as shown in Figure 4.19.

The air sample is connected on the “left” side of the line and traverses the mass flow controller (MFC) and desiccant (MS4A) before being frozen onto charcoal column AC1. A helium carrier gas stream is then introduced, and AC1 is heated to room temperature. The effluent gases are continually monitored using a quadrupole mass spectrometer which is connected using a capillary near the exit of AC1.

After the nitrogen, argon and oxygen peaks have passed, the gas stream is redirected through the getter and the cooled charcoal trap AC2. The krypton peak now leaved AC1, is cleaned from any remaining nitrogen and oxygen by the getter, and frozen onto AC2.

Afterwards, AC2 is heated again to release the krypton, which is then frozen onto the final sample container.

4.3.4. Optimisation of the separation procedure

While the general separation procedure outlined in the previous section is simple, robust, tried and tested, it requires large degree of optimisation in order to provide an acceptable yield and purity for small air samples of 1 L. This section identifies potential problems and describes the systematic experiments conducted to quantify their influence and obtain the optimal procedure for each step of the separation.

4.3.4.1. MS4A troubles

The vessel “MS4A” containing a 4 Å molecular sieve is dimensioned generously in order to desiccate several samples before regeneration is required, but offers a high

²⁰Filename: “KAAplot.py”

Table 4.6.: Relative yields in separation runs using a different number of flushing procedures for the MS4A molecular sieve. A very slight increase can be observed for the 2nd flush, while the 3rd flush does not increase the yield. Results are from 2016/11/21.

n flushes	yield $\pm 1\sigma$ [10^{-14} A·s/cm ³]	peak width [min]
1	0.96 ± 0.05	2.0
2	1.02 ± 0.06	1.9
3	1.01 ± 0.06	2.0

flow resistance due to the installed sinter filters. As a consequence, a large dead volume which is not easily evacuated of N₂ remains in front of the charcoal trap.

If MS4A is not shut off during the separation run, N₂, Ar and O₂ continually seep from it during the separation and contaminate the krypton peak, as seen in Figure 4.23. Closing off MS4A, on the other hand, bears the risk of trapping the remaining krypton within, reducing the yield. As a compromise, helium “flushing” has been introduced as an extra step before the heating and chromatography run: as soon as the pressure before the trap AC1 has dropped to 750 mbar, the helium carrier valve will be opened, increasing the pressure to 1500 mbar, and closed again. Now, the higher pressure accelerates the diffusion of the remaining sample into AC1.

The above procedure can be repeated several times to achieve a better yield, with every flush increasing the overall duration by 3–4 minutes. Mathematically, repeating the procedure 3 times will flush at least 94 % of the sample into AC1. Assuming that krypton and nitrogen share similar diffusion kinetics on 4 Å molecular sieve, this results in a tradeoff of 6 % yield versus a considerable increase in purity, as the remaining nitrogen is still much more abundant. The actual krypton loss is probably smaller, as krypton traverses the molecular sieve more readily than nitrogen does.

To assess how the number of flushings affects the yield, separation runs have been conducted, see Table 4.6. The results show a slight increase in yield for the first 2 flushings. After that the yield is identical within the margin of error. For the final separation procedure, three flushings have been implemented to be on the safe side.

4.3.4.2. Stability of results and error propagation

In order to assess the effect of changes to the separation procedure on performance and yield, the krypton peaks as observed by the quadrupole mass spectrometer are integrated and normalised for sample volume. The resulting yield is expressed in units of A·s/cm³. As already discussed, the quadrupole mass spectrometer peak is not an absolute measure of performance because of its long term variability, but suitable for a relative, short term comparison. This is the case whenever measurements are

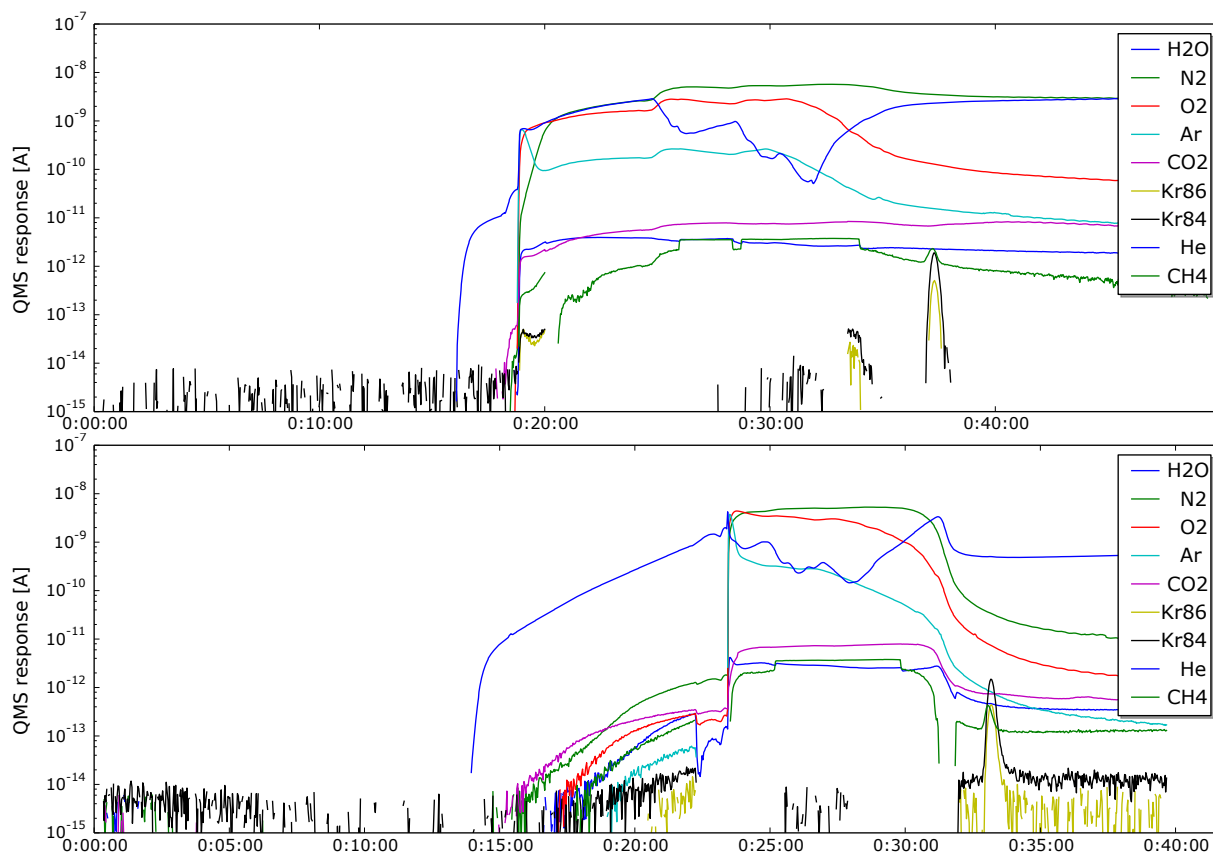


Figure 4.23.: Two separation runs to compare the effects of gases remaining in molecular sieve 4 Å. For the upper run, MS4A is not shut off and leaks nitrogen (28), argon (40) and other gases throughout the separation procedure. In the lower run, MS4A is shut off before the actual chromatography, and undesired gases drop sharply before the krypton peak passes. The actual krypton peak occurs about 12 minutes after heating the trap AC1. Experiments were conducted on 2015/09/23.

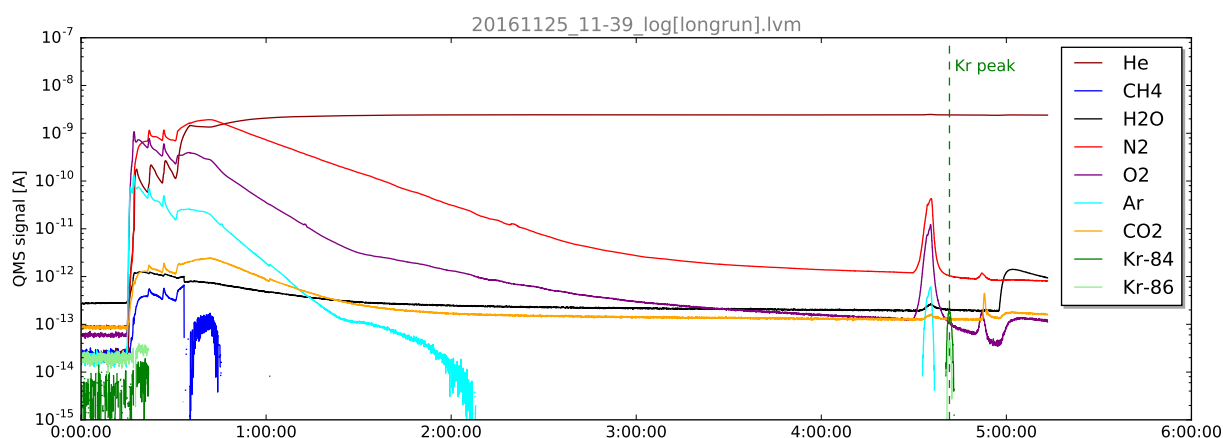


Figure 4.24.: After starting a separation procedure as normal by drawing the sample onto column AC1 at 80 °C and starting the He carrier stream, the temperature is not increased for 4 hours. Afterwards, the column is heated and the remaining gases are released: nitrogen, oxygen, argon as well as all of the krypton.

available which were conducted within a few days of each other.

The uncertainties for these peak integrals are mainly the sum of the statistical uncertainty of the peak area and the uncertainty of the sample volume determination. Based on a number of measurements²¹, the relative standard deviation for the peak area can be approximated to $1\sigma = 5.5\%$.

4.3.4.3. AC1 temperature and timing

The temperature of AC1 is central to the separation process, necessitating a good compromise between low temperature to retain the krypton and high temperature to release contaminants. An additional barrier holding back the krypton is provided by the sheer length of the charcoal column.

The boiling point of krypton is about -153 °C, but in activated charcoal, the krypton is effectively frozen at much higher temperatures. To determine the maximum allowable temperature, experiments were conducted on AC1 by setting a certain temperature, adsorbing the sample onto the column and starting a helium stream analogous to the regular separation procedure. The highest temperature not showing any breakthrough was -60 °C. Figure 4.24 shows one of these experiments at -80 °C, where no krypton was exiting the column after 4 hours of continuous carrier stream, with no more argon and only small amounts of nitrogen and oxygen seeping from the column.

To ensure the applicability of these results, separation runs have been conducted us-

²¹Measurements conducted on 2016/03/24, 2016/05/25, 2016/05/26, 2016/07/20, 2016/11/18.

Table 4.7.: Results of identical separation runs with the same sample size using different starting temperatures for trap AC1. The peak area is unaffected, but the peaks are broadened for higher temperatures. The results are from 2016/03/03–04.

T_{AC1} [°C]	peak width [min]	yield $\pm 1\sigma$ [10^{-15} A·s/cm ³]
-120	2.9	8.63 ± 0.48
-100	2.8	8.30 ± 0.46
-80	3.5	7.91 ± 0.44
-70	4.0	8.22 ± 0.45
-60	4.8	8.43 ± 0.46

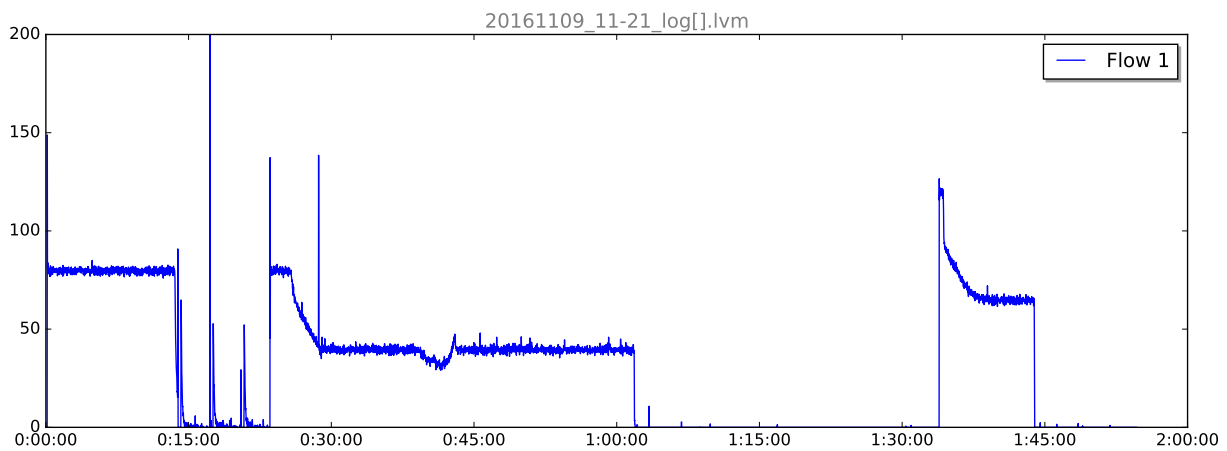


Figure 4.25.: Gas flow in cm³/min as measured by the flow meter during a normal separation procedure. Most critical is the time from 0:34:00 onward, when the heating commences. If heating had started prematurely or was conducted to quickly, the expanding sample would have pushed back against the carrier gas, reducing the flow rate.

ing different base temperatures for AC1, and the heating curves have been shortened accordingly. The results in Table 4.7 suggest that up to -60 °C, the peak area stays the same, indicating that no krypton is lost. Higher temperatures yield wider peaks, suggesting enhanced mobility of the krypton phase.

To benefit from reduced contamination, while observing a generous safety margin, the temperature for routine operation is set to -80 °C. The heating curve remains as outlined in Table 4.3 auf Seite 69, but starting at -80 °C and running for 3 minutes. Figure 4.25 shows the carrier flow during a separation procedure, demonstrating that the heating curve does not adversely affect the result by driving part of the sample out of the entry.

A higher starting temperature provides the added benefit of faster operation mainly

Table 4.8.: Test separation runs using increasingly long pauses (t_{pause}) between switching on the carrier gas and heating charcoal column AC1. The emerging krypton peak retains about the same size (yield) and width and always emerges at a definite time ($t_{\text{heat}}-t_{\text{peak}}$) after the start of heating.

t_{pause} [min]	$t_{\text{heat}}-t_{\text{peak}}$ [min]	yield $\pm 1\sigma$ [10^{-14} A·s/cm ³]	peak width [min]
0	12.5	1.03 ± 0.06	2.4
4	11.5	1.00 ± 0.06	2.0
10	10.0	1.05 ± 0.06	1.5
15	11.5	1.03 ± 0.06	2.1
20	11.0	1.01 ± 0.06	2.0

due to less time being required for cooling. Cooled passively, AC1 will reach -80 °C within 30 minutes, -100 °C within 40 minutes and -120 °C within 65 minutes. All of these times can be accelerated by directed user interaction, e.g. repeatedly pouring liquid nitrogen directly onto the trap, but the time between samples is nevertheless reduced significantly.

4.3.4.4. Pause before heating

Section 4.3.4.3 has shown how krypton is practically frozen on activated charcoal at -80 °C, while other air components retain at least some mobility. This effect is used to achieve additional sample purification by prolonging the time until heating the column. To investigate the effect on separation yield, a number of separation runs have been conducted using increasing pauses between the steps of switching on the carrier gas and heating AC1. The results listed in Table 4.8 indicate that the length of the pause does not seem to affect the krypton peak in any way: the yield and peak width remain the same. Moreover, the time between the start of heating and the emergence of the peak do not systematically deviate.

At the same time, a significant drop in argon contamination is apparent (see Figure 4.26), and other gases are also reduced.

Overall, the pause is an effective measure to increase purity, while also extending the time of the whole separation procedure. In the routine program, a pause of 20 minutes is implemented as a compromise.

4.3.4.5. AC1 end temperature

The speed of the krypton phase within the charcoal column is relatively slow even at room temperature. Although a clearly defined peak is the only visible occurrence, a rest of the sample may remain within the column after the peak is passed. Additional

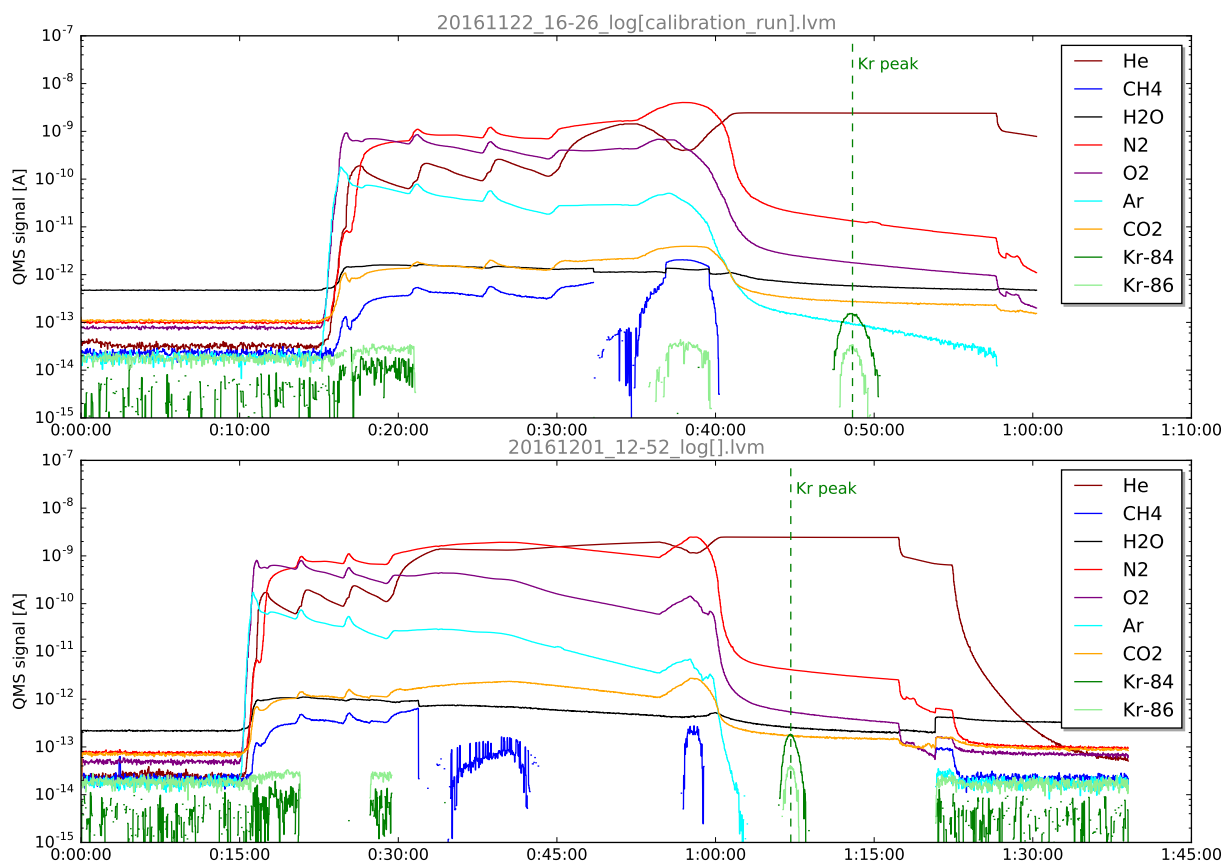


Figure 4.26.: The chromatograms of two separation runs using no pause (upper figure) and 20 minute pause (lower figure) between switching on the carrier gas and heating charcoal column AC1. During the pause, the temperature of AC1 remains at $-85\text{ }^{\circ}\text{C}$. The krypton peaks occur at 48 respectively 66 minutes; at that time, there is still a considerable amount of argon (light blue) seeping from the column in the run without a pause, whereas Ar is not detectable during the peak if a 20 minute pause was observed.

Table 4.9.: Resulting gas signals in a quadrupole mass spectrometer measurement of the purified sample with an identical separation procedure, but using two different temperatures for the capturing trap AC2. While krypton and argon remain constant, the nitrogen contamination has been reduced by 75 %. The experiments were conducted 2016/02/11.

T_{AC2} [°C]	I_{Kr} [A]	I_{Ar} [A]	I_{N2} [A]
-150	1.9e-12	6.5e-12	1.2e-12
-120	1.9e-12	6.4e-12	0.3e-12

heating facilitates the complete removal of krypton from the column and decreases the likelihood of cold spots due to irregular heating of the column.

The effects of increased working temperature during the chromatography have been investigated, heating the column up to 120 °C instead of 20 °C room temperature. Doing so increases the background in two ways. First, the elevated temperature accelerates the overall procedure, resulting in a sharper krypton peak, which occurs earlier and thus has more overlap with the nitrogen and argon peaks. Secondly, heating the charcoal causes an elevated CO₂ release, which puts more strain on the getter.

Despite these effects detrimental to sample purity, no increased yield was observed. The compromise is a temperature of 40 °C, which causes no CO₂ seepage but still decreases the chance of krypton remains.

4.3.4.6. AC2 temperature

Trap AC2 is much smaller than AC1, so while the considerations for finding the optimal adsorption temperature are similar, its small size offers a smaller surface for krypton to settle, so a lower temperature has been planned from the start. The focus of development has been placed on purifying the krypton during the chromatography and gettering stages.

Because of variations in peak position and size, and the automatic switching, the time window in which the gas stream is directed through AC2 is several minutes longer than the actual peak width. Any remaining nitrogen and argon contamination are spread out over all this time, possibly accumulating in AC2.

To find an optimal compromise, several temperatures for AC2 have been tested regarding their performance. Some of the results listed in Table 4.9 indicate that a slightly higher temperature will help reduce the remaining nitrogen contamination, but not argon.

In the end, and adsorption temperature of -120 °C has been chosen for AC2, which provides the same krypton yield than a lower temperature, but reduces any potentially remaining nitrogen contamination by 75 % compared to -150 °C.

Table 4.10.: Comparison of krypton separation line performance for different sample sizes using normal air. The yield seems to drop slightly for larger samples and peak width broadens considerably.

T_{AC1} [°C]	V [L]	yield [A·s/cm ³]	peak width [min]	$t_{heat}-t_{peak}$ [min]
-100	1	1.34e-14	3.0	18.5
	2	1.28e-14	4.3	18.0
	3	1.15e-14	5.5	17.0
	4	1.12e-14	7.3	16.5
	5	1.23e-14	10.1	13.0
-80	2	1.11e-14	5.9	18.0
	6	0.84e-14	17.6	14.0

4.3.4.7. Sample size

The krypton separation line is laid out with small samples of 1 L in mind. Depending on the device used to measure the purified sample, a larger size might be necessary. To evaluate separation performance, sample sizes of up to 6 L have been processed. The results are depicted in Table 4.10. The yield per litre is relatively constant and is seeing only a slight drop for increasing sample sizes, while the krypton peak itself is broadening about 30–40 % per additional litre.

When going above 5 L, one faces a different problem. Due to the broadening of the peak, the time between the start of heating and, consequently, the separation power are reduced and the peak might even visibly overlap with the other gases (see Figure 4.27). This may be alleviated using an extended pause before heating as described in Section 4.3.4.4, but is still a concern.

4.3.4.8. AC2 capture timing

The results presented in Sections 4.3.4.7 and 4.3.4.4 show that the exact position of the peak can vary to some degree. While, with identical heating speed, the time from the start of heating to the peak maximum is relatively constant, an increasing sample size causes the peak to occur earlier.

In the automated procedure, the time window for adsorption of krypton on trap AC2 is determined relative to the start of heating, meaning that larger samples require an adapted program with times specifically calibrated for the sample size. It has been explicitly avoided to trigger the opening of AC2 via the quadrupole mass spectrometer krypton signal as a manual operator would, because automatic peak detection is less robust.

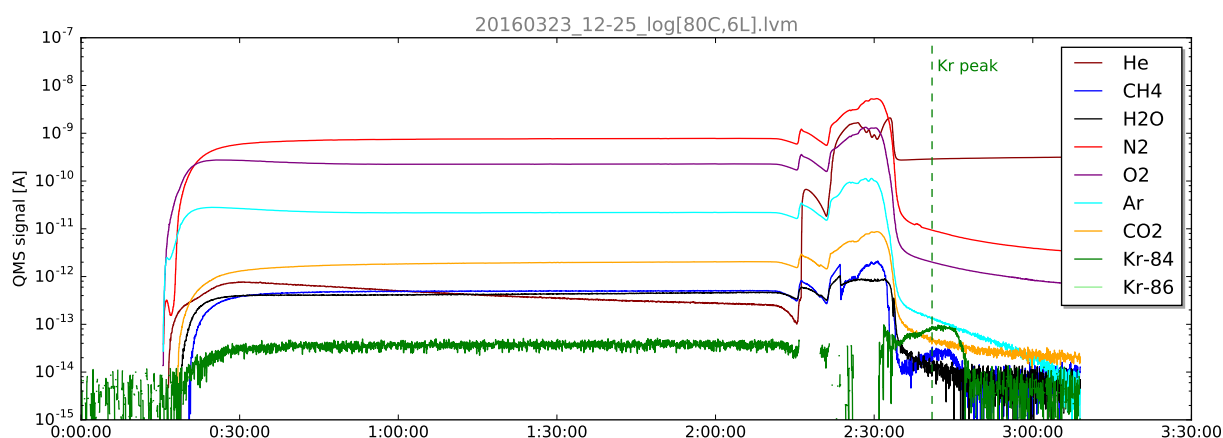


Figure 4.27.: Separation run in the krypton separation line for a large 6 L air sample. Note how the krypton peak strongly overlaps with the other gases.

4.3.4.9. Sample concentration

The krypton fraction of samples is small, even when using enriched samples instead of pure air. To investigate whether the sampling procedure needs to be adapted according to the krypton content of the sample, two test samples of 1 L with differing Kr content have been compared. Figure 4.28 shows that the enriched sample has a peak 8.9 times the size of the ambient air sample, the peak occurs at the same time, i.e. 13.5 minutes after the start of heating trap AC1.

Incidentally, this experiment was conducted using the same enriched standard sample as in Sections 5.2 and 5.3, which was assumed to contain a krypton concentration five times as large as that of ambient air. This result already hints at that the sample may have contained a higher concentration, about eightfold ambient value for mass 84 (see Section 5.3.4).

4.3.4.10. Transfer to krypton container

After storing the sample in trap AC2, it needs to be transferred to the sample container described in Section 4.2.8. This process cannot use a carrier gas and must rely on diffusion alone despite the low flow coefficient. While heating AC2 to a temperature of 200 °C and freezing the krypton container using liquid nitrogen, only the necessary valves are opened to keep the dead volume small.

Several experiments have been conducted to estimate transfer efficiency, transferring the sample back and forth between the krypton container and AC2. Measurements were limited to AC2 because the krypton container could not be easily connected to the quadrupole mass spectrometer without a significant dead volume, which reduces the pressure of krypton below the detection threshold. For the measurement,

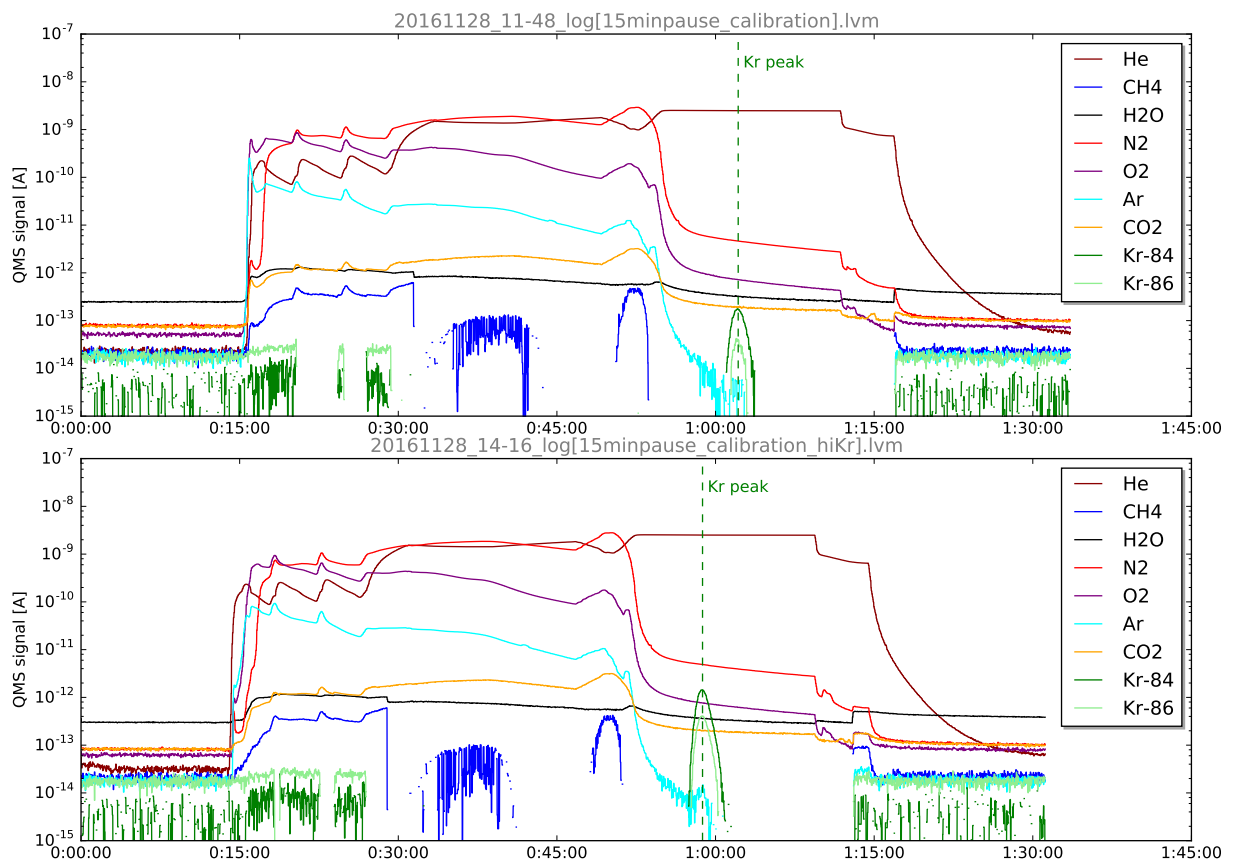


Figure 4.28.: Two separation runs using ambient air (upper graph) and air enriched in krypton (lower graph). As expected, the peaks occur at the same time relative to the start of heating the trap AC1. The higher Kr concentration is clearly visible by comparing the mass 84 peaks.

Table 4.11.: Krypton loss when transferring from one cryotrap to another. The first experiment was using a 5 minute time window and showed significant loss per transfer. No krypton loss was observed for a 10 minute transfer window. The measurements were conducted using a quadrupole mass spectrometer using a fixed helium pressure as reference. Results are not directly comparable between experiments.

experiment	transfer [min]	n transfers	I_{84}/I_4	loss per transfer [%]
2016/05/19	5	0	7.3 ± 2.3	
		2	3.9 ± 0.8	23 ± 16
		4	0.36 ± 0.14	46 ± 10
2016/05/24	10	0	0.54 ± 0.10	
		2	0.55 ± 0.12	-1 ± 15
2016/05/25	10	0	1.31 ± 0.18	
		2	1.37 ± 0.19	-2 ± 10
		4	1.29 ± 0.17	3 ± 10

10 mbar of helium were introduced into AC2 to serve as baseline and increase the flow from AC2 to the quadrupole mass spectrometer chamber.

The results in Table 4.11 indicate that a long transfer time is necessary to avoid sample loss. For a 5 minute transfer window, about one third was lost per transfer, with a high margin of error. Using a 10 minute window, no sample loss is observed.

4.3.4.11. Cross-contamination

Care has been taken to establish an effective cleaning procedure between successive samples:

- AC2 After the final sample transfer, AC2 is evacuated at 200 °C using the turbo pump for 10 minutes. It is a small trap, so this procedure should be more than sufficient.
- AC1 AC1 is then heated to 200 °C and flushed with the He carrier for 10 minutes, followed by evacuation for another 10 minutes.
- MS4A Finally, MS4A is flushed with He for 10 minutes to get rid of excess nitrogen, which should also remove any remaining krypton. At this point, MS4A is not baked because cooling takes a long time and prohibits more sample runs on the same day. Instead, heating to 300 °C takes place for two hours after the last sample to purge water and CO₂ and the MS4A can cool down over night.

Of course, these are precautionary measures, as ideally, the sampling procedure will not have left any krypton in any of the traps and dead volumes.

To observe whether cross contamination was detectable, on three occasions after preparing an enriched sample a blank separation run using pure nitrogen instead of a normal air sample. None of these had a krypton peak or enhanced krypton signal visible in its chromatogram. Of course, the quadrupole mass spectrometer will only observe on point in the line, but it accounts for the critical phase when the enriched krypton is transferred to trap AC2; any krypton that cannot be observed at this point would probably not end up in the purified sample.

Based on the experience with the peak sizes that can be clearly detected above background, it is estimated that a cross-contamination of 0.1 % would have been detectable using a blank sample. Further investigations will require experiments using highly enriched samples and a trace measurement capability.

Cross contamination in the krypton container has not been investigated, but should be negligible according to experience²².

4.3.4.12. Sample purity

To estimate the purity of a separated sample, charcoal trap AC2 has been temporarily fitted with a capillary connection leading to the quadrupole mass spectrometer. After the separation procedure, 15 mbar of He were introduced into AC2 before closing and heating the trap. This He pressure is sufficient to observe a signal at the quadrupole mass spectrometer. One such measurement is documented in Figure 4.29. In general, no impurities have been observed in these measurements, which does not necessarily mean that none are present. Impurities might be below the detection sensitivity of the quadrupole mass spectrometer, which only uses a Faraday cup. The signal for mass 84 is three orders of magnitude above the background. A comparison with a gas standard²³ suggests that impurities up to 20 % of N₂ and 30 % of Ar could go undetected in this case.

These degrees of impurity are sufficient for measurement in the atom trap trace analysis, but any remaining N₂ has to be removed before coming in contact with the MgF windows. Transport of the sample to the atom trap trace analysis also has the potential to introduce impurities, so an additional getter at the entry point is advised.

4.3.5. Final separation procedure

This section will describe the finalised procedure for separating krypton in the krypton separation line, building upon the components whose development is detailed in Sec-

²²Personal communication with laboratory personnel at University of Bern.

²³25 % Ar, 25 % Kr, 26 % N₂, 24 % He

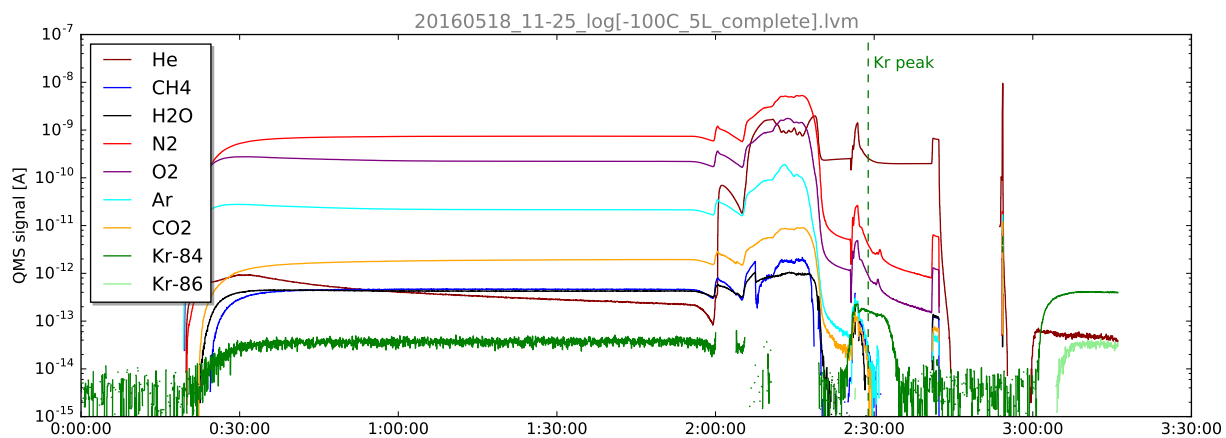


Figure 4.29.: Separation of 5 L of air using the krypton separation line. After separation, the sample has been mixed with He and can be observed in the quadrupole mass spectrometer, visible after the 3 hour mark. Notably, only Kr-84 and Kr-86 are visible, implying a high purity of the sample.

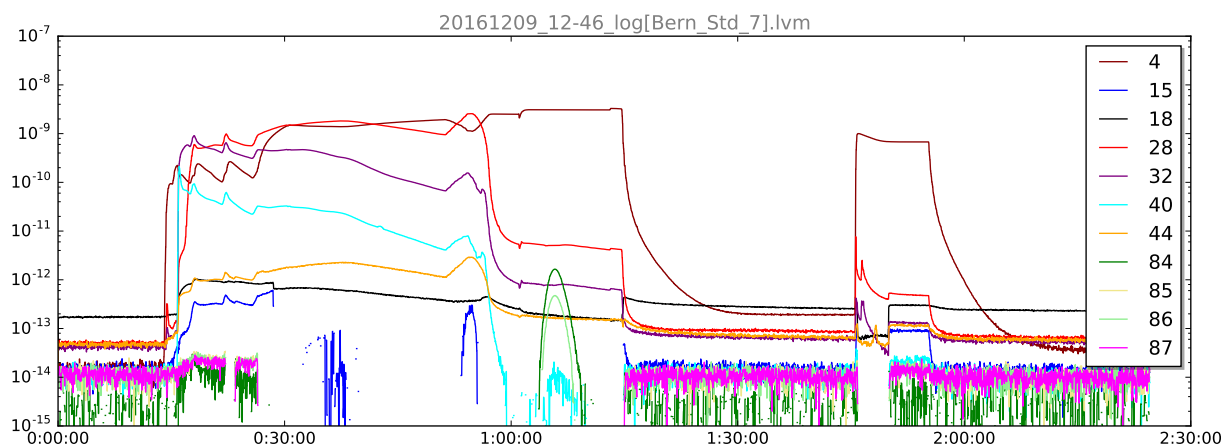


Figure 4.30.: Chromatogram of a typical separation run as recorded by the quadrupole mass spectrometer. All such chromatograms are watermarked with the file-name of the log file.

tion 4.2. For the layout of the separation line, please refer to Figure 4.19.

An exemplary separation run output is shown in Figure 4.30 and referred to throughout this section. The detailed program is listed in Annex A.

Before starting the separation, the operator is required to manually conduct some preliminary steps: the sampling bag is connected to the line via the entry valve, which is the manual valve below V1, which is then opened. AC1 and AC2 are cooled to -80 °C and -120 °C respectively. All components need to be evacuated if not already done so. A sample container must be connected to the manual valve below V18, opened and evacuated.

Upon activation of the automated procedure, V1 is opened and atmospheric pressure is pushing the sample out of the bag through the mass flow controller (MFC) and the moisture trap (MS4A) into AC1. All the while, the far end of AC1 is pumped using the turbo pump, and the other components (Getter, AC2) are shut off from the main line. Most of the sample will be frozen onto MS4A, the sample flow is limited to 80 cm³/min. At -120 °C, all gases except xenon and krypton will remain partially mobile, but their movement along the column is very slow.

When the sampling bag is empty and the pressure at PG1 decreases, V1 is closed. At this time, part of the sample is still present in MS4A. To speed up the adsorption process, the helium carrier gas is used to flush MS4A three times: each time the residual pressure drops below 750 mbar, V2 and V6 are opened to increase pressure to 1500 mbar, and closed again, while still pumping on the far end of AC1. Coincidentally, Ar, N₂ and O₂ will start to exit the column along with the carrier gas, so the turbo pump is bypassed to cope with the increasing pressure.

Afterwards, MS4A is disconnected and the carrier flow is set to 66 cm³/min by opening V2 and shutting off the pump by closing V20. When the pressure on the far end of the line has reached 1 atm, V19 is opened, guiding the carrier off gas stream out of the krypton separation line. This carrier gas stream is now continued for 20 minutes during which the air components are partially separated from the immobile krypton.

Now AC1 is slowly heated to 40 °C. All gases are completely desorbed and travel along the column, the exit of which is continually monitored by the quadrupole mass spectrometer. After about 20 minutes of heating, 55 minutes into the whole separation run, the levels of N₂, Ar and O₂ drop sharply. The gas stream is now rerouted through the getter and AC2 for 12 minutes. The getter is removing the remaining N₂ and O₂, leaving only argon and krypton which are adsorbed in AC2. A krypton peak will require about 2 minutes²⁴ to travel from AC1 to AC2, so AC2 should remain open for at least 2 minutes after the krypton signal to the quadrupole mass spectrometer has ceased.

²⁴Between AC1 and AC2 there is a volume of approximately 40 cm³, including tubing, valves and getter. When AC2 is active, its low flow coefficient will slow the carrier gas to approximately 50 cm³/min. Theoretically, the volume could be exchanged in under 1 minute, but additional time should be allowed to account for turbulence.

A few minutes after the peak has passed, V19 is closed. The entrance of AC2 is also closed and the trap is evacuated to remove excess helium, before completely shutting off AC2 by closing V17 and performing a rough evacuation of the whole separation line to minimise potential sources of contamination.

Now, all valves except V15, V16, V17 and V18 are closed, creating a direct connection between AC2 and the sample container, and AC2 is heated to 200 °C for 15 minutes to transfer the krypton. AC2 has been cooled by liquid nitrogen throughout the separation. The 15 minute time window is necessary to completely transfer the krypton despite the low flow coefficient between AC2 and the container.

Finally, V18 closes and the separation is finished. The operator may now close the manual valve and remove the sample container, which should be done before the level of nitrogen cooling it drops too low. The program will continue to evacuate and bake all components of the separation line in order to prepare for the next sample.

The sample can now be archived or transferred to measurement.

4.3.6. Routine operation

Using the procedure described above, a routine sample preparation can be upheld with only momentary attention of laboratory staff.

Before starting the separation, the dewars must be filled with liquid nitrogen and the traps cooled to -80 °C and -120 °C. While they are cooling, the purified sample vessel can be connected, evacuated and baked using a hot air gun, and of course the sampling bag must be connected. This preparation takes about half an hour, 15 minutes of which are waiting time.

The actual separation takes about 1.25 hours without any operator interference. Afterwards, a regeneration procedure is started which lasts another 20 minutes, during which the purified sample can be removed. Subsequently, the traps are set to cool down again, but before the working temperature for the next sample is reached, liquid nitrogen reservoirs require a refill, and the next sample bag and container must be connected.

When the working day is done, an enhanced baking procedure can be initiated over night to clean MS4A of water and remaining nitrogen, and the getter is set to 350 °C to regenerate.

Overall, each sample takes a bit over two hours to process, with up to 15 minutes of manual operation per sample, making for 4–5 samples that can be processed on a normal working day.

5. Evaluation of separation performance

In order to obtain a precise evaluation of the separation line's performance, samples were separated locally and measured at the University of Bern, where a suitable, calibrated gas chromatograph is available.

Using the local quadrupole mass spectrometer only serves as a relative reference because results are only precise if the measurements are conducted under controlled and calibrated conditions using well defined standard gases.

Even if such a standard could be fabricated locally, comparison is difficult due to the fact that the purified sample has an inconvenient size. A proper quantification requires the capability of precisely measuring pressures in the order of 1 mbar. A pirani gauge is not suitable for the task as the readout is highly dependent on the gas composition. Gas type independent gauges, like membrane gauges, which provide a resolution better than 10 % for this pressure range are not available on the market. A more suitable method of measuring the yield would be to utilise a noble gas mass spectrometer, which was not available for this work, but might be an option for future campaigns.

To compensate, another method was chosen, namely the radiological measurement of the sample's krypton-85 content. The trials were conducted using large ambient air samples as well as enriched samples to evaluate the performance at the target size of 1 L.

Unless stated otherwise, uncertainties of values are expressed using the standard deviation of 1σ .

5.1. Ambient air sample

As a first step, a large sample of ambient air was used. In order to provide a strong Kr-85 signal for measurement, a large air sample was taken and split: 5 L were processed using the krypton separation line and sent for measurement in the underground laboratory of the University of Bern. The remaining 30 L were also sent there to evaluate the krypton-85 concentration using Bern's routine procedure (see Section 3.4.2).

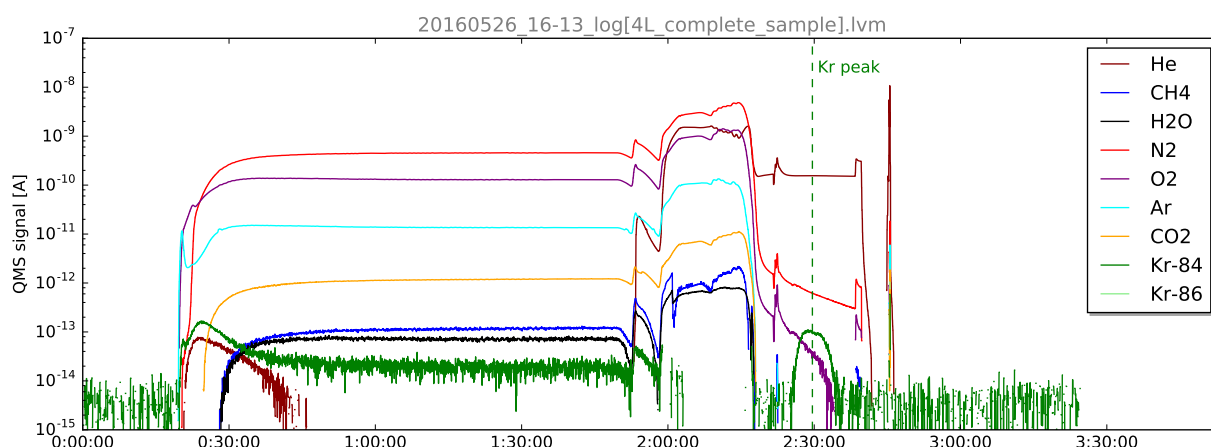


Figure 5.1.: Chromatogram of the separation routine for a 6 L ambient air sample. The krypton peak is displayed in green and marked.

5.1.1. Separation procedure

Unfiltered ambient air was sampled in the laboratory at University of Hamburg on 2016/05/26. The air was collected and compressed into a 50 L PVF¹ bag using a membrane pump, with the krypton separation line's mass flow controller used to determine the sampled volume of 34.7 ± 0.35 L. Approximately 6 L were then pumped into another PVF bag, which was in turn connected to the krypton separation line for separation.

All transfers and connections were made using PTFE tubing and push connect or quick connect couplings providing sufficient leak tightness for operation close to ambient pressure.

The separation procedure was largely conducted as described in Section 4.3.5, with a few deviations due to the fact that not all aspects of the sampling procedure were finalised at the time. Most importantly, no helium "flushings" were conducted (as in Section 4.3.4.1); of course, they are negligible in this case due to the sample volume being relatively large compared to the dead volume of MS4A. Also, no pause was inserted between the adsorption of the sample and heating of the column (see Section 4.3.4.4). Several test runs on the preceding days have been used to calibrate the time window for krypton capture on AC2, which was set from 13 to 29 minutes after the start of heating to accommodate the 9 minute long peak. The chromatogram (Figure 5.1) verifies that 3 minutes passed between the krypton peak and the closure of AC2, which is sufficient for a complete transfer. Also, instead of simply being routed out of the exhaust into the atmosphere, the carrier is being drained by the vacuum pump during the transfer between AC1 and AC2, resulting in a lower pressure in the

¹polyvinyl fluoride a.k.a. Tedlar®

Table 5.1.: Evaluation of the chromatogram of the separation routine for a 6 L ambient air sample.

V_{sample} [mL]	peak ₈₄ [A]	area ₈₄ [A·s/cm ³]	peak width [min]
6034 ± 60	$1.1 \cdot 10^{-13}$	$(5.87 \pm 0.32) \cdot 10^{-15}$	8.9

getter and AC2 and with the intention of avoiding the entrance of impurities from the exhaust. Implications of these procedural differences compared to the final separation method are discussed below.

A numerical evaluation of the procedure yields the results listed in Table 5.1. The relative yield of $6 \cdot 10^{-15}$ A·s/cm³ is as expected for the low pressure during the AC1-AC2 transfer. The peak width is also nominal for a sample of this size.

5.1.2. Measurement procedure

Both the air in the sampling bag and the purified sample have been sent to Bern University for comparison.

The 29 L air sample has been purified using the EFA procedure and measured using their beta-gamma coincidence setup, resulting in a krypton-85 activity concentration of 85.1 ± 2.0 dpm/cm³.

The purified sample has been transferred into the counting tube using the following setup. The sampling container No1 is connected to an intermediate volume V_K , which is connected to a liquid nitrogen cooled cryotrap KF, the other end of which is connected to the counting tube, with all connections initially closed. While heating No1 using a hot-air gun, about 100 mbar of P10 counting gas² are introduced into V_K and No1 is opened. Now, the valve leading to KF is opened, momentarily decreasing the pressure to 20 mbar, until the pressure has dropped to $6.3 \cdot 10^{-3}$ mbar due to the gas freezing on KF. This is repeated 3 times so that, comparing the volumes, 99.9999 % of the sample should theoretically be transferred to KF. Finally, KF is heated, the valve of the counting tube is opened and more counting gas is introduced, running through KF into the counting tube until the pressure reaches 2500 mbar.

The actual measurement is done in the low-level-counting laboratory at the University of Bern, which is located 35 m below surface level for background reduction.

²Argon with a 10 % methane content.

5.1.3. Yield

From the activity measurement of the separated sample, the yield can be calculated as

$$Y = \frac{V_c}{V_{exp}}$$

$$V_{exp} = C_{st} \cdot V_s \cdot 0.001$$

$$V_c = \frac{A_c}{a}$$

with Y [%] as the yield resulting from the expected volume V_{exp} [μL], the standard gas krypton concentration C_{st} [ppm], the sample volume V_s [cm^3], the volume V_c [cm^3] in the counting tube, the measured activity A_c [dpm] and the activity concentration a [dpm/ cm^3] of the standard gas.

The Kr-85 activity measured in the counting tube is 0.49 ± 0.05 dpm. Taking into account the activity concentration, the Kr amount in the sample is 5.76 ± 0.60 μL . With an estimated atmospheric concentration of 1.14 ppm, the initial air sample must have contained 6.87 ± 0.07 μL of Kr, so the final yield, corrected for 39 days of decay, is 83.1 ± 8.8 %. The large margin of error is mainly caused by the activity measurement of the final sample due to the low decay rate.

5.1.4. Evaluation

Despite the large error, the resulting yield of 80–90 % is satisfactory, especially taking into account that the krypton separation line was not optimized for larger air samples, and 6 L is close to the maximum the separation procedure can handle without major modifications.

5.2. Enriched samples, Series 1

For a precise measurement of the actual separation performance using small samples, a standard gas has been prepared at Bern University consisting largely of atmospheric air and an estimated krypton fraction of 5.45 ppm with a measured Kr-85 activity of 230 ± 8 dpm/ cm^3 .

A 35 L PVF bag containing this standard was received and refilled into 1 L composite foil bags for separation or storage.

Table 5.2.: Evaluation of the chromatogram (Figure 5.2) of the separation routine for a 6 L ambient air sample.

Sample	No	V [mL]	peak [10^{-11} A]	area [10^{-14} A·s/cm ³]	width [min]
Bern Std 1	1	1375 ± 14	3.72	2.70 ± 0.14	0.75
Bern Std 2	2	1438 ± 14	4.22	2.93 ± 0.16	0.80
Bern Std 6	4	987 ± 10	2.07	2.09 ± 0.11	0.66

5.2.1. Separation

Three samples have been processed using the krypton separation line with the procedure described in Section 5.1.1.

During separation, the krypton transfer to AC2 had shown irregularities, so the time windows were adjusted, as can be seen in Figure 5.2, but the peak was always rather too early than too late, so a complete transfer is expected in all cases.

A numerical evaluation of the chromatograms (Table 5.2) reveals another anomaly regarding the last sample, which displays a significantly lower peak area per sample volume, even taking into account the measurement uncertainty. A potential explanation for this may be the degeneration of the ionisation filament of the quadrupole mass spectrometer, which became apparent in later experiments and may have started at this point.

Compared to the calibration experiments of the preceding days using pure air, which averaged around $3 \cdot 10^{-15}$ A·s/cm³, the peak areas were higher than expected.

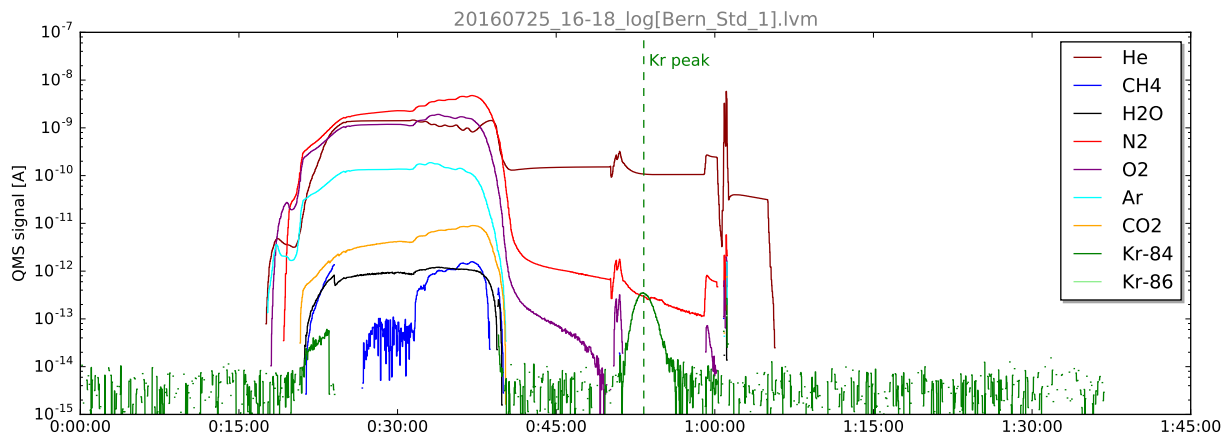
5.2.2. Measurement

The three purified samples have been extracted and measured as described in Section 5.1.2.

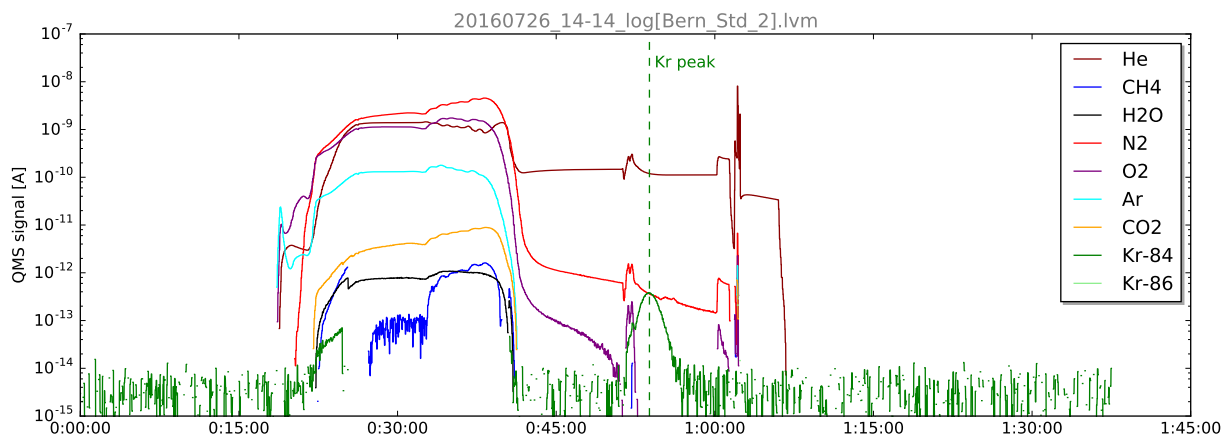
5.2.3. Yield

The yields have been determined by multiplying the results from the activity measurement with the known concentration of the standard, which has been measured at 230 ± 8 dpm/cm³, and comparing it with the expected krypton amount derived from the sample volume and concentration (5.45 ppm).

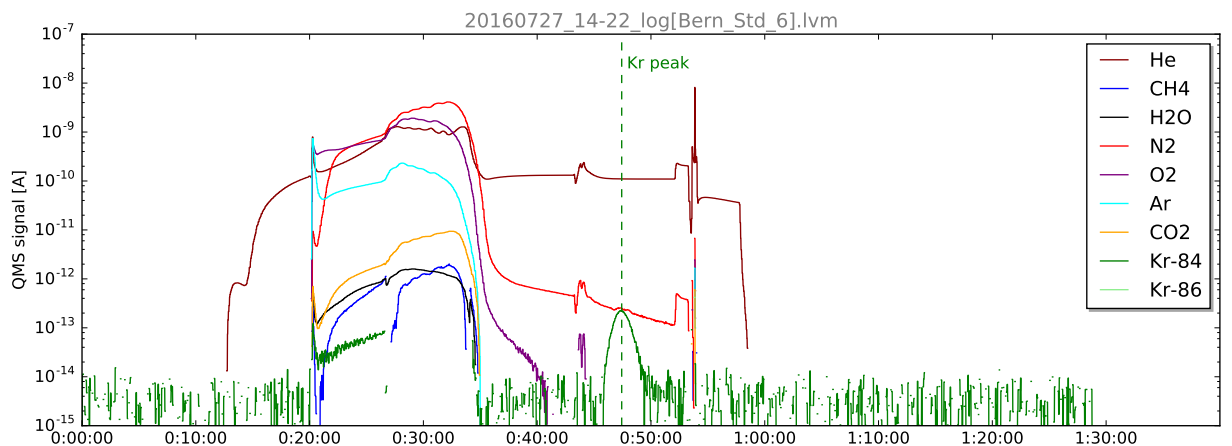
Results are displayed in Table 5.3 and while the average result of 77 % seems satisfactory, the individual yields vary wildly from 35–110 %. Of course, a separation yield beyond 100 % is highly implausible. The error margins are relatively small, at about 1 % relative error, and do not account for these variations. The yield increases for



(a) Sample "Bern Std 1"



(b) Sample "Bern Std 2"



(c) Sample "Bern Std 6"

Figure 5.2.: Separation chromatograms of several enriched samples obtained from Bern University.

Table 5.3.: Measurements of the separated samples from Series 1, the derived volumes and according yields.

Sample	A_{tube} [dpm]	V_{tube} [μL]	V_{expected} [μL]	yield [%]
Std 1	0.61 ± 0.05	2.65 ± 0.01	7.50	35.38 ± 0.39
Std 2	1.56 ± 0.04	6.78 ± 0.01	7.84	86.51 ± 0.87
Std 6	1.36 ± 0.06	5.91 ± 0.01	5.38	109.88 ± 1.13
<i>mean</i>				77 ± 38

each sample in the order of their preparation, which has been the same in Hamburg and Bern.

5.2.3.1. Memory effect

These results heavily imply a memory effect at work, although it is hard to determine at which point it may have taken place.

There are three potential points where a memory effect might occur: the molecular sieve MS4A used for desiccation, the carbon column AC1 and the trap AC2.

AC1 is an unlikely culprit, as already discussed in Section 4.3.4.11. Thanks to the placement of AC1 just before the quadrupole mass spectrometer capillary port, cross contamination could be tested during development and is definitely below 0.1 %

Cross contamination from MS4A is possible, the separation procedure used for Series 1 is not completely evacuating the trap. However, the trap is evacuated after each sample, during the regeneration procedure, so causing a large memory effect as observed is highly unlikely. Nevertheless, there is potential for some of the sample being retained in MS4A during the separation, which is addressed in Section 4.3.4.1 and compensated in the final separation procedure described in Section 4.3.5.

A memory effect in AC2 cannot be ruled out, but is also unlikely as it has not been observed in transfer experiments, such as those described in Section 4.3.4.10.

It is possible that a memory effect has affected the sample transfer from the sample container to the counting tube conducted in Section 5.1.2.

To make attribution of memory effects easier, the following sample batches were prepared in a different order in Bern than they were in Hamburg.

5.2.4. Evaluation

The samples from Series 1 have been successfully separated and measured, but the strongly varying yields cannot be adequately explained. The standard gas has a higher krypton concentration than pure air, but this should not impact the efficiency

Table 5.4.: Evaluation of the chromatogram (Figure 5.3) of the separation routine for a 6 L ambient air sample.

Sample	No	V [mL]	peak [10^{-12} A]	area [10^{-13} A·s/cm ³]	width [min]
Bern Std 7	2	1038 ± 10	1.4	1.38 ± 0.08	0.73
Bern Std 5	1	1138 ± 11	1.6	1.70 ± 0.09	0.82
Bern Std 4	4	1120 ± 11	1.5	1.52 ± 0.08	0.78

of the separation procedure according to the findings in Section 4.3.4.9. If a memory effect has led to higher yields in successive samples, one must assume that the minimum efficiency for the krypton separation line is 35 %. Another series of measurements was conducted for further study and is described in the next section.

In reaction to these results, a number of modifications have been made to the separation procedure to improve both yield and purity, arriving at the steps described in Section 4.3.5.

5.3. Enriched samples, Series 2

In order to obtain more reliable data on the extraction process, another series of samples has been prepared using the same standard gas, which had been stored in compound foil bags.

This measurement series was mostly carried out analogously to the the previous one, but with a number of improvements and measures have been implemented to avoid the unreliable results produced previously. These are described below.

5.3.1. Separation

This time, the separation procedure was carried out exactly as described in Section 4.3.5 and Appendix A. All parameters (Table 5.4) and chromatograms (Figure 5.3) are nominal, and the peaks are well defined and comfortably within the time window for transfer. The normalised peak area is smaller in the first peak, which may be due to the quadrupole mass spectrometer warming up.

A defect in the NuPure getter necessitated a switch from the 100 XL to the smaller Mini XL unit, so the gettering performance was reduced for this sample series. This is unlikely to influence the outcome, as the purity is not examined and the measurement procedure is not affected by an elevated nitrogen content.

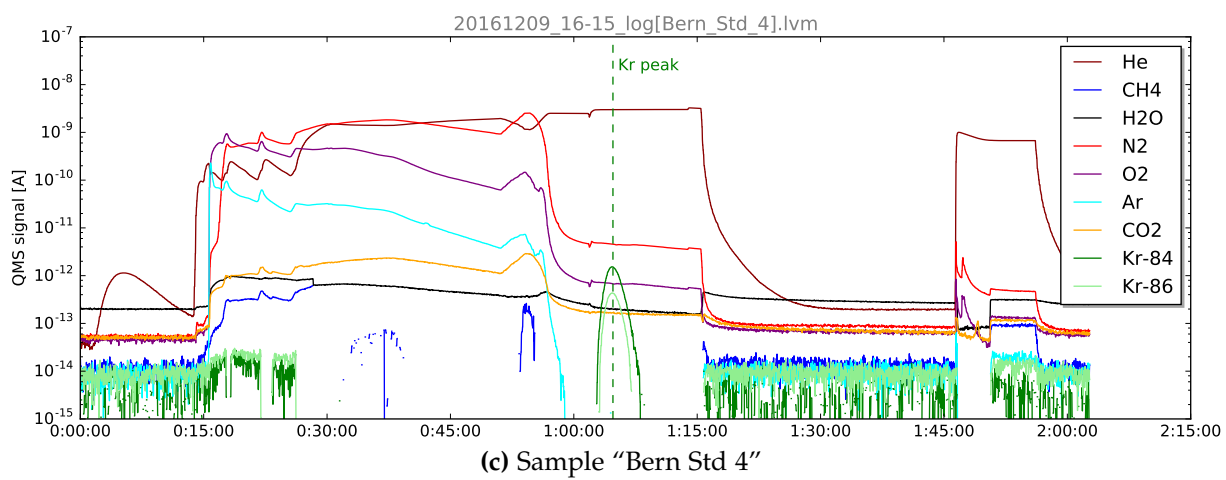
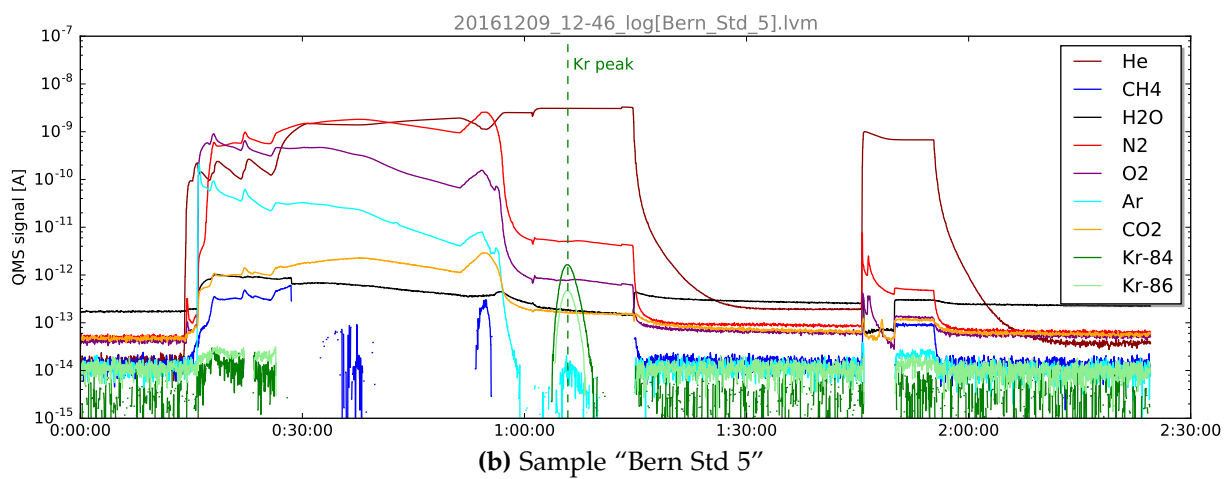
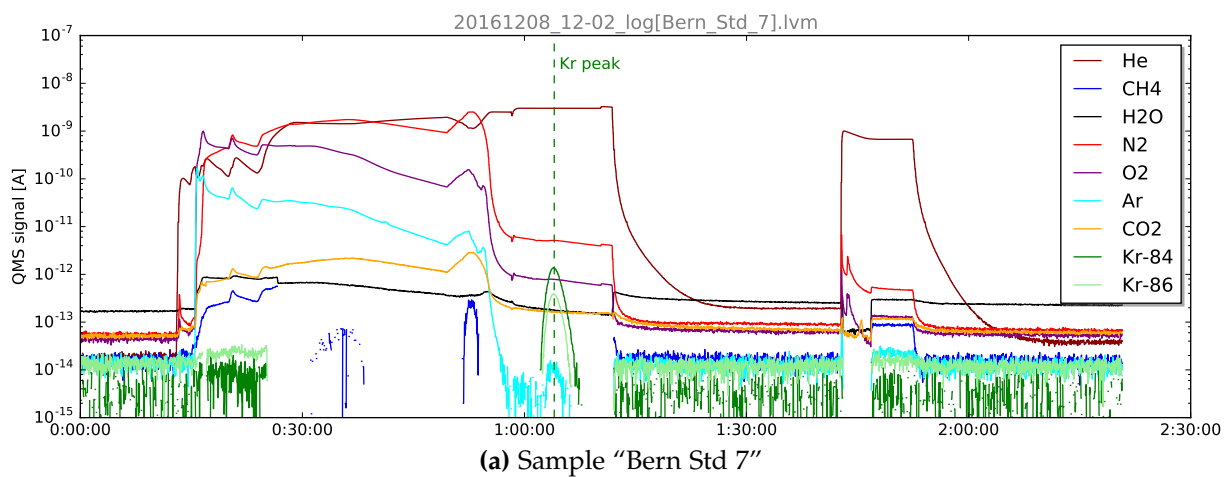


Figure 5.3.: Separation chromatograms of several enriched samples obtained from Bern University, Series 2.

Table 5.5.: Measurements of the separated samples from Series 1, the derived volumes and according yields.

Sample	No	A_{tube} [dpm]	V_{tube} [μL]	V_{expected} [μL]	yield [%]
Bern Std 5	1	0.721 ± 0.036	3.22 ± 0.01	6.16	52.29 ± 0.55
Bern Std 7	2	0.803 ± 0.029	3.58 ± 0.01	5.61	63.85 ± 0.65
Bern Std 4	4	0.778 ± 0.029	3.47 ± 0.01	6.06	57.28 ± 0.58
<i>mean</i>					57.8 ± 5.8

5.3.2. Measurement

The three purified samples have been extracted and measured as described in Section 5.1.2. Additional care has been taken to properly heat the transfer trap KF. Also, they have been prepared for measurement in a different order than they have been separated in the krypton separation line, to enable the attribution of memory effects.

5.3.3. Yield

The yields presented in Table 5.5 are more consistent than those of Series 1. No memory effect is present as evidenced by the results increasing neither in the order of separation, nor the order of measurement.

An average yield of 57.8 ± 5.8 % is observed.

5.3.4. Re-evaluation based on the composition of the standard gas

At the time of their separation for measurement Series 2, the standard gas samples had been in storage for five months. Although similar storage bag materials have been used for air sample storage (Hirota et al., 2004), the bags on hand are custom made and have not been tested for leak tightness over long periods of time.

To investigate whether the results of Series 2 may have been influenced by leakage of the storage bags, one of the remaining bags has been sent to the Institute of Environmental Physics of the University of Heidelberg for an analysis of the composition of the remaining standard gas. There, several cubic centimetres of the gas have been separated and processed using getters to isolate the noble gases for measurement in a sector-field static noble gas mass spectrometer (GV 5400, GV Instruments Ltd, Manchester, UK) to measure the most common stable noble gas isotopes (Sander et al., 2014). The resulting peak heights are compared with an atmospheric air standard and listed in Table 5.6.

Table 5.6.: Analysis of the noble gas contents of the standard gas used for measurement series 1 and 2 compared to atmospheric air. The Kr-84 content is significantly higher than the predicted 4.78. Also notable is a slight increase in He-4 content.

Isotope	He-3	He-4	Ne-20	Ne-22	Ar-36	Ar-40	Kr-84	Xe-132
abundance	0.99	1.08	0.99	0.99	0.99	0.99	7.33	0.98
error	0.02	0.01	0.01	0.01	0.01	0.01	0.10	0.03

The current atmospheric krypton concentration is 1.14 ppm, so for a sample containing 5.45 ppm, the Kr-84 peak should be elevated by a factor of 4.78. In the analysis, we find an elevation of 7.33 ± 0.10 , resulting in a Kr-84 content of 4.76 ± 0.06 ppm and an overall krypton content of 8.35 ± 0.11 ppm in the standard gas.

The reason for this disagreement remains unknown. While a leak in the storage bags could have led to a loss of standard gas and an influx of ambient air, this process would result in a reduced krypton concentration. Another explanation is the selective diffusion of different gas components through the sampling bag membrane, but this is also highly unlikely: a diffusion process to select krypton over the other noble gases is not known and could not explain the large drift that is observed. An error during the mixing of the standard gas cannot be ruled out.

Another class of potential mistakes is those which lead to different krypton concentrations across the sampling bags in which the standard gas was stored at the University of Hamburg laboratory. The PVF bag with the original standard gas was in transit for two days, which would be enough to homogeneously mix the components of the standard gas even if they had not been properly mixed to begin with. "De-mixing" of the gases during transfer into the sampling bags is not possible. The only conceivable cause for an elevated krypton concentration may be a contamination of one of the sampling bags, but while large samples of pure krypton have been handled during the development of the krypton separation line, no pure krypton has ever been stored in any of the bags. It is possible that some experiment has left a higher krypton concentration in parts of the krypton separation line which has in turn leaked into one of the bags, but no scenario of this type could be constructed from the laboratory records.

As the yield estimation is directly based on the krypton concentration of the standard gas, corrected yields can be derived and are listed in Table 5.7. These yields are even smaller, averaging around 38 % for Series 2. After correction, the yields from Series 1 become more plausible, even if still highly variable and subject to a potential memory effect.

Table 5.7.: The yields of Series 1 and Series 2, corrected for the elevated krypton content found in a an analysis of the standard gas used for the measurements. The original results were calculated for a krypton content of 5.45 ppm, when the analysis showed a content of 8.35 ppm.

Series	Sample	No	yield [%]	corrected yield [%]
2	Bern Std 5	1	52.29 ± 0.55	33.89 ± 0.57
2	Bern Std 7	2	63.85 ± 0.65	41.38 ± 0.69
2	Bern Std 4	4	57.28 ± 0.58	37.13 ± 0.62
	<i>mean</i>		57.8 ± 5.8	37.7 ± 3.8
1	Bern Std 1	1	35.38 ± 0.39	23.10 ± 0.40
1	Bern Std 2	2	86.51 ± 0.87	56.49 ± 0.94
1	Bern Std 6	4	109.88 ± 1.13	71.75 ± 1.20
	<i>mean</i>		77 ± 38	50 ± 25

5.4. Overall performance of the krypton separation line

Overall, the experiments have shown that the separation line successfully extracts a sufficient amount of krypton from ambient air samples.

The most reliable performance data have been collected on Series 2 of the samples and represent the yield of the final separation method detailed in Section 4.3.5. Depending on whether or not the corrections in Section 5.3.4 apply, the overall yield is around 38 % or, less likely, 58 %. At first glance, this performance is considerably lower than comparable methods working at higher sample volumes (Loosli et al., 1999; Yokochi et al., 2008; Yang et al., 2015) or even newer methods that target small sample sizes using a 5 Å molecular sieve setup (Tu et al., 2014).

However, most comparable efforts, for example Tu et al. (2014), measure the separation performance on the purified sample directly after the separation. Instead of being a best-case value, the separation yield in this work is actually representative of a real world sample, including transfer steps, shipping and handling at the remote laboratory.

In other words, while the actual separation performance may even be higher than 38 %, this yield represents the minimum amount of krypton that will actually be available for the atom trap trace analysis. In case of the average sample volume of 1100 mL, this amounts to 0.5 µL available for measurement. An increase in sample size to 2 L is feasible with the equipment available at the University of Hamburg and will yield the target amount of 1 µL, which is sufficient for measurement via atom trap trace analysis, especially if an advanced all-optical excitation scheme is

employed (Jiang et al., 2012).

The optimal air sample volume for separation is 1–5 L. Larger samples can be separated by splitting them and treating them successively; if the processed sample container is not removed and cooled continuously, all partial krypton samples can be stored in the same container.

6. Conclusions

After the planning, experimentation and development of all components as documented in this thesis, the krypton separation line has been built and programmed to comply with all requirements for supplying krypton samples for measurement using atom trap trace analysis. It is able to reliably extract the krypton fraction from very small air samples and shows that for such a separation, only one activated charcoal chromatography column is necessary when the temperature can be controlled precisely.

The separation process itself is fully automated, the operator is only required to refill liquid nitrogen and change the sampling bag and the purified sample vessel for each run. While the development of a separation method robust enough for automation was successful, different sample sizes behave uniquely, and adapted separation scripts need to be run depending on the approximate air volume to be separated.

Air volumes of 1–5 L per pass can be separated, larger samples can be processed by splitting them. With a separation recovery yield of 38 %, sample volumes may have to be increased to 2 L depending on the operational atom trap trace analysis performance. Processing of a sample takes 2–3 hours including regenerating and cooling all adsorbents, with at most 30 minutes of operator attention required. The sample contains no measurable impurities like argon, nitrogen or hydrocarbons, although a second gettering stage after transfer is advised to protect the vacuum ultra violet lamps necessary for optical excitation of the Kr atoms. The final krypton sample is collected in a vessel appropriate for long range transfer, if necessary.

The krypton separation line is constructed to be easily reassembled and modified to accommodate additional components or undertake repairs. Separation and regeneration procedures can be written and stored in files using a simple instruction syntax easily accessible to laboratory personnel without LabView programming knowledge.

The krypton separation line represents another important step to implementing a complete sampling and measurement infrastructure for krypton-85 at the Centre for Science and Peace Research, enabling the use of large numbers of small air samples for verification and environmental sciences.

7. Outlook

The krypton separation line as is will suffice to prepare atmospheric air samples for atom trap trace analysis. Some modifications may be necessary to treat different samples.

Samples of soil gas are commonly highly enriched (up to 90 %) in methane. The performance of the separation line for a high methane sample has not been investigated, but it is common to preprocess such samples using a copper furnace to reduce the methane content before beginning separation. Depending on the amount of gas that is left, the separation procedure may have to be modified.

Similarly, gas samples of high humidity, such as degassed water samples, may overload the desiccant column. A water trap may be necessary, with the crucial requirement of not reducing the krypton content of the sample.

When taking samples from the stack or the inside of a reprocessing plant, additional measures may be necessary to deal with hazardous contaminants such as hydrogen or hydrazine.

Bibliography

- Ahlsvede, Jochen; Simon Hebel; Martin B. Kalinowski; and Ole Ross (2009): *Update of the global krypton-85 emission inventory, Occasional Paper No. 9*. Tech. rep., Weizsäcker-Centre for Science and Peace Research, University of Hamburg.
- Ahlsvede, Jochen; Simon Hebel; J. Ole Ross; Robert Schoetter; and Martin B. Kalinowski (2013): Update and improvement of the global krypton-85 emission inventory. *Journal of Environmental Radioactivity*, 115:34–42.
- Avenhaus, Rudolf; Nicholas Kyriakopoulos; Michel Richard; and Gotthard Stein (2006): *Verifying Treaty Compliance*. No. ISBN-13: 978-3-540-33853-6 S. Springer.
- Bernatowicz, T. J. and F. A. Podosek (1986): Adsorption and isotopic fractionation of Xe. *Geochimica et Cosmochimica Acta*, 50:1503–1507.
- Briggs, G.A. (1973): *Diffusion Estimation of Small Emissions*. Tech. Rep. Contribution No. 79, Atmospheric Turbulence and Diffusion Laboratory, Oak Ridge, TN.
- Briggs, Gary A. (1985): Analytical Parameterizations of Diffusion: The Convective Boundary Layer. *Journal of Climate and Applied Meteorology*, 24(11):1167–1186.
- Brunauer, S.; P. Emmett; and E. Teller (1938): Adsorption of gases in multimolecular layers. *Journal of the American Chemical Society*.
- Carrott, P. J. M. (1995): Molecular sieve behaviour of activated carbons. *Carbon*, 33(9):1307–1312.
- Chen, C. Y.; Y. M. Li; K. Bailey; T. P. O'Connor; L. Young; and Z.-T. Lu (1999): Ultrasensitive Isotope Trace Analyses with a Magneto-Optical Trap. *Science*, 286(5442):1139–1141.
- Cimbák, Š. and P. Povinec (1985): ⁸⁵Kr atmospheric concentration in Bratislava from 1980 to 1983. *Environment International*, 11(1):65–69.
- Collon, P.; W. Kutschera; H. H. Loosli; B. E. Lehmann; R. Purtschert; A. Love; L. Sampson; D. Anthony; D. Cole; B. Davis; D. J. Morrissey; B. M. Sherrill; M. Steiner; R. C. Pardo; and M. Paul (2000): Kr-81 in the Great Artesian Basin, Australia: a new method for dating very old groundwater. *Earth and Planetary Science Letters*, 182:103–113.

- Connan, O.; L. Solier; D. Hebert; D. Maro; M. Lamotte; C. Voiseux; P. Laguionie; O. Cazimajou; S. Le Cavelier; C. Godinot; M. Morillon; L. Thomas; and S. Percot (2014): Near-field krypton-85 measurements in stable meteorological conditions around the AREVA NC La Hague reprocessing plant: estimation of atmospheric transfer coefficients. *Journal of Environmental Radioactivity*, 137:142–149.
- Connan, Olivier; Kilian Smith; Catherine Organo; Luc Solier; Denis Maro; and Didier Hébert (2013): Comparison of RIMPUFF, HYSPLIT, ADMS atmospheric dispersion model outputs, using emergency response procedures, with ⁸⁵Kr measurements made in the vicinity of nuclear reprocessing plant. *Journal of Environmental Radioactivity*, 124:266–277.
- Daerr, Heiner; Markus Kohler; Peter Sahling; Sandra Tippenhauer; Ariyan Arabi-Hashemi; Christoph Becker; Klaus Sengstock; and Martin B. Kalinowski (2011): A novel vacuum ultra violet lamp for metastable rare gas experiments. *Review of Scientific Instruments*, 82(073106).
- England, T. R. and B. F. Rider (Oct 1994): *Evaluation and Compilation of Fission Product Yields*. Tech. Rep. ENDF-349, Los Alamos National Laboratory, <http://t2.lanl.gov/publications/yields/>. LA-UR-94-3106.
- Ewing, J.H. and F.G. Ramberg (Aug 14 1984): Thermal mass flowmetering. US Patent 4,464,932.
- Ferber, G.J.; K. Telegadas; J.L. Heffter; and M.E. Smith (1977): Air concentrations of krypton-85 in the midwest United States during January–May 1974. *Atmospheric Environment* (1967), 11(4):379–385.
- Fischer, Michael (Jul 2011): *Molecular simulations of hydrogen storage and gas separation in metal-organic frameworks*. Ph.D. thesis, University of Hamburg.
- Göring, Friderike (2014): *Aufbau und Test einer vollautomatischen Luftsammelanlage (Construction and test of a fully automated air sampling device)*. Bachelor's thesis, Centre for Science and Peace Research, University of Hamburg.
- Harrison, R.G. and H.M. ApSimon (1994): Krypton-85 pollution and atmospheric electricity. *Atmospheric Environment*, 28(4):637–648.
- Hebel, Simon (2010): Genesis and equilibrium of natural lithospheric radionobles and its influence on subsurface noble gas samples for CTBT on-site inspections. *Pure and Applied Geophysics*, 167:463–470.
- Hirota, Michio; Kazuhiro Nemoto; Akira Wada; Yasuhito Igarashi; Michio Aoyama; Hidekazu Matsueda; Katsumi Hirose; Hartmut Sartorius; Clemens Schlosser;

- Sabine Schmid; Wolfgang Weiss; and Kenji Fujii (2004): Spatial and Temporal Variations of Atmospheric ^{85}Kr Observed During 1995–2001 in Japan: Estimation of Atmospheric ^{85}Kr Inventory in the Northern Hemisphere. *Journal of Radiation Research*.
- IAEA (1972): The structure and content of agreements between the Agency and states required in connection with the Treaty on the Non-Proliferation of Nuclear Weapons (INFCIRC/153). International Atomic Energy Agency.
- IAEA (1997): Model Protocol additional to the agreement(s) between state(s) and the International Atomic Energy Agency for the application of safeguards (INFCIRC/540). International Atomic Energy Agency.
- IAEA-STR-351 (2006): *Technical Meeting on Noble Gas Monitoring, Sampling and Analysis for Safeguards Applications, 12–16 September 2005*. Tech. rep., International Atomic Energy Agency.
- IPFM (2015): *Plutonium Separation in Nuclear Power Programs*. Tech. rep., International Panel on Fissile Materials.
- Jiang, W.; K. Bailey; Z.-T. Lu; P. Mueller; T.P. O'Connor; C.-F. Cheng; S.-M. Hu; R. Purtschert; N.C. Sturchio; Y.R. Sun; W.D. Williams; and G.-M. Yang (2012): An atom counter for measuring ^{81}Kr and ^{85}Kr in environmental samples. *Geochimica et Cosmochimica Acta*, 91:1–6.
- Jousten, Karl; Wolfgang Jitschin; Rudolf Lachenmann; Alfons Jünemann; Boris Kossek; Uwe Friedrichsen; Erik Lippelt; Harald Grave; Klaus Galda; Karl-Heinz Bernhardt; Stephan Plaetz; Norbert Müller; Robert Ellefson; Werner Große-Bley; Felix Altenheimer; Uwe Meißner; and Bernhard Schimunek (2006): *Wutz – Handbuch Vakuumtechnik*. Vieweg, 9th edn.
- Kalinowski, Martin B.; Hartmut Sartorius; Stefan Uhl; and Wolfgang Weiss (2004): Conclusions on plutonium separation from atmospheric krypton-85 measured at various distances from the Karlsruhe reprocessing plant. *Journal of Environmental Radioactivity*, 73:203–222.
- Klingberg, F.; S. Hebel; and M.B. Kalinowski (2011): *Simulation of atmospheric noble gas concentrations to assess sampling procedures for the detection of unreported reprocessing*. Phase I, 2nd Year Status Report JOPAG/01.09-PRG-373, Centre for Science and Peace Research, University of Hamburg.
- Kohler, M.; H. Daerr; P. Sahling; C. Sieveke; N. Jerschabek; C. Becker; and K. Sengstock (2014): All-optical production and trapping of metastable noble gas atoms down to the single atom regime. *Europhysics Letters*, 108(13001).

- Kohler, Markus (2011): *Vakuum-Ultra-Violette-Lichtquelle und Konzeptionen für die Ultrasparenanalyse von seltenen Kryptonisotopen*. Ph.D. thesis, University of Hamburg.
- Levins, Desmond M.; Ronald W. Glass; Marion M. Chiles; Daniel J. Inman; and David C. Watkin (1977): Beta-scintillation monitor for krypton-85 at high pressures. *Nuclear Instruments and Methods*, 146(3):517–525.
- Lide, D. R., ed. (2005): *CRC Handbook of Chemistry and Physics*. Taylor&Francis, London.
- Linde (2008): *Produktdatenblatt Helium 5.0*. Tech. rep., Linde AG.
- Loosli, H. H.; B. E. Lehmann; and W.R. Smethie (1999): *Environmental tracers in subsurface hydrology*, Kluwer, chap. Noble gas radioisotopes (Ar-37, Kr-85, Ar-39, Kr-81), pp. 379–396.
- Lott, Dempsey E. (2001): Improvements in noble gas separation methodology: a nude cryogenic trap. *Geochemistry, Geophysics, Geosystems*, 2:1068.
- Metcalf, Harold J. and Peter van der Straten (1999): *Laser Cooling and Trapping*. Springer-Verlag New York, Inc.
- Mieville, Rodney L. and Ken K. Robinson (2010): *Carbon molecular sieve and other porous carbons – Synthesis and applications*. Tech. rep., Mega-Carbon Company.
- MKS Instruments (1996): *"MKS Type 358C Master-Flo™ Mass Flow Meter and MKS Type 1359C Master-Flo™ Mass Flow Controller" Manual*.
- Momoshima, Noriyuki; Fumio Inoue; Shinji Sugihara; Jun Shimada; and Makoto Taniguchi (2010): An improved method for Kr-85 analysis by liquid scintillation counting and its application to atmospheric Kr-85 determination. *Journal of Environmental Radioactivity*, 101:615–621.
- Munakata, Kenzo; Teruki Fukumatsu; Satoshi Yamatsuki; Kenji Tanaka; and Masabumi Nishikawa (1999): Adsorption equilibria of krypton, xenon, nitrogen and their mixtures on molecular sieve 5A and activated charcoal. *Journal of Nuclear Science and Technology*, 36:818–829.
- Munakata, Kenzo; Hirofumi Okabe; Dmitri Ivanovski; Seigo Kanjo; and Yasuhito Igarashi (2006): Screening test for adsorbent for Kr at liquid argon temperature under nitrogen atmosphere. *Journal of Nuclear Science and Technology*.
- Munakata, Kenzo; Takashi Shinozaki; and Hirofumi Okabe (2008): Adsorption of krypton on adsorbents at cryogenic temperatures. *Journal of Power and Energy Systems*, 2(1):171–177.

- Munakata, Kenzo; Satoshi Yamatsuki; Kenji Tanaka; and Teruki Fukumatsu (2000): Screening test of adsorbents for recovery of krypton. *Journal of Nuclear Science and Technology*, 37(1):84–89.
- Pfeiffer (2012): *Pfeiffer HiPace 80, Manual*.
- Purtschert, Roland; Reika Yokochi; and Neil Sturchio (Sep 2009): Kr-81 dating of old groundwater.
- Riedmann, Robin A. (2011): *Separation of Argon from atmospheric air and Measurements of Ar-37 for CTBT purposes*. Ph.D. thesis, University of Bern.
- Ross, J. Ole (2010): *Simulation of atmospheric krypton-85 transport to assess the detectability of clandestine nuclear reprocessing*. Ph.D. thesis, International Max Planck Research School on Earth System Modelling.
- Ross, O.; J. Ahlswede; R. Annewandter; R. Schoetter; P. Stanoszek; and M. Kalinowski (2009): *Simulation of atmospheric noble gas concentrations to assess sampling procedures for the detection of clandestine reprocessing*. Phase I, 1st Year Status Report JOPAG/01.09-PRG-373, Centre for Science and Peace Research, University of Hamburg.
- Saey, Paul R. J. (2009): The influence of radiopharmaceutical isotope production on the global radionon background. *Journal of Environmental Radioactivity*, 100(5):396–406.
- Sander, Tim; Thomas Marx; Jürgen Engel; and Werner Aeschbach-Hertig (2014): Reproducibility and accuracy of noble gas measurements on water samples in the microlitre range. *Rapid Communications in Mass Spectrometry*, (28):42–48.
- Sartorius, H.; C. Schlosser; S. Schmid; and W. Weiss (2002): *Verfahren zur Bestimmung der Aktivitätskonzentration der atmosphärischen Edelgase Krypton-85 und Xenon-133*. Loseblattsammlung FS-78-15-AKU Empfehlungen zur Überwachung der Umweltradioaktivität, Bundesamt für Strahlenschutz.
- Schlosser, Clemens and Franziska Klingberg (2014): Krypton-85 Monitoring at BfS in Germany and Possible Applications for Safeguards. In: *Symposium on International Safeguards, IAEA, Vienna, Austria, 20–24 October 2014*.
- Schoeppner, Michael and Alexander Glaser (2016): Present and future potential of krypton-85 for the detection of clandestine reprocessing plants for treaty verification. *Journal of Environmental Radioactivity*, 162–163:300–309.

- Simgen, Hardy (2003): *Hochempfindlicher Nachweis radioaktiver Edelgasnuklide und natürlicher Radionuklide aus der Uran-Zerfallsreihe*. Ph.D. thesis, Ruprecht-Karls-Universität Heidelberg.
- Stockburger, H.; H. Sartorius; and A. Sittkus (1977): Messung der Krypton-85- und Xenon-133-Aktivität der atmosphärischen Luft. *Zeitschrift für Naturforschung*, 32a:1249–1253.
- Stute, M. and P. Schlosser (1993): Principles and application of the noble gas paleothermometer. In: *Continental Isotopic Indicators of Climate, AGU Monograph No 78*, P. K. Swart et al., pp. 89–100.
- Thallapally, Praveen K.; Grate W. Jay; and Radha K. Motkuri (2012): Facile capture and release at room temperature using a metal-organic framework: a comparison with activated charcoal. *Chemical Communications*, 48:347–349.
- Tu, Le-Yi; Guo-Min Yang; Cun-Feng Cheng; Gu-Liang Liu; Xiang-Yang Zhang; and Shui-Ming Hu (2014): Analysis of Krypton-85 and Krypton-81 in a Few Liters of Air. *Analytical Chemistry*, (86):4002–4007.
- Turner, D. B. (1970): *Workbook of Atmospheric Dispersion Estimates*. USEPA, ASRL, Research Triangle Park, North Carolina, US.
- UNSCEAR (1982): *Ionizing Radiation: Sources & Biological Effects*. Tech. rep., United Nations Scientific Committee on the Effects of Atomic Radiation.
- von Hippel, F.; D. H. Albright; and B. G. Levi (1986): *Quantities of Fissile Materials in US and Soviet Nuclear Weapons Arsenals*. Tech. rep., Center for Energy and Environmental Studies, Princeton University.
- Whichello, Julian; Cynthia Annese; and Andrew Monteith and (2010): Novel Technologies for IAEA Safeguards. In: *Symposium for International Safeguards, Preparing for Future Verification Challenges*.
- Wilhelmová, Ludmila; Zdeněk Dvořák; Milan Tomášek; and Karel Štukheil (1986): Application of the CaF₂(Eu) scintillator to ⁸⁵Kr monitoring in atmospheric air samples. *International Journal of Radiation Applications and Instrumentation. Part A. Applied Radiation and Isotopes*, 37(5):429–432.
- Winger, K.; J. Feichtera; M.B. Kalinowski; H. Sartorius; and C. Schlosser (2005): A new compilation of the atmospheric ⁸⁵krypton inventories from 1945 to 2000 and its evaluation in a global transport model. *Journal of Environmental Radioactivity*, 80:183–215.

Yang, Guo-min; Le-yi Tua; Cun-feng Chenga; Xiang-yang Zhang; and Shui-ming Hua (2015): Counting Radio-Krypton Atoms with a Laser. *CHINESE JOURNAL OF CHEMICAL PHYSICS*, 28(4).

Yang, Ralph T. (2003): *Adsorbents: Fundamentals and Applications*. Wiley & Sons, Inc.

Yokochi, Reika (2016): Recent developments on field gas extraction and sample preparation methods for radiokrypton dating of groundwater. *Journal of Hydrology*, 540:368–378.

Yokochi, Reika; Linnea J. Heraty; and Neil C. Sturchio (2008): Method for purification of krypton from environmental samples for analysis of radiokrypton isotopes. *Analytical Chemistry*, 80(22):8688–8693.

A. Final separation procedure

parts	new status per part	trigger	
V3;V4;V5;V6;V7;V8;V9;V10;V11;Setflow 1;V18	off;on;on;off;on;on;off;on;on;80;off	t	00:01
V1	on	dt	00:05
V1	on	dt	00:05
V1;V21;V22	off;off;off	PG1	<750
V20	on	dt	00:01
V2;V6	on;on	dt	00:01
V2;V6	off;off	dt	00:20
V2;V6	on;on	PG1	<750
V2;V6	off;off	dt	00:20
V2;V6	on;on	PG1	<750
V2;V6	off;off	dt	00:20
V2;V20	on;off	PG1	<750
V19	on	PG3	>1050
V4;V5;V3;Setflow 1	off;off;on;40	dt	00:10
V24	off	dt	20:00
AC1 set	-70	dt	00:30
AC1 set	-60	dt	00:30
AC1 set	-50	dt	00:30
AC1 set	-40	dt	00:30
AC1 set	-20	dt	00:30
AC1 set	0	dt	00:30
AC1 set	40	dt	00:30

parts	new status per part	trigger	
V12;V15	off;off	dt	8:00
V13;V16	on;on	dt	00:02
V17;V14	on;on	dt	00:05
V2;V16;V17;V10;V11;AC1 set;AC1 vent;V19	off;off;off;off;off;20;off;off	dt	12:00
V15;V12;V20	on;on;on	dt	00:01
V20;V21;V22	off;on;on	PG3	<2
V13;V14	off;off	PG2	<0,005
V21;V22	off;off	dt	00:01
V20;V11;V10;V9;V6	on;on;on;on;on	dt	00:01
V20;V11;V10;V9;V6	on;on;on;on;on	dt	00:10
V20;V21;V22	off;on;on	PG3	<2
V10;V11;V7;V8	off;off;off;off	PG2	<0,05
V20;V21;V22	on;off;off	dt	00:01
V5;V4	on;on	dt	00:01
V5;V4	on;on	dt	00:10
V5;V4	off;off	PG3	<20
V20;V21;V22	off;on;on	PG3	<2
V15;V17	off;on	PG2	<0,05
V15;V17	off;on	dt	00:10
V17;V15;V12	off;on;off	PG2	<0,05
V20;V21;V22;V18	on;off;off;off	PG2	<0,005
V20;V21;V22;V18	on;off;off;off	dt	00:05
V20;V21;V22	off;on;on	PG3	<2
V23	off	PG2	<0,005
AC2 vent;AC2 set;V16;V17	off;200;on;on	dt	00:01
V18	on	dt	5:00
V18	off	dt	10:00
V23	on	dt	00:05

parts	new status per part	trigger	
V16;V17;V20;V21;V22;AC2 set	off;off;on;off;off;20	dt	10:00
V10;V11;AC1 vent;AC1 set;V12	on;on;off;200;on	dt	00:01
V6;V7;V8;V9;V2;Setflow 1	off;on;on;off;on;120	dt	00:01
V2;V6;V9	off;on;on	dt	10:00
V20;V21;V22;V7;V8	off;on;on;off;off	PG3	<2
V10;V11;AC1 set	off;off;20	dt	10:00
V20;V21;V22	on;off;off	dt	00:01
V4;V5;V7;V8	on;on;on;on	dt	00:01
V24	off	dt	00:10
V6;V3;V2;Setflow 1	off;off;on;120	PG3	<3
V2;V3;V6	off;on;on	dt	10:00
V7;V8;V20;V21;V22	off;off;off;on;on	PG3	<1
end	end	end	end

Acknowledgements

First and foremost, I would like to thank Prof. Dr. Gerald Kirchner for his supervision and guidance, and Dr. Roland Purtschert, without whose invaluable help and expertise this work would not have been possible.

The students and staff of the laboratories at University of Hamburg and University of Bern taught the countless skills required to envision and construct this separation line, and were never short of helping hands, especially Dr. Markus Kohler, Carsten Sieveke, Rüdiger Schanda and Christoph Gerber.

Dr. Reika Yokochi and Dr. Axel Suckow provided crucial advice in the early stages of this work.

Prof. Dr. Martin Kalinowski introduced me to scientific peace research and enabled me to start this thesis.

My heartfelt thanks also go to Ellen and my parents for their unwavering support.

Eidesstattliche Versicherung (Declaration on oath)

Hiermit versichere ich an Eides statt, die vorliegende Dissertationsschrift selbst verfasst und keine anderen als die angegebenen Hilfsmittel und Quellen benutzt zu haben.

Die eingereichte schriftliche Fassung entspricht der auf dem elektronischen Speichermedium.

Die Dissertation wurde in der vorgelegten oder einer ähnlichen Form nicht schon einmal in einem früheren Promotionsverfahren angenommen oder als ungenügend beurteilt.

Hamburg, den 26.03.2018

Unterschrift der Doktorandin / des Doktoranden